



Universidad de Concepción  
Dirección de Postgrado  
Facultad de Ciencias Naturales y Oceanográficas  
Programa de Doctorado en Oceanografía

**Interacciones físicas-biológicas que determinan la  
variabilidad en biomasa y producción del zooplancton en  
la zona de surgencia de Chile - Centro Sur: el rol de  
procesos advectivos y la interacción fitoplancton-  
zooplancton**

Tesis para optar al grado de Doctor en Oceanografía

Ana Belén Venegas Ramos.

Concepción – Chile

2023

Profesor guía: Rubén Escribano

Depto. Oceanografía, Facultad de Ciencias Naturales y Oceanográficas

Universidad de Concepción

# Universidad de Concepción

## Dirección de Postgrado

La Tesis de *Doctorado en Oceanografía* titulada “*Interacciones físicas-biológicas que determinan la variabilidad en biomasa y producción del zooplancton en la zona de surgencia de Chile - Centro Sur: el rol de procesos advectivos y la interacción fitoplancton-zooplancton*”, de la Sra. Ana Belén Venegas y realizada bajo la Facultad de Ciencias Naturales y Oceanográficas, Universidad de Concepción, ha sido aprobada por la siguiente Comisión de Evaluación:

Dr. Rubén Escribano

Profesor guía

Universidad de Concepción

---

Dra. Carolina Parada.

Profesora Co-guía

Universidad de Concepción

---

Dra. Vera Oerder.

Miembro Comité de Tesis.

Universidad de Concepción

---

Dr. Pierre Amael Auger

Miembro Comité de Tesis

Laboratoire d'océanographie physique et spatiale

---

Dr. Ricardo Castro Santis

Miembro Comité de Tesis

Universidad Tecnológica Metropolitana

---

Dr. Fernando Córdova Lepe

Miembro Comité de Tesis

Universidad católica del maule

---

Dra. Lidia Yebra.

Examinadora Externa

Instituto Español de Oceanografía CSIC

---

Dra. Pamela Hidalgo

Director

Programa de Doctorado en Oceanografía

Universidad de Concepción

---

Dedicatoria.

A mi familia... En especial a mis hijos,  
Antonella Yaikin y Leonardo Yaikin.

A mi esposo Joshua Yaikin, mi gran compañero.

Agradecimiento.

Agradezco a todos aquellos que de alguna u otra forma hicieron posible el desarrollo y termino de esta tesis, a mi familia por siempre apoyarme y mi esposo por siempre estar para mí.

A mi profesor guía, Dr. Rubén Escribano, por su confianza y dedicación en mi formación profesional y desarrollo personal, por su cariño y preocupación desde el comienzo de este viaje sin él no sería posible este logro, al Dr. Pierre-Amaël por sus contribuciones impagables, sus constantes revisiones y sugerencias, apoyo en todo momento, recibimiento en Brest y su paciencia infinita, un pilar fundamental en este proceso.

A la Dra. Paulina Mancilla, por su apoyo y cooperación indispensable para el termino de esta tesis.

A los docentes y compañeros del programa de Doctorado por su apoyo y formación, en especial a mis compañeros de generación por ser unos amigos inigualables.

Agradezco a las distintas fuentes de financiamiento que me permitieron desarrollar mi programa de Doctorado: Beca de Doctorado Nacional (CONICYT-PFCHA/doctorado nacional/2018-21180829), Beca Gastos Operacionales (CONICY -242190249). Beca de Pasantía Doctoral (CONICY -752190085), Beca del Instituto Milenio de Oceanografía, Beca de Pasantía internacional escuela de graduados N°1211.

## Índice de Contenidos

Resumen .....	i
Abstract .....	iii
1.- INTRODUCCIÓN .....	5
2.- MATERIAL Y MÉTODOS.....	11
3.RESULTADOS.....	18
3.1.- Capítulo 1 “Comprensión de la variabilidad estacional de la biomasa del mesozooplancton en el sistema de surgencia de Chile centro-sur: una aproximación con modelado” .....	18
3.2.- Capítulo 2 “Evaluando la respuesta funcional Holling tipo IV para la interacción diatomeas-zooplancton”.....	34
4.- DISCUSIÓN.....	54
5.- CONCLUSIONES.....	60
6.- REFERENCIAS.....	61
7.- ANEXOS.....	71

## Índice de Figuras

- Figura 1.** Área de estudio configuración del modelo, el círculo rojo representa ubicación de la estación 18.....11
- Figura 2.** Correlación espacial del punto de grilla de la estación 18 con cada punto del dominio de estudio, para la biomasa del mesozooplancton.....54
- Figura 3.** Gráficas simulación del modelo NPZ para diferentes valores del parámetro inhibitorio (Beta).....58
- Figura 4.** Gráficas simulación del modelo NPZ para diferentes valores del parámetro de mortalidad.....58

## Índice de Tablas.

<b>Tabla 1.</b> Valores R y P de correlaciones de los datos de la estación 18 y modelo para la temperatura y los sesgos entre ambas series de datos.....	13
<b>Tabla 2.</b> Valores R y P de correlaciones de los datos de la estación 18 y modelo para la salinidad y los sesgos entre ambas series de datos.....	13
<b>Tabla 3.</b> Valores R y P de correlaciones de los datos de la estación 18 y modelo para el nitrato y los sesgos entre ambas series de datos.....	14
<b>Tabla 4.</b> Valores R y P de correlaciones de los datos de la estación 18 y modelo para la clorofila y los sesgos entre ambas series de datos.....	14
<b>Tabla 5.</b> Desfases temporales de los diferentes flujos y variables biológicas, obtenidas desde las ecuaciones del modelo.....	15

## *Curriculum Vitae*

Ana Belén Venegas  
Nacida el 3 de agosto, 1989, en Los Ángeles, Chile

2008-2013: Profesor de Matemáticas y Educación Tecnológica, Licenciado en Educación Universidad de Concepción, Chile.

2014-2016: Magíster en Matemáticas aplicadas, Universidad del Bío-Bío, Chile.

### ÁREAS DE INVESTIGACIÓN

Principal: Oceanografía biológica.

Secundaria: Modelos biogeoquímicos.

Otras: Educación interdisciplinaria, Matemáticas aplicadas a la oceanografía.

### EXPERIENCIA DOCENTE

2023:

Universidad del Bío-Bío, Cálculo I para Ingeniería en Construcción, Álgebra y trigonometría para Ingeniería en Ejecución Mecánica e Ingeniería Civil mecánica, Álgebra lineal para Ingeniería Civil Química, Cálculo integral para Ingeniería en Ejecución Eléctrica.

Universidad de Concepción: Matemática I para Pedagogía en Ciencias Naturales y Biología e Ingeniería en Biotecnología Vegetal, Geometría y trigonometría para Ingeniería en Geomática, Introducción a las ciencias básicas para Biotecnología Marina y Acuicultura, Razonamiento Algebraico para Educación General Básica, Introducción a los modelos de crecimiento vegetal para Ingeniería en Biotecnología Vegetal.

Universidad Andrés Bello. Docente, Sistemas lineales y Ecuaciones diferenciales para Ingenierías.

2022:

Universidad del Bío-Bío, Álgebra I para Ingeniería Comercial, Álgebra y trigonometría para Ingeniería en Ejecución Mecánica e Ingeniería Civil Mecánica. Álgebra lineal para Ingeniería Civil Industrial e Ingeniería Civil Mecánica.



Universidad de Concepción: Matemática I para Pedagogía en Ciencias Naturales y Biología e Ingeniería en Biotecnología Vegetal, Geometría y trigonometría para Ingeniería en Geomática, Razonamiento algebraico para Pedagogía General Básica, El océano como recurso para el trabajo interdisciplinar para Pedagogías, Introducción a las ciencias básicas para Biotecnología Marina y Acuicultura (Concepción).

Universidad Andrés Bello. Docente ayudante, Sistemas lineales y ecuaciones diferenciales para Ingenierías.

2021:

Universidad del Bío-Bío, Álgebra I para Ingeniería Comercial, Álgebra y trigonometría para Ingeniería en Ejecución Mecánica. Álgebra lineal para Ingeniería Civil Industrial e Ingeniería Civil Mecánica.

Universidad Católica de la santísima Concepción: Profesora de prácticas en cálculo I, profesora de Matlab para Calculo III y Ecuaciones diferenciales, para carreras de Ingeniería.

Universidad de Concepción: Razonamiento algebraico para Pedagogía General Básica, Historia de las matemáticas para Pedagogía en Matemáticas.

2020:

Universidad del Bío-Bío: Tópicos de matemáticas aplicadas para Ingeniería en Ejecución Electrónica, Ecuaciones diferenciales para Ingeniería Civil Informática, Álgebra I para Ingeniería Comercial, Álgebra lineal para Ingeniería Civil Industrial e Ingeniería Civil Mecánica.

2019:

Universidad del Bío-Bío. Cálculo integral para Ingeniería Civil Mecánica e Ingeniería Civil Eléctrica, Cálculo II para Contador Auditor, Cálculo diferencial para Ingeniería en Ejecución Informática, Cálculo II para Ingeniería Civil Eléctrica, Cálculo I para Ingeniería Ejecución en Computación e Informática.

2018:

Universidad de Concepción. Comprensión de procesos en ciencias naturales y oceanográficas utilizando herramientas matemáticas para Biología Marina y Biotecnología Marina y Acuicultura

2016:

Universidad Santo Tomás: Profesor Asistente. Matemática básica para Enfermería y Nutrición, Matemática para Ingeniería Comercial, Introducción a la matemática para Ingeniería Comercial.

Universidad del Bío-Bío: Matemática para Arquitectura.

2015:

Universidad Santo Tomás: Introducción a la matemática para Ingeniería Comercial, Matemática básica para Enfermería y Nutrición Matemática para Ingeniería Comercial

2014:

Universidad del Bío-Bío: Cálculo diferencial para Ingeniería Civil Mecánica, Álgebra y trigonometría para Ingeniería Civil Industrial Cálculo diferencial para Contador Auditor Público, Cálculo integral para Ingeniería Civil Civil

2013:

Preuniversitario Cpech, Los Ángeles. Profesora de Matemáticas.

Universidad de Concepción, Campus Los Ángeles: Alumna ayudante para la asignatura de Geometría I para Pedagogía en Matemática y Educación Tecnológica, Matemática II y IV para Pedagogía en Ciencias Naturales y Biología, Alumna guía del programa CADE (Centro de Apoyo al Desarrollo del Estudiante),

2012:

Práctica Profesional, Liceo Bicentenario Los Ángeles A-59.

2010-2012:

Universidad de Concepción, Campus Los Ángeles. Alumna ayudante para las asignaturas de Geometría I y II para Pedagogía en Matemática y Educación Tecnológica.

## GESTIÓN ACADEMICA:

2021-2023:

Universidad del Bío-Bío. Coordinadora de asignatura Álgebra y Trigonometría para ingenierías en ejecución.

2023:

Universidad del Bío-Bío. Coordinadora de asignatura Calculo Integral para ingenierías en ejecución.

## ESTADÍAS DE INVESTIGACIÓN O ENTRENAMIENTO

Pasantía en Centro de Investigación: Laboratoire d'océanographie physique et spatiale - (LOPS), Dr. Pierre-Amael Aüger, Brest, Francia Diciembre 2019-Abril 2020.

## RESUMEN.

Interacciones físicas-biológicas que determinan la variabilidad en biomasa y producción del zooplancton en la zona de surgencia de Chile - Centro Sur: el rol de procesos advectivos y la interacción fitoplancton-zooplancton.

Ana Belén Venegas Ramos, 2023, Profesor Guía, Rubén Escribano.

Los grandes ecosistemas de surgencia costera, también conocidos como "Sistemas de Corrientes de Borde Oriental" (EBUS), son de gran importancia tanto ecológica como económica debido a que sostienen una alta productividad biológica y pesquera. En ellos, el zooplancton es uno de los componentes clave puesto que sustenta la productividad de estos ecosistemas, siendo responsable de la transferencia de energía entre los productores primarios a los niveles tróficos superiores, incluyendo peces, por lo cual la biomasa y producción del zooplancton en su conjunto es un pilar clave en la productividad de los EBUS.

El EBUS que se encuentra frente a Chile Centro Sur (30-39° S) se caracteriza por la presencia de un frente de surgencia, con un máximo observado en primavera-verano, que desplaza hacia la superficie agua ecuatorial subsuperficial, fertilizando la capa fótica y promoviendo el crecimiento del plancton, la abundancia de peces pelágicos pequeños, aves y mamíferos, lo cual los convierte en ecosistemas de gran importancia biológica /económica. Este sistema se caracteriza por una alta variabilidad en escalas tanto temporales como espaciales debido al proceso de surgencia costera, el cual impacta en los organismos que se desarrollan en estas regiones. Por lo cual, determinar los factores que influyen en la variabilidad en la biomasa del zooplancton es de suma importancia para poder pronosticar los cambios que los EBUS puedan presentar en su productividad bajo un escenario de cambio climático.

Esta tesis se centra en someter a prueba dos hipótesis: 1) bajo condiciones de surgencia intensificada, los procesos advectivos contribuyen a una pérdida significativa de la biomasa del zooplancton desde la zona de surgencia, impactando negativamente la producción frente a Chile Centro-Sur, y 2) en el sistema de surgencia costera de Chile centro-sur del Pacífico sur oriental, para un período de surgencia intensa primavera-verano, la respuesta funcional del zooplancton frente a altas concentraciones del fitoplancton se manifiesta con un efecto inhibitorio de parte de las diatomeas sobre el zooplancton afectando negativamente su crecimiento y producción.

Para testear tales hipótesis se planteó un primer objetivo científico: I) Determinar la importancia relativa de la advección horizontal *versus* la producción local de biomasa del zooplancton, en el sistema de surgencia costera frente a Chile centro-sur. Para esto se utilizó un enfoque de modelado, utilizando las salidas de una configuración del modelo ROMS-PISCES para la región de surgencia de Chile centro sur (35.2°-37.8°S). Con este modelo se reconstruyó la variabilidad oceanográfica para el período agosto de 2002 a diciembre de 2008 para la zona costera asociada a la estación de monitoreo fija Estación 18, ubicada al noroeste de la bahía de Concepción frente a Dichato en la región del Bío Bío (36°30.80'S, 73°7.75' W), Chile. El estudio evaluó la influencia de la productividad local *versus* los factores advectivos en la variabilidad de la biomasa del zooplancton en la zona de surgencia del centro-sur de Chile, se determinó que en los meses de primavera – verano los términos advectivos son de gran importancia para la variabilidad de la biomasa en la zona de surgencia, donde el flujo desde sur a norte contribuye sustancialmente al aumento de la biomasa en la zona, en cambio el flujo hacia el oeste es la principal fuente de pérdida de biomasa.

Con respecto al segundo objetivo se propuso conocer el impacto de la respuesta funcional tipo Holling IV sobre el crecimiento del zooplancton a través de la implementación de un modelo analítico nutrientes-fitoplancton-zooplancton (NPZ) para condiciones de altas concentraciones de fitoplancton en sistemas altamente productivos. Para esto se realizó un análisis cualitativo de las soluciones de un modelo de NPZ en tiempo finito e infinito, de estos 3 compartimientos (Nutrientes-Fitoplancton-Zooplancton). Así se estudió la variación de la biomasa del zooplancton considerando la toxicidad de las diatomeas cuando estas se encuentran en grandes concentraciones. Se observó que al incluir una respuesta funcional Holling IV para representar la toxicidad de las diatomeas durante el periodo de surgencia activa, se reproducen apropiadamente las magnitudes y variaciones de la biomasa del zooplancton en la zona de estudio, y se evidencia la importancia del factor inhibitorio de las diatomeas y el parámetro de mortalidad en la variación de la biomasa del zooplancton.

El estudio provee evidencia apoyando ambas hipótesis planteadas y sugiere que ambos procesos con base física y biológica deberían ser considerados en las observaciones de campo y en el desarrollo de modelos biogeoquímicos que involucran la dinámica y producción del zooplancton en sistemas de surgencia altamente productivos.

## ABSTRACT.

Physical-biological interactions that determine the variability in biomass and zooplankton production in the upwelling zone of Chile - South Central: the role of advective processes and the phytoplankton-zooplankton interaction.

Ana Belén Venegas Ramos, 2023, Profesor Guía, Rubén Escribano

Large coastal upwelling ecosystems, also known as EBUS "Eastern Boundary Upwelling Systems", are of great ecological and economic importance because they support high biological and fisheries productivity. In them, zooplankton is one of the key components since they support the productivity of these ecosystems, being responsible for the transfer of energy between primary producers to higher trophic levels, including fish, which is why the biomass and production of zooplankton in their Together it is a key pillar in the productivity of the EBUS.

The EBUS located off central-southern Chile (30-39° S) is characterized by the presence of an upwelling front, with a maximum observed in spring-summer, which displaces subsurface equatorial water to the surface, fertilizing the photic layer and promoting the growth of plankton, the abundance of small pelagic fish, birds and mammals, which makes it an ecosystem of great biological/economic importance. This system is characterized by high variability on both temporal and spatial scales due to the coastal upwelling process, which impacts the organisms that develop in these regions. Therefore, determining the factors that influence the variability in zooplankton biomass is of utmost importance to be able to predict the changes that EBUS may present in their productivity under a climate change scenario.

This thesis focuses on testing two hypotheses: 1) under conditions of intensified upwelling, advective processes contribute to a significant loss of zooplankton biomass from the upwelling zone, negatively impacting its production off central-southern Chile, and 2) in the coastal upwelling system of south-central Chile in the eastern South Pacific, for a period of intense spring-summer upwelling, the functional response of zooplankton to high concentrations of phytoplankton is manifested with an inhibitory effect of the diatoms on zooplankton, negatively affecting their growth and production.

To test such hypotheses, a first scientific objective was proposed: I) Determine the relative importance of horizontal advection *versus* local zooplankton biomass production, in the coastal upwelling system off central-southern Chile. For this, a modeling approach was used, using the outputs of a configuration of the ROMS-PISCES model for the upwelling region of south-central Chile ( $35.2^{\circ}$ - $37.8^{\circ}$ S). With this model, the oceanographic variability was reconstructed for the period August 2002 to December 2008 for the coastal zone associated with the fixed monitoring Station 18, located northwest of Concepción Bay in front of Dichato in the Bio Bio region ( $36^{\circ}30.80'S$ ,  $73^{\circ}7.75'W$ ), Chile. The study evaluated the influence of local productivity *versus* advective factors on the variability of zooplankton biomass in the upwelling zone of central-southern Chile. It was determined that in the spring-summer months advective terms are of great importance for the variability of biomass in the upwelling zone of central-southern Chile, where the flow from south to north contributes substantially to the increase in biomass in the area, while the flow to the west is the main source of biomass loss.

With respect to the second objective, it was proposed to know the impact of the Holling IV type functional response on the growth of zooplankton through the implementation of a nutrient-phytoplankton-zooplankton (NPZ) analytical model for conditions of high phytoplankton concentrations in highly productive systems. For this, a qualitative analysis of the solutions of an NPZ model in finite and infinite time, of these 3 compartments (Nutrients-Phytoplankton-Zooplankton), was carried out. Thus, the variation in zooplankton biomass was studied considering the toxicity of diatoms when they are found in high concentrations. It was observed that by including a Holling IV functional response to represent the toxicity of diatoms during the period of active upwelling, the magnitudes, and variations of zooplankton biomass in the study area are appropriately reproduced, and the importance of the inhibitory factor is evident of diatoms and the mortality parameter in the variation of zooplankton biomass.

The study provides evidence supporting both hypotheses and suggests that both physically and biologically based processes should be considered in field observations and in the development of biogeochemical models involving the dynamics and production of zooplankton in highly productive upwelling systems.

## INTRODUCCIÓN

El zooplancton marino es clave en la trama trófica pelágica, al ser responsable de gran parte de la transferencia de materia y energía desde los productores primarios a los consumidores tales como peces (Saiz et al., 2007, Hjort, 1914). El zooplancton está fundamentalmente compuesto por organismos de ciclos de vida corto (<1 año), muy sensibles a los cambios ambientales, los cuales responden rápidamente en términos de abundancia y composición a variables como la temperatura (Peterson et al., 2006), cantidad y calidad de alimento (Vargas et al., 2006), estratificación y oxigenación (Seibel, 2010), entre otras. Estas variables ambientales están sujetas a cambios en diversas escalas espaciales y temporales, y por lo tanto la estructura comunitaria del zooplancton puede verse alterada en el escenario de cambio climático actual, siendo por lo tanto considerado como un modelo biológico adecuado para estudiar los efectos de la variabilidad climática sobre el ecosistema marino y sus componentes biológicos, así como en los ciclos biogeoquímicos (Buttay et al., 2017).

La dinámica del zooplancton adquiere particular relevancia en los sistemas de alta productividad biológica, tales como los sistemas de surgencia de borde oriental (EBUS), que sustentan grandes pesquerías y cuya productividad está relacionada a la surgencia costera (Mann & Lazier, 1991). La surgencia costera es un proceso físico que resulta de la transferencia de momentum desde el viento hacia el océano, combinado con la rotación terrestre, lo cual provoca el movimiento horizontal de la capa superficial adyacente a la costa, también llamada capa de Ekman, en 90° a la izquierda de la dirección del viento en el hemisferio sur (Yoshida, 1959; Gill, 1982), es decir, mar afuera, lo cual produce divergencia costera y movimientos verticales de agua hacia la superficie, generando cambios en la capa fótica, tales como la disminución de la temperatura, oxígeno, pH y aumento de la salinidad y cantidad de nutrientes. Este aumento de nutrientes provenientes desde las capas más profundas trae consigo un aumento de la productividad primaria (Mann & Lazier, 1991), que promueve también el crecimiento del zooplancton.

El Sistema de la Corriente de Humboldt frente a las costas de Chile es altamente productivo (Montero et al., 2007; Quiñones et al., 2010), en particular la zona de surgencia de Chile centro-sur (30°-40°S) es de gran relevancia tanto ecológica como económica dado que sustenta una fuerte pesquería basada en peces pelágicos y demersales (Arcos et al., 2001). En esta región se reconocen varios centros de surgencias costeras (Fonseca & Farías, 1987), que presentan una fuerte variación estacional. Al respecto,



Cáceres & Arcos (1991), Figueroa & Moffat (2000), y Sobarzo et al. (2007), determinaron que la surgencia costera en dicha zona es un proceso fuertemente estacional el cual se caracteriza por afloramientos intensos y continuos en primavera/verano y surgencias débiles o inexistentes durante otoño/invierno.

Con respecto a la influencia de la surgencia en el zooplancton, Buttay et al. (2017), utilizando series de tiempo en la Plataforma Ibérica Noreste, corroboraron una fuerte asociación entre la variabilidad meteorológica-hidrográfica, la biomasa total y abundancia del zooplancton, las cuales fluctuaban en sincronía con la surgencia. Escribano et al. (2007), por otra parte, mediante el análisis de una serie temporal ubicada a 30 km desde la costa de Dichato, Chile (36°30' S) determinaron que la biomasa del zooplancton fue mayor en promedio en primavera y verano y menor en invierno y otoño, coincidiendo con los periodos de surgencia activa y sin surgencia, respectivamente.

Los modelos climáticos proyectan un calentamiento global de la superficie del océano para las próximas décadas de aproximadamente +3°C, una desoxigenación del interior del océano de aproximadamente 3%, y una disminución en la productividad primaria neta marina total de aproximadamente un 8% (Lefort et al., 2015). En este contexto se considera de suma importancia comprender los factores y mecanismos que controlan la variación y producción del zooplancton, dado que las variaciones tanto biogeoquímicas como ecológicas que pueden provocar las alteraciones en la estructura comunitaria y producción del zooplancton son cruciales para poder predecir las respuestas del ecosistema marino en un contexto de cambio climático (Beaugrand et al., 2002; Richardson & Schoeman, 2004; Hays et al., 2005; Lauria et al. 2013, Brun et al. 2019).

Bakun et al. (2010), plantean la hipótesis de que el calentamiento global aumentará los gradientes de temperatura tierra-océano, producto de un calentamiento diferencial, donde la tierra aumentaría más rápidamente de temperatura que el océano, provocando que incrementen los vientos favorables a la surgencia. Esta intensificación del fenómeno de surgencia traería consigo mayor turbulencia y un transporte más rápido afuera de la costa de las aguas superficiales (Bakun et al., 2015). Diversos estudios han evidenciado este fenómeno en los sistemas de surgencia, por ejemplo, el sistema de corriente de Humboldt (Wang et al., 2015), de Perú (Bakun & Weeks, 2008), Noroeste de África (Santos et al., 2005), Sudáfrica (Shannon et al., 1992) y California (Mendelssohn & Schwing, 2002). Además se señala que esta tendencia en la intensificación continuará (Garreaud & Falvey, 2009; Bakun et al., 2015; Xiu et al., 2018), lo que sugiere que frente a Chile centro-sur el

calentamiento global podría traer consigo un aumento en la intensidad de la surgencia costera, provocando un mayor aporte de nutrientes a las capas superficiales, así como un aumento en los procesos advectivos que puede producir de pérdidas de biomasa de zooplancton fuera de la zona de surgencia hacia la zona de transición costera y oceánica, causado por un aumento de la advección horizontal.

Un mayor suministro de nutrientes a la capa fótica puede provocar un aumento en las floraciones de fitoplancton, el cual, en los EBUS se caracteriza por densas floraciones de especies de diatomeas, a menudo cosmopolitas (ej. 5 especies reportadas en Ianora et al., 2004). Estas diatomeas son fuente de alimento de copépodos planctónicos (Lebour, 1922; Marchal & Orr, 1995), y se considera que la floración de primavera de diatomeas inicia y apoya la producción secundaria, así como el crecimiento de larvas de peces que dependen, principalmente, de huevos y nauplios de copépodos planctónicos como fuente de alimento (Turner, 1984; Mann, 1993). Sin embargo, los estudios muestran que un alto porcentaje (>20%) de la biomasa del fitoplancton sedimenta sin ser pastoreada, producto de que las poblaciones de sus principales depredadores, los copépodos calanoideos, alcanzan su punto máximo posteriormente a la floración (Colebrook et al., 1986; Verity et al., 1996; Miralto et al., 2003). Una posible explicación a este desacople se debe a la liberación de sustancias tóxicas, tales como aldehídos poliinsaturados (PUA), por parte del fitoplancton como una estrategia de defensa hacia los copépodos herbívoros, estas toxinas, según estudios realizados por Poulet et al. (2007), pueden afectar negativamente el zooplancton, inhibiendo su capacidad reproductiva e impactando directamente su crecimiento, debido a una menor producción de huevos y menor sobrevivencia de nauplios.

Los aldehídos poliinsaturados (PUA), se derivan a partir de ácidos grasos cuando las células están físicamente dañadas (Miralto et al., 1999; Pohnert, 2002), y se postula que estos compuestos derivados de diatomeas son la principal causa de las fallas en la reproducción y el desarrollo de los copépodos (Miralto et al. 1999, Ianora et al. 2004). Este efecto ha sido observado en diversos estudios de campo asociados a una alta concentración de diatomeas, por ejemplo en el Mar Adriático (Ianora et al., 2004), Bahía Dabob: Pacífico norte (Halsband-Lenk et al., 2005), aguas costeras frente a Roscoff: Canal de la Mancha (Poulet et al., 2006), sistema de surgencia del Pacífico sur (Vargas et al., 2006), fiordos de Noruega (Koski, 2007), y en laboratorios en los que se determinó que, cuando los copépodos son alimentados con monocultivos de ciertos tipos de

diatomeas, se inhibe la frecuencia de eclosión (Ianora et al., 1996, 2004; Ban et al., 1997). Esta inhibición puede representar un mecanismo de defensa de las diatomeas contra el pastoreo de los copépodos, prolongando de esta manera el florecimiento de las diatomeas (Ban et al., 1997).

Como se mencionó anteriormente, comprender los mecanismos y procesos que regulan la variabilidad de la biomasa y producción del zooplancton es sumamente importante para poder predecir los cambios de los ecosistemas marinos producto del cambio climático. Sin embargo la información disponible en la región de Chile centro-sur es limitada, lo cual complejiza tratar de realizar predicciones confiables sobre los cambios en las poblaciones de peces cuyo sustento está estrechamente relacionado al zooplancton (Beaugrand et al., 2003; Araujo et al., 2006), es por esto que contar con estudios de series temporales es relevante para evaluar la variabilidad del ecosistema marino frente a los cambios ambientales (Richardson & Schoeman, 2004; Mackas et al., 2007).

Una herramienta cada vez más utilizada que no solo evidencian los cambios en el tiempo de las variables de estudio, sino que además permiten comprender y evaluar los procesos que subyacen estos cambios mediante diversas ecuaciones y respuestas funcionales es la modelación matemática, puesto que es posible evaluar los efectos en los cambios de determinadas condiciones o parámetros, ya sean ambientales o fisiológicas, por ejemplo, cambios en la temperatura, advección, radiación o cambios en las tasas de mortalidad, tasas de crecimiento, porcentaje de asimilación, etc. Mediante simulaciones las cuales requieren una cantidad de tiempo y recursos considerablemente menor que realizar experimentos en laboratorios o *in situ*.

Los modelos biogeoquímicos se desarrollan como una herramienta que permite estudiar los cambios en la productividad biológica y los flujos de carbono y de los nutrientes más importantes en los ecosistemas, describiendo los procesos biogeoquímicos subyacentes a estos cambios y de esta forma poder estudiar los factores que influenciaron estos cambios en el pasado y poder de esta forma pronosticar las respuestas del ecosistema en el futuro a los cambios ambientales (Aumont et al., 2015).

Uno de estos modelos biogeoquímicos es PISCES por sus siglas en inglés (Pelagic Interactions Scheme for Carbon and Ecosystem Studies) el cual es un modelo biogeoquímico compuesto por ecuaciones que describen la interacción de dos clases de fitoplancton, 2 clases de zooplancton, las cuales están diferenciadas por el tamaño, 5 tipos

de nutrientes (C, F, N, Si, Fe), materia orgánica disuelta (MOD) y materia orgánica particulada (MOP), en el cual uno de los supuestos es que la razón de Redfield es constante en el océano global (Aumont et al., 2015). Este modelo puede ser utilizado para estudios en diversas escalas tanto espaciales como temporales.

Además, el modelo PISCES se acopla al modelo físico ROMS permitiendo de esta forma que los procesos físicos sean forzantes de los procesos biogeoquímicos. Este modelo físico (Shchepetkin & McWilliams, 2005), simula la circulación de las masas de agua, utilizando coordenadas sigma en la vertical y resuelve las ecuaciones hidrostáticas primitivas con un esquema explícito de superficie libre, al utilizar el modelo acoplado ROMS-PISCES permite evaluar y comprender los procesos y forzantes que están determinando las variaciones observadas en las variables de interés tales como la biomasa del fitoplancton y zooplancton.

Por otra parte, bajo un enfoque de modelado encontramos los modelos NPZ (Nutrient-Phytoplankton-Zooplankton), los cuales se han usado ampliamente para estudiar la dinámica de las comunidades planctónicas (Franks, 2002). Estos modelos consisten en una ecuación de evolución de nutrientes, fitoplancton y zooplancton, donde se incluyen efectos de mortalidad, consumo de nutrientes por el fitoplancton y consumo de fitoplancton por el zooplancton, entre otros. Uno de los supuestos importantes en este tipo de modelos es que estos campos NPZ, se resuelven en la capa fótica (Steele, 1958), y no consideran la física como forzante de estos procesos. Mediante un análisis de sensibilidad, Mitra et al. (2014), determinaron que los parámetros de los modelos NPZ, que tienen un mayor potencial de afectar la dinámica del modelo, son aquellos que describen el pastoreo, la eficiencia de asimilación y la mortalidad.

En base a lo planteado anteriormente se formula el siguiente objetivo general.

Determinar la importancia relativa y contribución de la advección horizontal *versus* la interacción fitoplancton tóxico-zooplancton en la modulación de la variabilidad de la biomasa del zooplancton, y de las tasas de producción del zooplancton en un sistema de surgencia costera de corriente de borde oriental (EBUS).

## HIPÓTESIS Y OBJETIVOS ESPECIFICOS

Hipótesis:

H1: En el sistema de surgencia costera de Chile centro-sur del Pacífico sur oriental, para un período de surgencia intensa primavera-verano, la respuesta funcional del zooplancton frente a altas concentraciones del fitoplancton se manifiesta con un efecto inhibitorio de la producción de biomasa del zooplancton.

H2: Bajo condiciones de surgencia intensificada, los procesos advectivos contribuyen a una pérdida significativa de la biomasa del zooplancton desde la zona de surgencia, impactando negativamente la producción de biomasa del zooplancton frente a Chile centro-sur.

Objetivos específicos:

Objetivo 1: Determinar la importancia relativa de la advección horizontal *versus* la producción local de biomasa del zooplancton y el efecto de la migración vertical en esto, en el sistema de surgencia costera frente a Chile centro-sur.

Objetivo 2: Determinar la importancia relativa de la advección horizontal *versus* la toxicidad por diatomeas en la producción de biomasa del zooplancton y el efecto de la toxicidad sobre la variabilidad espacio temporal de la biomasa de zooplancton en el sistema de surgencia costera frente a Chile centro-sur.

## MATERIALES Y METODOS

Área de estudio: los datos utilizados para evaluar el comportamiento de ambos modelos fueron obtenidos de la serie de tiempo ubicada a 30Km de la costa, a 36°30.80' sur y 73°7.75'oeste con 90 metros de profundidad llamada “estación 18”.

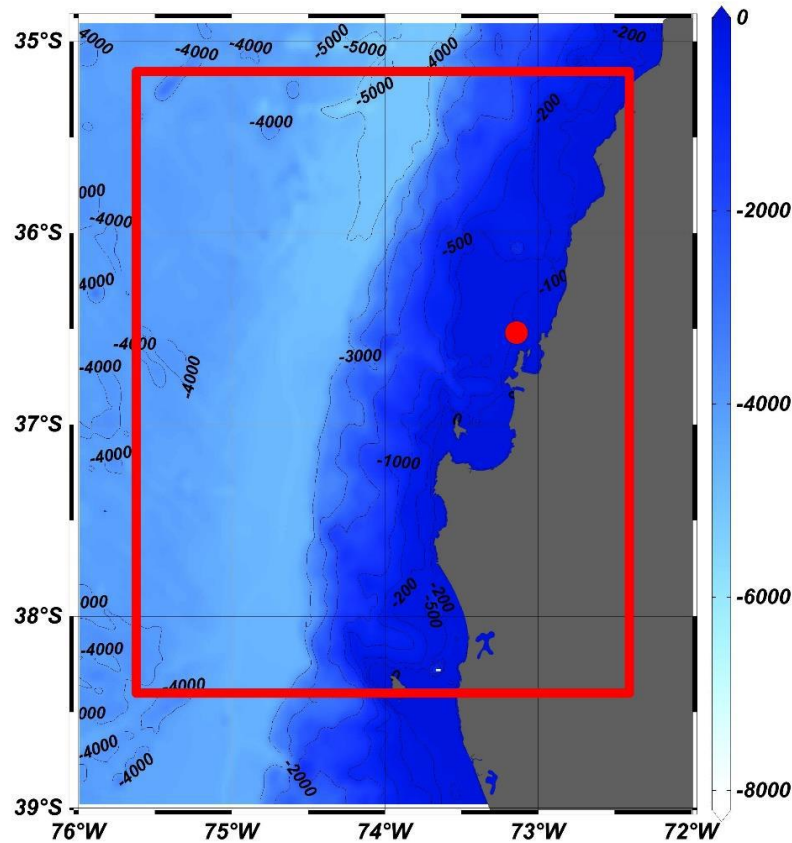


**Figura 1.** Área de estudio configuración del modelo, el círculo rojo representa ubicación de la estación 18.

Se utilizaron datos mensuales desde agosto de 2002 a diciembre de 2008 de la estación de monitoreo. Las variables utilizadas de la serie fueron, salinidad, temperatura, nutrientes (nitrato, fosfato, silicatos), clorofila, los cuales están dados para 9 profundidades (0, 5, 10, 15, 20, 30, 40, 50, 80 metros), se utilizó la biomasa del mesozoplancton integrada de 0 a 80 metros y las salidas de una configuración del modelo ROMS-PISCES desde agosto de 2002 hasta diciembre de 2008 con resolución horizontal  $1/12^\circ$  y resolución temporal 3 días. El modelo biogeoquímico PISCES (Pelagic Interactions Scheme for Carbon & Ecosystem Studies) (Aumont et al., 2015; Aumont &

Bopp, 2006) fue forzado por el modelo regional de circulación oceánica ROMS (Regional Ocean Modeling System) (Shchepetkin & McWilliams, 2005). ROMS es un modelo de ecuaciones primitivas hidrostáticas de superficie libre, seguimiento del terreno (sigma) y coordenadas curvilíneas. PISCES es un modelo biogeoquímico basado en tipos funcionales del plancton (Le Quéré et al., 2005), que simula los ciclos biogeoquímicos del carbono y los nutrientes primarios (nitrato, amonio, fosfato, silicato y hierro). El modelo simula dos clases de tamaño funcional de fitoplancton (nanofitoplancton y diatomeas) y zooplancton (micro- y mesozooplancton), así como detritus (células muertas y gránulos fecales). La síntesis de carbono por parte del fitoplancton depende de la luz, la temperatura y la disponibilidad externa de nutrientes

Para hacer coincidir el periodo de tiempo del modelo con los datos disponibles en la estación 18, se determinaron las fechas más cercanas a las fechas de muestreo y se construyó de esta forma una serie temporal similar a la serie de tiempo de la estación de monitoreo. Estos datos se interpolaron a las profundidades de las observaciones, es decir, 0, 5, 10, 15, 20, 30, 40, 50 y 80 metros y se verificaron las correlaciones entre las variables físicas, nutrientes y clorofila en 6 puntos del modelo cercanos a la ubicación geográfica de la estación 18 y con una profundidad similar, con los datos de correlación y se determinó el punto que mejor caracteriza a la estación 18 en cuanto a temperatura, salinidad y oxígeno y profundidad. En el trabajo de Escribano (2007) se muestra que la biomasa del zooplancton se correlaciona fuertemente con la profundidad de la ZMO y por lo cual el oxígeno es una variable ambiental crucial. Del total de datos obtenidos se utilizaron 80 datos de muestreos en variables físicas y nutrientes, correspondientes al total de fechas de las observaciones en el periodo indicado.

Se calculó la correlación y significancia de este punto con cada uno de los puntos del dominio en ventanas de tiempo de 5, 30 y 60 días y de esta forma poder determinar cuan representativo de la región es el punto seleccionado.

Una vez obtenida la serie de tiempo con el punto del dominio elegido se construyeron gráficos de profundidad de los datos simulados y observados, de los cuales se determinaron visualmente dos capas: una superficial de 0 a 20 metros representativa de la capa de mezcla y una capa profunda de 20 a 80 metros. En ambas capas se calcularon los promedios ponderados (observación y modelo) en 0-20 metros, 20-80 metros y 0-80 metros de las variables físicas y nutrientes y se determinó la correlación y desviaciones

estándar de la salinidad, temperatura, clorofila y nutrientes, con el objetivo de evaluar el desempeño del modelo.

De lo cual se determinó una concordancia en los ciclos y variaciones, pero con discrepancias evidentes en las magnitudes (ver tabla 1, 2, 2 y 4), en especial del oxígeno disuelto y la salinidad (ver tabla 2). Se consideró la capa de 0 a 20 metros como representante de la capa de mezcla en la cual ocurren la mayor parte de las interacciones biológicas. Se determinó que el modelo, representaba los ciclos estacionales de la estación 18 y se realizaron las climatologías y las series promedios en las profundidades de 0-20, 20-80 y 0-80 metros de cada una de las variables del modelo y la observación y análisis de correlación entre ambas bases de datos en cada capa definida.

	0-20m			20-80m			0-80m		
	R	P	Sesgo	R	P	Sesgo	R	P	Sesgo
Temperatura	0.57	0.05	0.77	0.8	0.00	0.49	0.57	0.05	0.52

**Tabla 1.** Valores R y P de correlaciones de los datos de la estación 18 y modelo para la temperatura y los sesgos entre ambas series de datos.

	0-20m			20-80m			0-80m		
	R	P	Sesgo	R	P	Sesgo	R	P	Sesgo
Salinidad	0.81	0.00	-0.24	0.73	0.00	-0.46	0.80	0.05	-0.36

**Tabla 2.** Valores R y P de correlaciones de los datos de la estación 18 y modelo para la salinidad y los sesgos entre ambas series de datos



	0-20m			20-80m			0-80m		
	R	P	Sesgo	R	P	Sesgo	R	P	Sesgo
Nitrato	0.07	0.83	-9.32	0.56	0.06	-10.29	0.36	0.24	-9.66

**Tabla 3.** Valores R y P de correlaciones de los datos de la estación 18 y modelo para el nitrato y los sesgos entre ambas series de datos.

	0-20m			20-80m			0-80m		
	R	P	Sesgo	R	P	Sesgo	R	P	Sesgo
Clorofila	0.79	0.00	-1.15	0.25	0.43	0.95	0.71	0.00	-0.28

**Tabla 4.** Valores R y P de correlaciones de los datos de la estación 18 y modelo para la clorofila y los sesgos entre ambas series de datos.

En cuanto a la biomasa del zooplancton se tienen un total de 73 muestreos de biomasa de mesozooplancton (>200 micras) desde 2002 a 2008, correspondientes a los datos disponibles en la observación. Se calculó la biomasa integrada para la observación y el modelo en el punto de grilla seleccionado anteriormente. Se determinaron los datos anómalos de la serie temporal y fueron eliminados para el análisis obteniendo finalmente 67 datos para la biomasa del mesozooplancton, se realizaron gráficos del total de datos y datos climatológicos con el objetivo de determinar si el modelo representa la variabilidad estacional.

Para evaluar que procesos tienen una mayor influencia se utilizó un balance de los aportes a los términos de la ecuación de evolución de mesozooplancton en el modelo ROMS-PISCES respetando el principio de conservación de masa y determinación de *lags* entre los flujos advectivos y producción biológica, con el fin de evaluar la concordancia entre los procesos.

Forzante	Respuesta	
Variable/ Proceso	Variable/ Proceso	Tiempo lag (días)
Flujo desde abajo, NO <sub>3</sub>	Flujo hacia el norte	2
Flujo desde abajo, NO <sub>3</sub>	Producción diatomeas	4
Flujo hacia el norte, diatomeas	Producción diatomeas	3
Flujo hacia el norte, diatomeas	Producción zooplancton	8
Producción diatomeas	Producción zooplancton	7
Flujo hacia el norte, diatomeas	Biomasa de diatomeas	20
Producción diatomeas	Biomasa de zooplancton	18
Flujo hacia el norte, diatomeas	Flujo hacia el norte, mesozoplancton	0

**Tabla 5.** Desfases temporales de los diferentes flujos y variables biológicas, obtenidas desde las ecuaciones del modelo.

Para el segundo objetivo se planteó un modelo NPZ (0D) según el esquema de Franks (2002), en el cual la respuesta funcional del zooplancton frente al fitoplancton está dada por una respuesta Holling IV, que permite determinar el efecto de las diatomeas tóxicas en el crecimiento del zooplancton, el sistema de ecuaciones planteados es:

$$\frac{dN}{dt} = a + \partial_p P + \partial_z Z + \frac{\mu \gamma P Z}{K_Z + P + \beta P^2} - \frac{rNP}{K_p + N}$$

$$\frac{dP}{dt} = \frac{rNP}{K_p + N} - \frac{\mu P Z}{K_Z + P + \beta P^2} - \partial_p P$$

$$\frac{dZ}{dt} = \frac{\varepsilon \mu P Z}{K_Z + P + \beta P^2} - \partial_z Z$$

Donde

- $r$ : Tasa de crecimiento máxima específica del fitoplancton.
- $K_z, K_p$ : Constante de saturación media para el zooplancton y el fitoplancton respectivamente.
- $\partial_z, \partial_p$ : Tasa de mortalidad del zooplancton y fitoplancton respectivamente.
- $\varepsilon$ : Eficiencia de asimilación del zooplancton.
- $\gamma$ : Fracción no asimilada por el zooplancton.
- $\beta$ : Parámetro inhibitorio del fitoplancton.
- $\mu$ : Tasa de crecimiento máxima específica del zooplancton.

Se hizo un análisis cualitativo de las ecuaciones diferenciales en el primer octante ( $N > 0, P > 0, Z > 0$ ) al ser la región de interés en procesos biológicos, se describió el comportamiento de las orbitas en cada plano (NZ, NP, PZ) y se determinó que no existían puntos de equilibrio finitos para el sistema descrito, además se realizó un análisis de comportamiento del sistema en tiempo infinito para lo cual se utilizó el teorema de compactificación de Poincaré.

Se compararon los resultados de una simulación de 60 días del modelo NPZ propuesto utilizando como condiciones iniciales los datos obtenidos de la serie de tiempo del modelo Roms-Pisces, con los datos obtenidos de la serie de tiempo “estación 18” y los datos de la simulación biogeoquímica-física obtenidas del modelo ROMS-PISCES, para lo cual se

utilizaron los datos de los meses de enero y febrero del año 2003 de la estación 18. De estos datos se extrajeron los correspondientes a nitratos y clorofila a 20 metros de profundidad como representativo de la capa de mezcla, además se consideró la biomasa del zooplancton en el mismo periodo indicado anteriormente y dividida por la profundidad de la muestra para obtener una serie de datos sin dimensión espacial.

La biomasa en el muestreo fue estimada en peso seco y luego se convirtió a  $\frac{mgC}{m^2}$  (Escribano et al., 2007). Para comparar con los datos simuladas en el modelo NPZ (0D) planteado los datos de biomasa del zooplancton y clorofila (como indicador de biomasa del fitoplancton) fueron convertidos a  $\frac{\mu gN}{L}$  utilizando la razón de Redfield, dado que el modelo ROMS-PISCES utiliza esta razón como constante a nivel global. Además se utilizó la misma serie de tiempo extraída del modelo ROMS-PISCES construida para el primer objetivo y para poder comparar con los datos obtenidos en el modelo propuestos se utilizaron los datos de biomasa del fitoplancton y zooplancton y nitrato a 20 metros de profundidad en  $\frac{\mu gN}{L}$ .

Se realizaron gráficos para comparar las tres series de datos, para nitrato, biomasa del fitoplancton y biomasa del zooplancton.

## Capítulo I:

“Understanding Seasonal Variability of Mesozooplankton Biomass in the Upwelling System of Central-Southern Chile: A Modelling Approach”

“Comprensión de la variabilidad estacional de la biomasa del mesozooplancton en el sistema de surgencia de Chile centro-sur: una aproximación con modelado”.

Progress in Oceanography 2023

## RESUMEN.

Comprender los mecanismos que influyen en la variabilidad de la biomasa de zooplancton en los sistemas de surgencia de borde oriental (EBUS) es un paso crítico en la estimación de la producción secundaria en el océano, particularmente en el contexto del modelado biogeoquímico y la evaluación de la productividad de estos ecosistemas. En este estudio, utilizamos una simulación retrospectiva físico-biogeoquímica (2002-2008) para investigar las fuentes de variabilidad estacional e interanual de la biomasa del mesozooplancton en la zona de surgencia del centro-sur de Chile.

Las observaciones mensuales fueron obtenidas desde una serie de tiempo oceanográfica realizada en la Estación 18 (36°30'S) frente a la costa de Concepción, Chile. El primer paso fue evaluar la coherencia entre los resultados del modelo y las observaciones de campo de las variables físicas y biogeoquímicas, incluyendo la biomasa del mesozooplancton.

Se midieron los factores que influyen en la variación en el volumen de biomasa en la Estación 18. En el modelo, los flujos advectivos a lo largo la costa y a través de la plataforma controlan la mayor parte de la biomasa. El efecto de advección parece ser más pronunciado durante la temporada de surgencias (primavera-verano austral) que en invierno, a pesar de esto la advección sigue contribuyendo significativamente a la variación de la biomasa.

Nuestro modelo físico-biogeoquímico ROMS-PISCES aplicado en este EBUS demostró que la advección a lo largo de la costa y a través de la plataforma juega un papel crucial en la variabilidad espacial y temporal de la biomasa del zooplancton en la zona de surgencia. Por lo tanto, es esencial considerar estos procesos físicos al interpretar observaciones de datos de series de tiempo de estaciones fijas.

Palabras clave: Biomasa de zooplancton, Modelización, Advección, Surgencia en Chile.



# Understanding seasonal variability of mesozooplankton biomass in the upwelling system of central-southern Chile: A modelling approach

Ana Venegas <sup>a, e</sup>, Pierre Amael-Auger <sup>b</sup>, Ruben Escribano <sup>c, e, \*</sup>, Carolina Parada <sup>d, e, f</sup>

<sup>a</sup> Doctoral Program in Oceanography, Department of Oceanography, Facultad de Ciencias Naturales y Oceanográficas, Universidad de Concepción, Concepción, Chile

<sup>b</sup> Laboratory for Ocean Physics and Remote Sensing, Institute of Research for Development (IRD), Marseille, France

<sup>c</sup> Departamento de Oceanografía, Universidad de Concepción, Chile

<sup>d</sup> Departamento de Geofísica, Universidad de Concepción, Chile

<sup>e</sup> Instituto Milenio de Oceanografía, Universidad de Concepción, Chile

<sup>f</sup> Center for Ecology and Sustainable Management of Oceanic Islands (ESMOI), Departamento de Biología Marina, Facultad de Ciencias del Mar, Universidad Católica del Norte, Coquimbo, Chile

## ARTICLE INFO

### Keywords:

Zooplankton biomass  
Modelling  
Advection  
Upwelling  
Chile

## ABSTRACT

Understanding the mechanisms that influence variability in zooplankton biomass in eastern boundary upwelling systems (EBUS) is a critical step in estimating secondary production in the ocean, particularly in the context of biogeochemical modelling and assessing ecosystem productivity. In this study, we utilised a physical-biogeochemical hindcast simulation (2002–2008) to investigate the sources of seasonal and interannual variability of mesozooplankton biomass within the upwelling zone of central-southern Chile. Monthly observations were obtained from an oceanographic time-series conducted at Station 18 (36°30'S) off the coast of Concepción, Chile. The first step was to assess the coherence between model outputs and field observations of physical and biogeochemical variables, including the biomass of mesozooplankton. The factors accounting for the variation in biomass at Station 18 were then assessed. In the model, advective flows along the shore and across the shelf control the majority of biomass. The advection effect appears to be more pronounced during the upwelling season (austral spring-summer) than in winter, although it still significantly contributes to biomass variation during the latter. Our physical-biogeochemical model ROMS-PISCES applied on this EBUS showed that alongshore and cross-shelf advection play a crucial role in driving spatial and temporal variability in zooplankton biomass within the upwelling zone. Therefore, it is essential to consider these physical processes when interpreting observational data from fixed time series stations.

## 1. Introduction

Zooplankton dynamics in the ocean play a crucial role in the carbon cycle and the production of various fish species that are exploited and maintain large fisheries (Pauly et al., 2002). Therefore, changes in the biomass and production of zooplankton are considered critical factors in predicting the future reactions of marine systems to global warming (Beaugrand et al., 2003; Richardson and Schoeman, 2004; Hays et al., 2005).

Temperature (Peterson et al., 2006; Escribano et al., 2014), stratification and oxygenation (Seibel, 2011), as well as food quantity and quality (Vargas et al., 2006; Vargas et al., 2010), have all been found to be associated with zooplankton biomass and production. Large-scale processes, such as global warming (Beaugrand, 2003; McGowan et al.,

2003) and the Pacific decadal oscillation (PDO) (Medellín-Mora et al., 2019), can have a significant impact on the biomass and production of zooplankton. To comprehend the dynamics of zooplankton, it is crucial to focus on zooplankton production as the primary factor driving biomass variation. Therefore, it is imperative to study the mechanisms that control zooplankton growth from an ecological perspective. In this regard, there has been a long-standing debate about whether food sources or temperature are the primary drivers for zooplankton growth (Huntley and Boyd, 1984; Hirst and Bunker, 2003). However, there is agreement that variation in zooplankton biomass must ultimately be governed by a combination of top-down and bottom-up processes (Smocker and Hernández-León, 2013).

The dynamics of zooplankton biomass are highly relevant in highly productive marine regions, such as eastern boundary upwelling systems

\* Corresponding author at: Instituto Milenio de Oceanografía, Universidad de Concepción, Chile.

E-mail address: [rescribano@udec.cl](mailto:rescribano@udec.cl) (R. Escribano).

<https://doi.org/10.1016/j.pocean.2023.103193>

Received 24 April 2023; Received in revised form 14 December 2023; Accepted 14 December 2023  
0079-6611/© 20XX

(EBUS), in which fishery production supports the economies of bordering countries (Mann and Lazier, 1991; Pauly, 2002). Despite its importance, the productivity of zooplankton and the factors that control it have rarely been addressed in studies focused on the dynamics of EBUS (Escribano et al., 2016; Medellín-Mora et al., 2019). Many questions remain regarding the driving forces that affect its seasonal and interannual variability.

The central-southern upwelling region of Chile (30–40° S) is one of the most highly productive EBUS in the world's ocean, exhibiting at times levels of primary production  $> 10 \text{ g C m}^{-2} \text{ d}^{-1}$  (Montero et al., 2007). This region experiences a highly seasonal upwelling regime that intensifies during the austral spring-summer (October–March) and significantly decreases throughout the autumn–winter (May–September) (Sobarzo et al., 2007). During the spring-summer season, primary production increases to  $10\text{--}20 \text{ g C m}^{-2} \text{ d}^{-1}$  (Montero et al., 2007), sustaining a high fishery production based on pelagic and demersal fish species (Arcos et al., 2001; Escribano and Schneider, 2007). In this region, the zooplankton dynamics are strongly associated with the variability of coastal upwelling, which is driven by alongshore winds blowing towards the equator (Riquelme-Bugueño et al., 2013; Escribano et al., 2007). However, the mechanisms involved in this process are unclear. For instance, it is known that upwelling can enhance advection and mesoscale activity in the coastal zone (Hormazábal et al., 2013), which in turn creates an unstable and advective environment that zooplankton must adapt to (Peterson, 1998; Escribano et al., 2016). The outcome of the interaction between advective forces and zooplankton biomass is uncertain, which is a critical issue in the context of rising upwelling intensity at high latitudes in EBUSs (Garreaud and Falvelly, 2009; Wang et al., 2015; Rykaczewski et al., 2015; Xiu et al., 2018). In this context, the upwelling zone in central-southern Chile may serve as a suitable natural laboratory for evaluating the effects of biological and physical factors that control the variability of zooplankton biomass and production.

In this region, an oceanographic time series investigation was conducted over the continental shelf in central southern Chile, at the fixed Station 18 (36° 30'S) starting in August 2002. This monthly time series includes mesozooplankton sampling, resulting in a significant database on the variations of mesozooplankton biomass and their environment. To identify the key processes driving the temporal dynamics of observed variations, we used a numerical modelling approach. Other studies conducted in the south-eastern Pacific EBUS have used the same physical-biogeochemical modelling tools to investigate the mechanisms responsible for the spatial–temporal fluctuations in phytoplankton productivity and dissolved oxygen levels (e.g. Vergara et al., 2017; Espinoza-Morriberon et al., 2016; Echevin et al., 2014; Montes et al., 2014). However, no study has been conducted on the dynamics of zooplankton. Here, the biogeochemical model Pelagic Interactions Scheme for Carbon and Ecosystem Studies (PISCES) developed by Aumont et al. (2015) is used. A model coupled with the regional ocean circulation Regional Ocean Modeling System (ROMS) (Shchepetkin and McWilliams, 2005) was used to investigate the influence of horizontal advection, recirculation processes and local production on regulating the seasonal variation of zooplankton biomass in the upwelling zone off central-southern Chile. This modelling approach aims to assess the influence of advective processes in causing variation in zooplankton biomass in the upwelling zone and test the hypothesis that zooplankton dispersion driven by alongshore and cross-shelf advection can negatively impact the biomass and secondary production in the coastal zone off central-southern Chile.

## 2. Methods

### 2.1. Field data

We used oceanographic data from a time series study that commenced in August 2002 at Station 18 (36°30.80'S and 73°07.75'W), a

location situated about 30 km away from the coast at a bottom depth of 90 m (Fig. 1). A monthly sampling strategy provided us with data to assess hydrographically (Sobarzo et al., 2007; Schneider et al., 2016), biogeochemical and biological variables (phytoplankton and zooplankton) across intra-seasonal, seasonal and interannual time scales (Escribano and Schneider, 2007; Escribano and Morales, 2012). Each month, 2–3 casts measuring temperature, salinity, and dissolved oxygen (CTDO) were conducted on a single day, usually in mid-month. These measurements were taken using an autonomous Seabird SBE-25 CTDO device, which was coupled with a 12-bottle Rosette system for collecting water samples. Water samples were collected at nine different depths to determine salinity, nutrient levels (including nitrate, phosphate, and silicate), chlorophyll-a (chl-a) concentrations and dissolved oxygen levels. Schneider et al. (2016) and Anabalón et al. (2016) provide details for all these measurements. During each sampling event, either one or two zooplankton tows were also carried out with a 1 m<sup>2</sup> Tucker trawl net equipped with three 200 µm mesh-size nets and a General Oceanics calibrated flowmeter for depth-stratified sampling, such that three strata were sampled, 0–80 m, 80–50 m and 50–0 m. In this investigation, integrated samples (0–80 m) were used, and biomass was estimated based on dry weight and then converted to  $\text{mg C m}^{-2}$ . Briefly, the sample was split in two using a Motoda Splitter and then a half was dried at 60 °C for 24 h. From the dried sample a fraction was used for organic C measurement by elemental analysis CHN, so that C could be estimated for the bulk of zooplankton biomass and then standardized to  $\text{mg C m}^{-3}$  using the filtered volume by the net with the flowmeter data (further details are in Escribano et al., 2007).

### 2.2. Physical-biogeochemical model

Our modelling approach was based on a three-dimensional physical-biogeochemical hindcast simulation with an eddy-resolving resolution of  $1/12^\circ$  (~7–9 km). The PISCES biogeochemical model (Aumont et al., 2015; Aumont and Bopp, 2006) was driven by the ROMS regional ocean circulation model (Shchepetkin and McWilliams, 2005). ROMS is a free-surface, terrain-following (sigma) and curvilinear coordinates, hydrostatic, and primitive equations model. PISCES is a biogeochemical model that is based on plankton functional types (Le Quééré et al., 2005). It simulates the biogeochemical cycles of carbon and primary nutrients, including nitrate, ammonium, phosphate, silicate, and iron. The model simulates two functional size classes of phytoplankton (nanophytoplankton and diatoms) and zooplankton (micro- and mesozooplankton), as well as detritus (dead cells and faecal pellets). Light, temperature and external nutrient availability all influence the synthesis of carbon by phytoplankton. Diatoms differ from nanophytoplankton in their silicate requirements, a higher requirement in DFe (Sunda and Huntsman, 1997) and higher half-saturation constants due to their smaller surface-to-volume ratio. Predation preferences (connected to the prey/predator size ratio), grazing rates and mortality parameterisation distinguish microzooplankton from mesozooplankton. Small and large particulate organic detritus differ only in their sinking velocity (5 and 30 m a day, respectively). PISCES has been widely used on a global scale (e.g. Aumont et al., 2015; Aumont & Bopp, 2006; Gorgues et al., 2010), at the basin scale (e.g. Gorgues et al., 2005) and in regional upwelling studies (e.g. Albert et al., 2010; Auger et al., 2015, 2016; Echevin et al., 2008; Vergara et al., 2017). A schematic representation of the structure of ROMS-PISCES model is shown in Fig. S1 (Supp. Mat.).

The model domain extended horizontally from 12°N to 41°S and from the coast to 95°W, with lateral open boundaries to the north, south and west, while the vertical grid consisted of 32 levels. Model outputs were available from January 2002 to December 2008 at a 3-day frequency, although for our simulations and biomass budget estimates, we used outputs from August 2002 to December 2008, which coincided with our time series data.



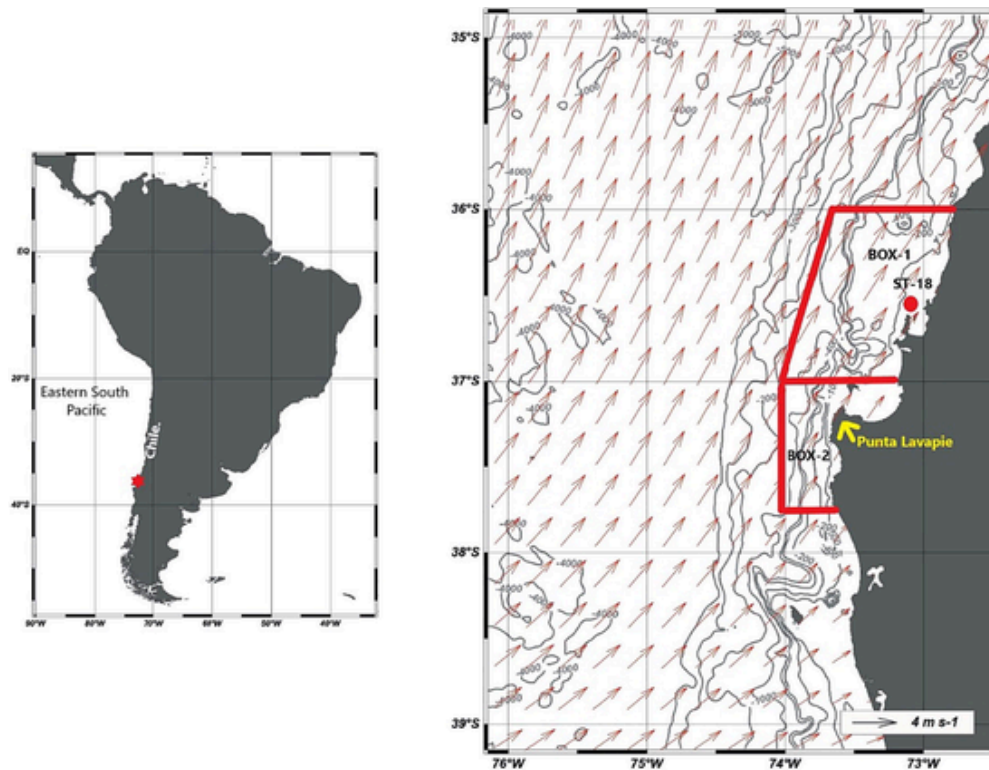


Fig. 1. The coastal upwelling zone off central-southern Chile in the southeast Pacific, illustrating the location of Station 18 (St-18) and the spatial boundaries of the analysis domain of the ROMS-PISCES hindcast simulation (see Section 2.2). Box 1 and Box 2 were areas defined to assess model performance. Vectors show the average geostrophic currents during the period 2002–2008 from satellite data available at the NOAA (<http://apdrc.soest.hawaii.edu/>).

### 2.3. Statistical analyses and model performance

To compare model and *in situ* data, physical (temperature and salinity) and biogeochemical (nitrate, phosphate, silicate, chlorophyll-a and oxygen) model variables were interpolated at the sampling depths of the *in-situ* data time series (0, 5, 10, 15, 20, 30, 40, 50, 80). Mesozooplankton biomass was integrated throughout the water column (0–80 m). The model data was used to determine the closest dates to the samplings at Station 18, resulting in a sample size of 67 months for zooplankton and 80 hydrographic casts from August 2002 to December 2008.

Model outputs were compared to *in situ* data, both visually and statistically. For the statistical comparison, we considered two depth layers based on the observed vertical structure of the water column at Station 18: the upper layer (0–20 m) and the deeper layer (20–80 m). The upper layer had a warmer and more homogeneous temperature during the spring-summer season, while the deeper layer had colder and more stable conditions year-round. Each variable was then vertically averaged across each layer in both the modelled and observed data. The mean deviation (biases) and correlation between simulated and observed time series for all physical and biogeochemical variables were estimated using Pearson correlation for time series data and Student's *t*-test comparisons for the mean values of two vertical layers.

### 2.4. Model diagnostics

To determine the factors that regulate the ecosystem dynamics at Station 18, we conducted budgets for nitrate (the primary limiting nutrient), diatom (assumed as the primary prey for mesozooplankton) and mesozooplankton biomass (in carbon for plankton) within a coastal box centred around Station 18 (Box 1 in Fig. 1). This box was defined from the coast to 0.6° offshore (ca. 70 km) in the zonal direction, ranging from 36°S to 37°S in the meridional direction (36°–37° S), and extends

vertically from the free surface down to 80 m. Advective (currents) and diffusive (turbulent mixing) fluxes of nitrate ( $\text{mmol m}^{-2} \text{s}^{-1}$ ), diatom and mesozooplankton biomass ( $\mu\text{g C m}^{-2} \text{s}^{-1}$ ) were averaged over each edge of the box: the southern and northern boundaries for alongshore fluxes, the western boundary for cross-shelf fluxes and the bottom boundary for vertical fluxes. Net biological fluxes (biological source minus sink) were also computed to offer an integrated view of the biological source and sink terms of nitrate, diatom and mesozooplankton biomass ( $\text{mg C m}^{-2} \text{s}^{-1}$ ). The respective contributions of advective and/or diffusive transport at the box boundaries, as well as the net biological rate, can be assessed. Concentrations of nitrate ( $\text{mol m}^{-3}$ ), diatom biomass and mesozooplankton biomass ( $\mu\text{g C m}^{-3}$ ) were also averaged within the box. The calculations were performed at each model time step, which occurred every three days. A daily seasonal climatology was then determined by interpolating the 3-day time series to obtain daily values. Since the main advective flux originates from the southern area of the study zone (see Fig. 1), we defined the second modelling Box-2, southern Station 18 (Fig. 1). The budget of mesozooplankton biomass from Box-1 was thus compared to the biomass budget from Box-2 (both shown Fig. 1). This analysis, based on model outputs, allowed us to quantify in relative terms the effects of advective fluxes on the variation of zooplankton biomass within our defined modelling Box-1.

Model diagnostics were also assessed through spatial autocorrelation, which was defined for each grid point as the temporal correlation between the time series at that grid point and the time series at Station 18. This estimate was made to determine the extent to which Station 18 represents the variability in biological processes across the upwelling region. For this purpose, spatial autocorrelation was calculated separately for diatoms, estimated in terms of chl-a concentration and mesozooplankton biomass in the 0–20 m and 0–80 m strata, respectively.

### 3. Results

#### 3.1. Model performance

##### 3.1.1. Seasonal cycle

Monthly climatological data based on CTD casts revealed a pronounced/clear seasonality in oceanographic conditions at station 18 during the time series data. The upward movement of cold water from the subsurface caused by coastal upwelling was observed to reach its peak in late winter/spring (August-December) and gradually decrease over the summer (December-March) (Fig. 2a). In late spring/summer (November-March), a surface temperature maximum is distributed over the first 10 m. However, during autumn (April-June), the water column gets mixed, resulting in a maximum mixed-layer depth of 50 m in early winter (June) (Fig. 2a). The seasonality depicted in Fig. 2B appears to be well-reproduced by the model. However, the maximum summer surface temperature generally extends deeper into the water column

(20–30 m). Consequently, when comparing the seasonal cycle of modelled and observed data for different layers (Fig. 2C, Fig. 2D and Fig. 2E), it is evident that the model overestimates the temperature for both the 0–20 m and 20–80 m depths during most of the upwelling phase (spring-summer). By contrast, the modelled data fits well with *in situ* observations during autumn–winter, especially for the 0–80 m layer (Fig. 2C), with a modest underestimation in the 0–20 m layer in September (Fig. 2D) and an overestimation in the 20–80 m layer from late winter through the spring-summer (Fig. 2E). Despite deviations between modelled and observed data, there was a significant correlation in the seasonal temperature variability across the three layers (Table 1).

Based on climatological data, the lowest salinities (< 30 PSU) were observed in the near-surface layer at station 18 during winter (June-August), (Fig. 3A). This was associated with river runoff and rainy conditions in winter (June-August), then increased towards summer (December-March) (near-surface salinity > 34 PSU), which was linked to the upwelling of Equatorial Subsurface Water (ESSW). The model re-

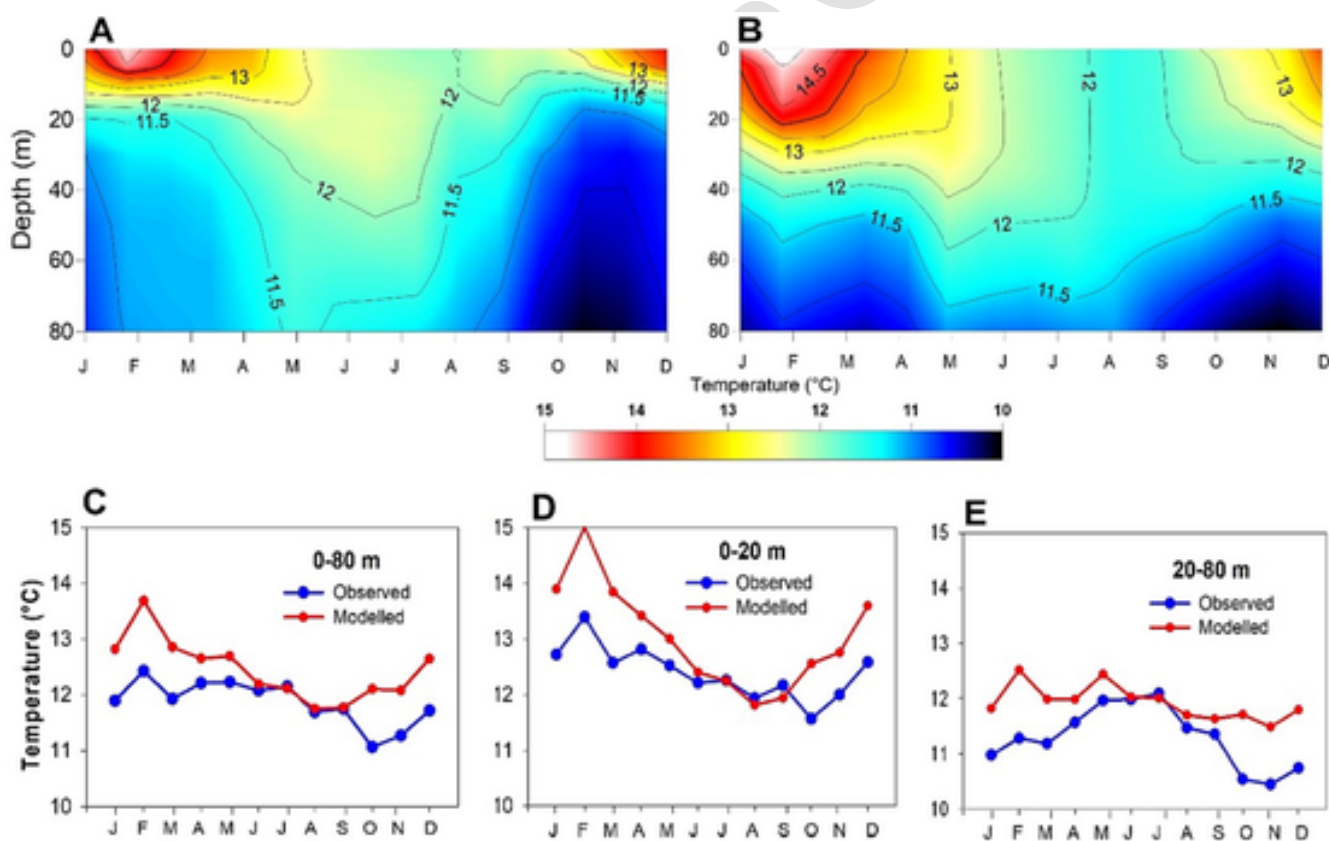


Fig. 2. Mean annual cycle (monthly climatology) of temperature (°C) at Station 18 obtained from monthly time series covering the 2002–2008 period: observed data from CTD casts (A) and model data (B). From the same climatological data, the mean temperatures were derived for the 0–80 m layer (C), the 0–20 m layer (D) and the 50–80 m layer (E).

Table 1

Pearson correlation analysis between observed and modelled mean values (climatological data) of hydrographic and biogeochemical variables at Station 18. This is based on monthly climatologies based on monthly observation and model data time series between 2002 and 2008. Mean values are for three vertical layers. R = Pearson correlation coefficient, P = probability, Bias = deviation of the modelled means to observed ones. ZooB = zooplankton biomass.

Variable	0–20 m			20–80 m			0–80 m		
	R	P	Bias	R	P	Bias	R	P	Bias
Temp. (°)	0.57	0.05	+0.77	0.80	<0.01	+0.49	0.57	0.05	+0.52
Salinity (Psu)	0.81	<0.01	–0.24	0.73	<0.01	–0.46	0.80	0.05	–0.36
Oxygen (mL L <sup>-1</sup> )	0.81	>0.05	+2.38	0.68	>0.05	+3.51	0.62	<0.05	–3.10
chl-a (mg m <sup>-3</sup> )	0.79	<0.01	1.15	0.25	0.43	+0.95	0.71	<0.01	–0.28
NO <sub>3</sub> (mm m <sup>-3</sup> )	0.07	0.83	–9.32	0.56	0.06	–10.29	0.36	0.24	–9.66
ZooB (mg C/m <sup>-2</sup> (- -))							0.23	0.48	+78.26

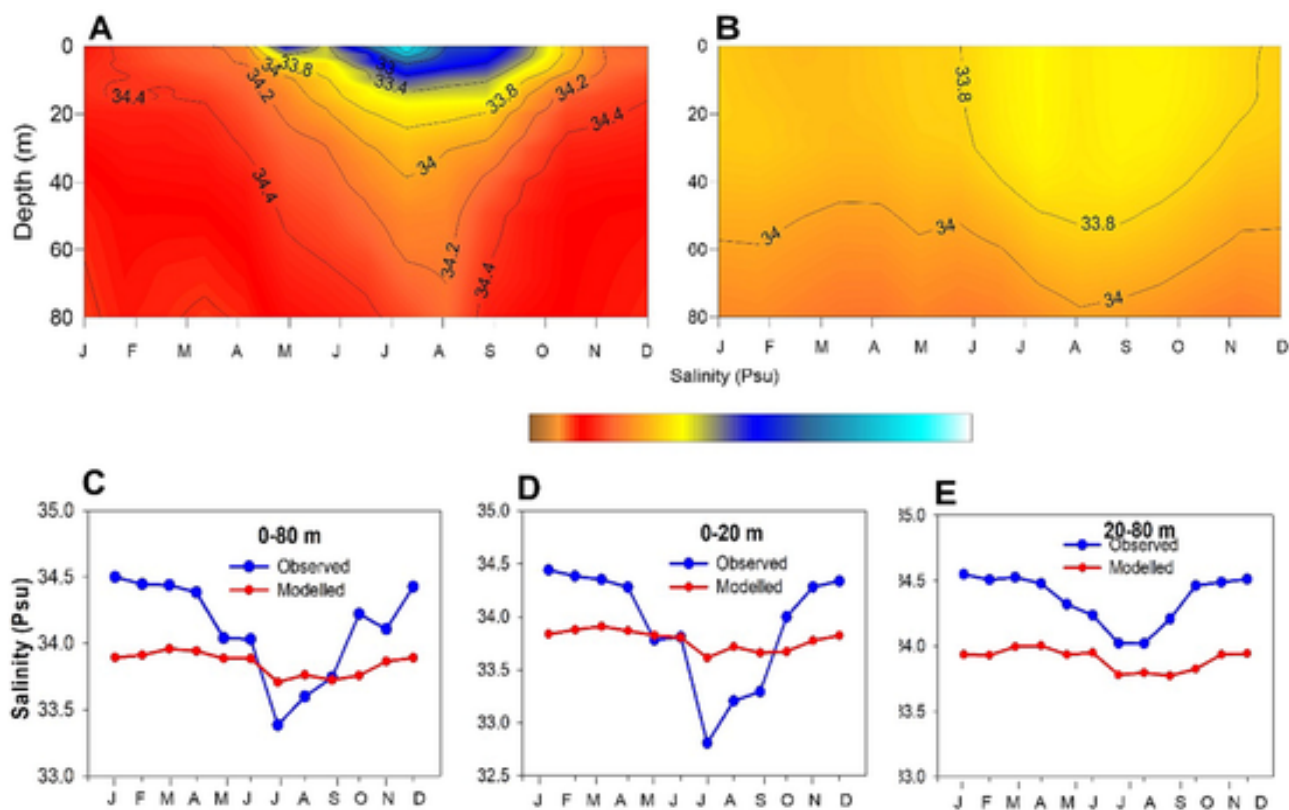


Fig. 3. Mean annual cycle (monthly climatology) of salinity (Psu) at Station 18 obtained from monthly time series covering the 2002–2008 period: observed data from CTD casts (A) and model data (B). From the same climatological data, the mean salinities were derived for the 0–80 m layer (C), the 0–20 m layer (D) and the 50–80 m layer (E).

produces this seasonal pattern, albeit with a significantly lower amplitude (Fig. 3B). The model strongly overestimates the salinity in the upper 20 m during winter (Fig. 3D). Moreover, salinity appears to be substantially underestimated throughout the water column during the summer (Fig. 3C) and below a depth of 20 m throughout the year (Fig. 3E). Correlations between modelled and observed mean values are significant for all three layers, as they are for temperature (Table 1).

Regarding oxygen concentrations (Fig. 4), the seasonal pattern was clearly marked by the ascent of the oxycline and the oxygen minimum zone (OMZ,  $<1 \text{ mL O}_2 \text{ L}^{-1}$ ) every year during the upwelling season (spring-summer) (Fig. 4A). The model appears to replicate the seasonal pattern effectively (Fig. 4B), although oxygen levels appear to be considerably overestimated and the presence and ascent of the OMZ are not reflected in the modelled data (Fig. 4B). The model overestimates oxygen concentration at all vertical levels due to a lack of representation of seasonal variation in the OMZ distribution (Fig. 4C, Fig. 4D and Fig. 4E). This considerable disparity between the modelled and observed data is also reflected in the absence of a significant correlation between mean values in the upper 20 m and the layer below 20 m, even though monthly means appear to be correlated when the whole water column was considered (Table 1).

The observed climatological data from the time series of chlorophyll-*a* concentration (chl-*a*), which serves as a proxy for phytoplankton biomass, shows a strong seasonal pattern. This pattern is characterised by an intense bloom of phytoplankton that emerges in early summer and mostly occupies the upper 20 m and greatly diminished chl-*a* ( $<1 \text{ mg m}^{-3}$ ) during the winter (Fig. 5A). The model appears to capture this seasonal pattern accurately, but with a lower amplitude (Fig. 5B). Nonetheless, there are important differences in the estimates of chl-*a* throughout the annual cycle. For instance, when considering vertical layers, it can be shown that the modelled data underestimate values during the spring-summer season in the whole water column

(Fig. 5C) and in the upper 20 m (Fig. 5D). On the other hand, overestimated values are found for most of the year below 20 m (Fig. 5E). Indeed, the mean values in the deep layer ( $>20 \text{ m}$ ) are uncorrelated, whereas significant correlations are found in the monthly means of the upper 20 m and the entire water column (Table 1).

The seasonal patterns of nitrate, phosphate and silicate observed at Station 18 are accurately reflected in the model outcomes, although the macronutrient concentrations are generally underestimated, as shown in Fig. S1, Fig. S2 and Fig. S3 (Supplemental Material). There is a significant correlation between average concentrations of phosphate and silicate in both the modelled and observed data ( $R = 0.87$ ,  $p < 0.01$  and  $R = 0.51$ ,  $p < 0.01$ , respectively) for the whole water column (0–80 m). However, for nitrate, this correlation is non-significant for both the 0–20 m layer and the entire 0–80 m layer (Table 1).

The mean seasonal cycle of zooplankton biomass, as derived from a monthly climatology, is unclear and appears to be only partially related to seasonal upwelling (Fig. 6). The highest biomass is generally found in the spring/summer (September–January), while the lowest values are found in the autumn/winter (February–August), with a minimum in June. However, a peak in biomass is typically observed in mid-autumn (May), although there is significant interannual variability. In fact, except during the winter, high interannual variability blurs the seasonal cycle. The seasonal pattern and high interannual variability appear well-reproduced by the model, although there is greater interannual variability in May, which corresponds with the above-mentioned peak in biomass. There is strong variation within and among months in both the observed and modelled data. However, the non-parametric ranking test Kruskal-Wallis indicated that both series did not differ to each other ( $p > 0.05$ ).

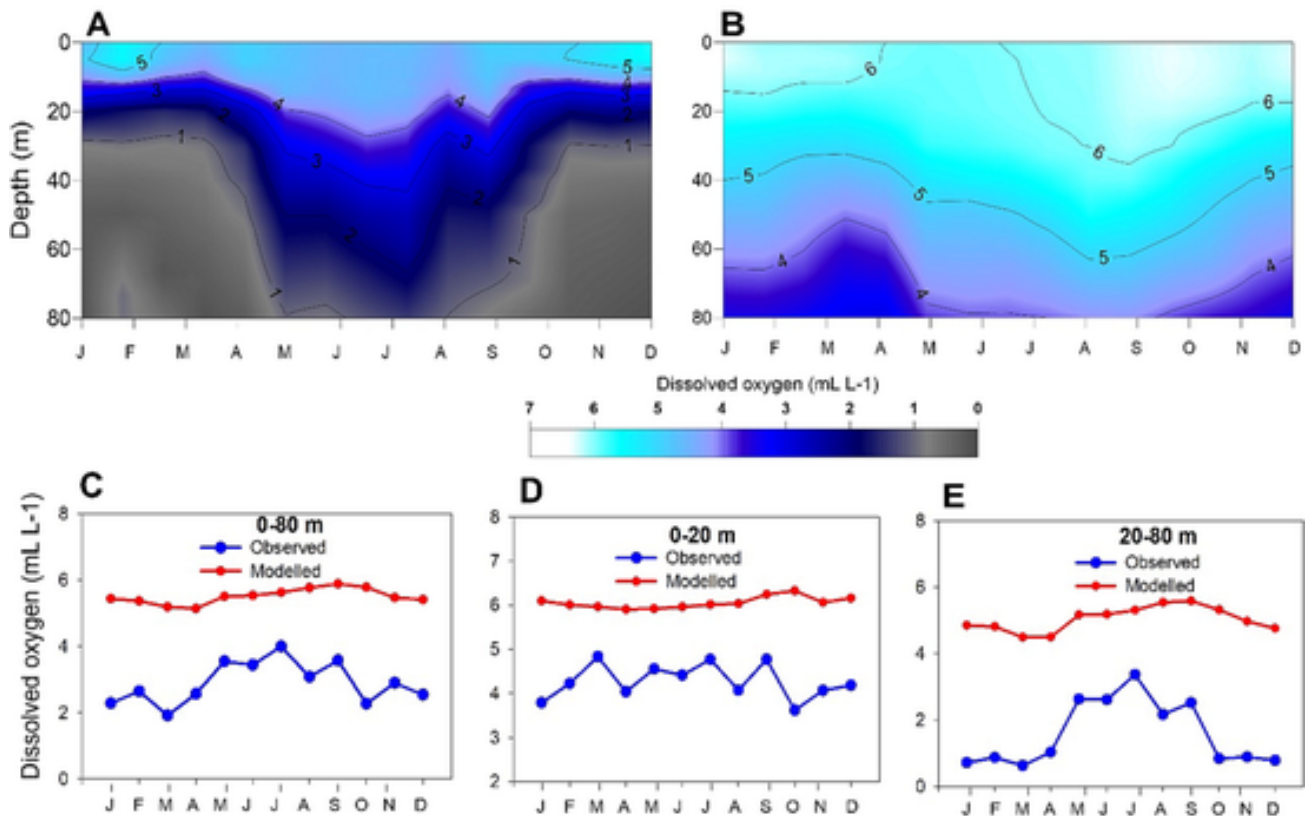


Fig. 4. Mean annual cycle (monthly climatology) of dissolved oxygen ( $\text{mL L}^{-1}$ ) at Station 18, obtained from monthly time series covering the 2002–2008 period: observed data from CTD casts (A) and model data (B). From the same climatological data, the mean concentrations of oxygen were derived for the 0–80 m layer (C), the 0–20 m layer (D) and the 50–80 m layer (E).

### 3.1.2. Interannual variability

The interannual variability of physical, chemical, and biological data was investigated by examining the complete monthly time series for both observed and modelled data. Strong year-to-year variations were observed in the seasonal upwelling cycle, as indicated by the *in situ* temperature. For example, there was strong near-surface warming during the summers of 2003 and 2005, while the winter of 2007 was considerably cooler (Fig. 7A). These interannual patterns are in general terms reproduced by the model (Fig. 7B), although in some years model outputs overestimate near surface warming during the summer, such as in 2002 and 2007. The average simulated temperature is slightly higher ( $<1^\circ\text{C}$  on average) in the upper 20 m, whereas slight positive deviations ( $<0.5^\circ\text{C}$ ) are recorded below 20 m (Table 2). These deviations are all statistically significant, according to the *t*-test (Table 2).

Regarding salinity, *in situ* data demonstrate that the seasonal upwelling is reflected each year by the ascent of high salinity water ( $>34.5$ ), which can penetrate the near-surface layer mostly during summertime (Fig. 7C). This pattern, however, fluctuated from year to year, revealing changes in upwelling intensity. For example, in 2002–2003, upwelling was substantially stronger than in previous years, whereas, in the summer of 2006–2007, upwelling was much weaker (Fig. 7C). In addition, low-salinity water was found near the surface due to winter-time rainfall and freshwater runoff from rivers, although there was interannual variation. For instance, the winters of 2005 and 2006 received more rainfall than other years (Fig. 7C). All these interannual patterns are not well represented in the simulated data (Fig. 7D), which exhibits lower salinity values below the mixed layer and does not accurately reflect the winter conditions. Positive deviations in subsurface water ( $>20\text{ m}$ ) and negative deviations in the mixed layer were found to be highly significant when comparing observed and simulated data (Table 2).

The time series of *in situ* dissolved oxygen shows interannual variability, which is characterised by the ascent of oxygen-depleted water ( $<1\text{ mL O}_2\text{ L}^{-1}$ ), coinciding with the spring-summer upwelling period every year, following a similar pattern to that of temperature (Fig. 8A). The upper boundary of the OMZ ( $<1\text{ mL O}_2\text{ L}^{-1}$ ) can intrude on the upper 30 m during summertime in all years sampled. By contrast, the model simulation clearly overestimates the oxygen concentration, causing the OMZ to not appear within the 0–80 m water column, despite representing the spring-summer ascent of low-oxygen water (Fig. 8B). These positive deviations of  $>2\text{ mL O}_2\text{ L}^{-1}$  in the upper 20 m and  $>3.5\text{ mL O}_2\text{ L}^{-1}$  below 20 m between the observed and modelled data are highly significant (Table 2).

Interannual variability in phytoplankton biomass revealed a strong spring-summer bloom, with chl-*a* appearing aggregated in the upper 30 m during this period, reaching values of  $>30\text{ mg chl-}a\text{ m}^{-3}$  (Fig. 8C). The intensity of spring-summer blooms exhibited some interannual variability that seems to be accurately replicated by modelled data. However, peaks in chl-*a* are slightly less intense and underestimated by the model. These deviations of model estimates from observed values are thus non-significant within the upper 20 m during the summer blooms (Fig. 8D) (Table 2).

The complete monthly time series of zooplankton biomass for both observed and modelled data is displayed in Fig. 9A. This shows that the model can reproduce some patterns of interannual variability that were reported by *in situ* data, especially at the beginning of the study period (before 2007). However, the apparent decreasing trend observed over the study period is not reproduced by the model, as illustrated by negative deviations during the first three years and positive deviations thereafter (Fig. 9B).

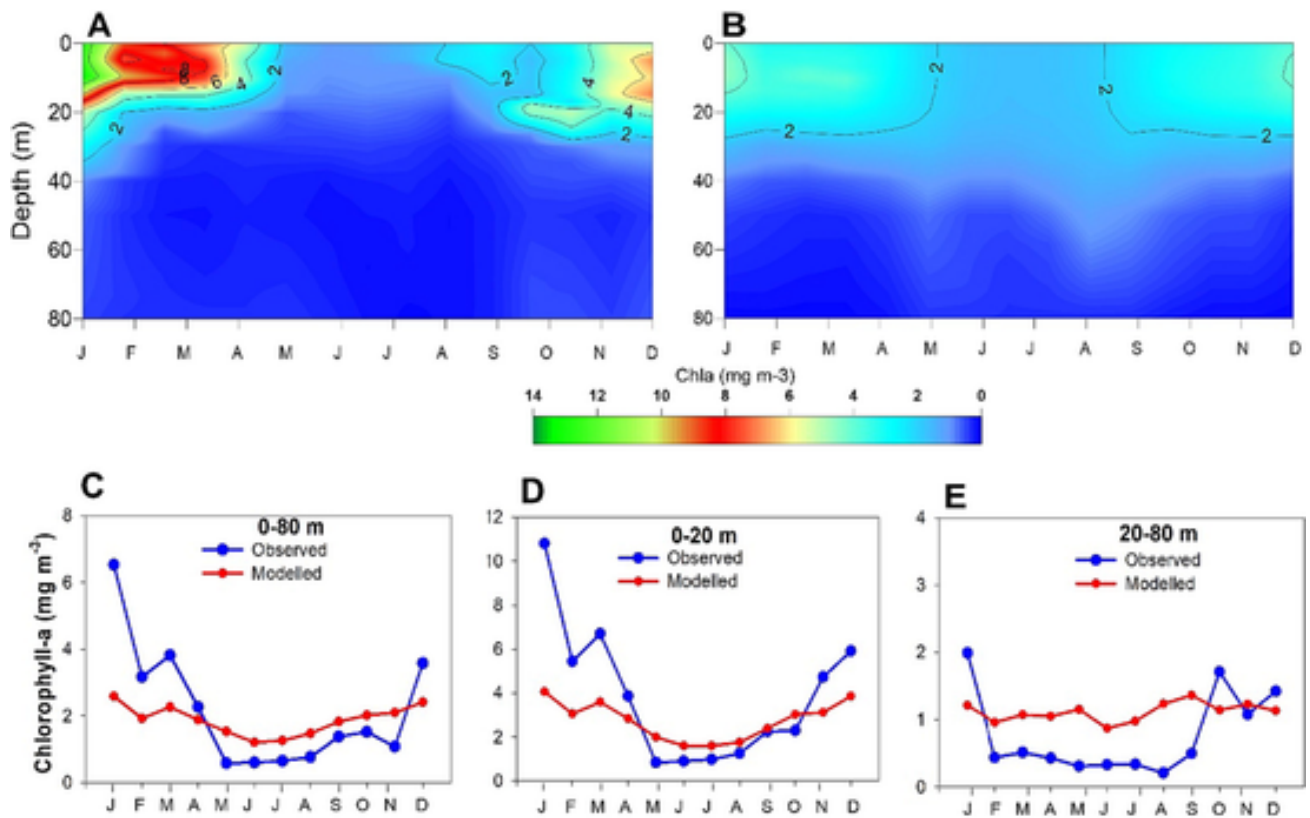


Fig. 5. Mean annual cycle (monthly climatology) of chlorophyll-a ( $\text{mg Chl m}^{-3}$ ) at Station 18, obtained from monthly time series covering the 2002–2008 period: observed data from CTD casts (A) and model data (B). From the same climatological data, the mean chlorophyll-a concentrations were derived for the 0–80 m layer (C), the 0–20 m layer (D) and the 50–80 m layer (E).

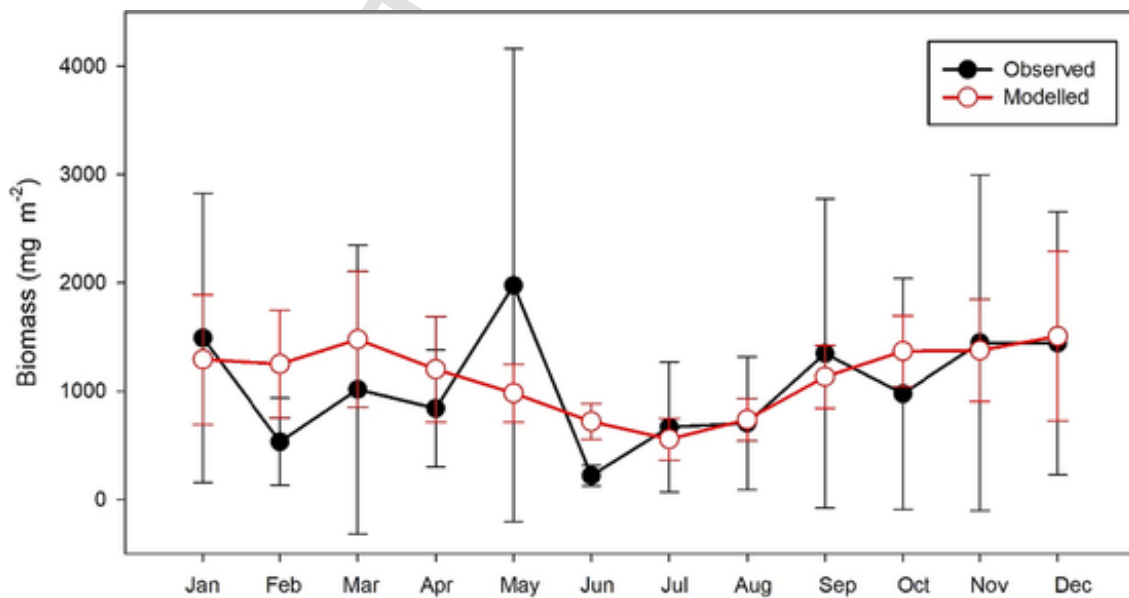


Fig. 6. Mean annual cycle (monthly climatology) of depth-integrated (0–80 m) zooplankton biomass at Station 18 from a monthly time series covering the 2002–2008 period of *in situ* (filled circles) and model estimates (open circles). The vertical bars indicate the standard deviation.

### 3.2. Zooplankton biomass variation and budget

Fig. 10 shows the seasonal cycles of the source and sink terms (i.e. advective and diffusive tracer fluxes and net biological flux) for nitrate, diatom and mesozooplankton budgets in the coastal box surrounding Station 18 (see Section 2.4). The net biological flux represents the actual estimates of nitrate, diatoms, and zooplankton bio-

mass. These advective and diffusive fluxes represent model outputs from PISCES-ROMS simulations for the entire study period (2002–2008) after a budget for the modelled box-1 shown in Fig. 1 in a common unit for diatoms and zooplankton biomass ( $\text{mg C s}^{-1}$ ). Note that diffusion, i.e. horizontal and vertical mixing, has negligible effects on nitrate concentration and plankton biomass when compared to advection.

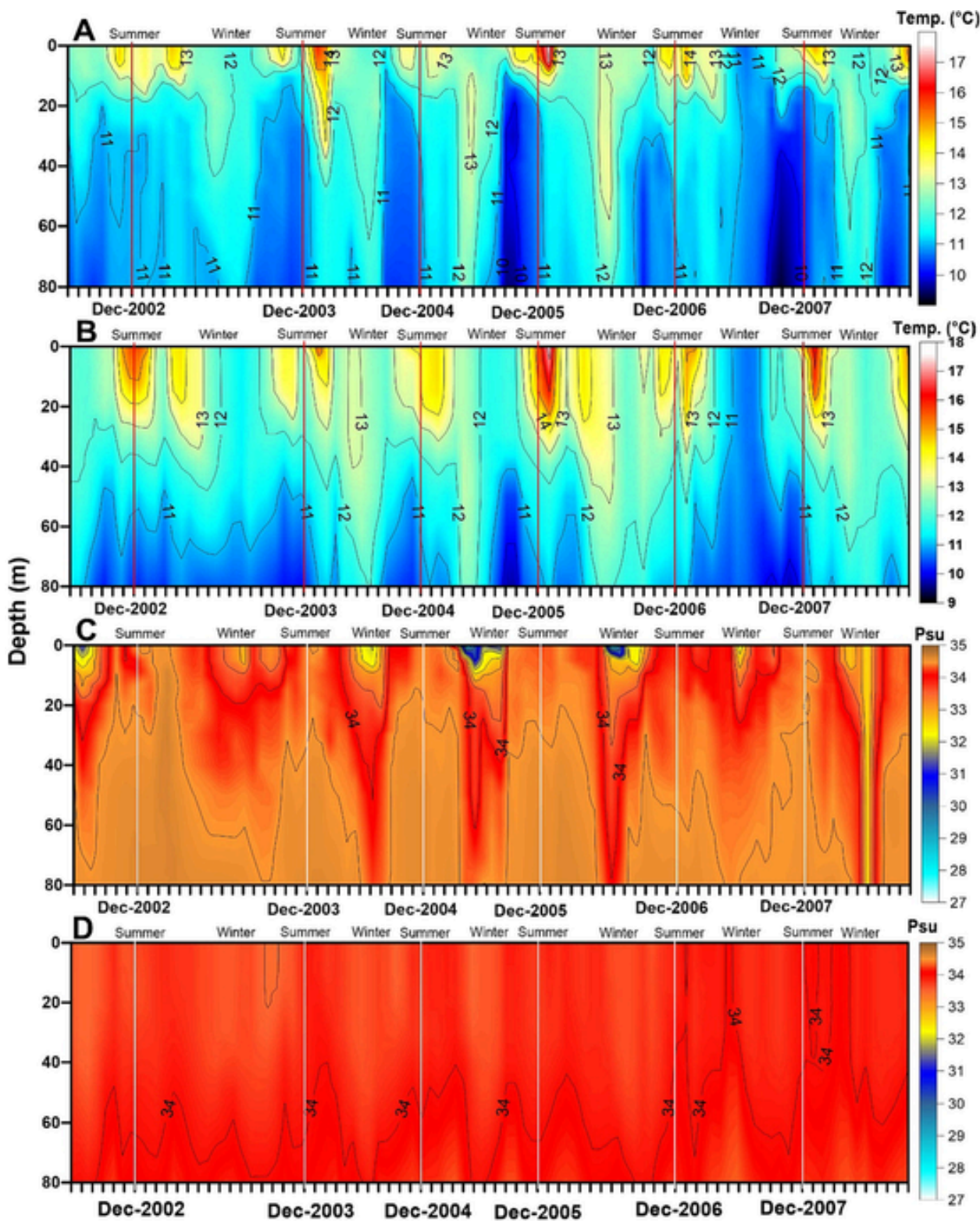


Fig. 7. Monthly time series at Station 18 (2002–2008) of temperature from CTD casts (A) and simulated by the model (B), and of salinity from CTD casts (C) and simulated by the model (D).

The nitrate supply is primarily dominated by nitrate advection from the south, which generally exceeds the input caused by coastal upwelling. The main sinks are due to northward and westward advection, which exceeds biological uptake (Fig. 10A). Nitrate supplies are at a minimum in early winter (June–July) and then increase during winter/spring due to the dominance of southerly advection over coastal up-

welling, reaching a maximum in late spring (November). Nitrate sinks follow a consistent seasonal pattern, although strong fluctuations are observed for northward and westward advection, indicating a balance between both pathways. The latter implies that the circulation of surface water masses in the coastal region of Station 18 is driven by coastal upwelling, alongshore flow towards the equator, and cross-shore export

**Table 2**

Testing the significance (Student *t*-test) of model deviations from observed values after PISCES model outputs of hydrographic and biogeochemical variables at Station 18. This is based on the monthly observation and model data time series between 2002 and 2008. Mean values are for two vertical layers.

Layer		Temperature	Salinity	Oxygen	Chla	NO3
0–20	<i>t</i> -test	4.101	2.292	12.595	1.543	8.991
	P	<0.01	<0.05	<0.01	>0.05	<0.01
	Bias	+0.78	+2.76	+2.38	+1.15	−9.33
	<i>t</i> -test	4.739	11.851	17.212	2.633	14.007
20–80	P	<0.01	<0.01	<0.01	0.023	<0.01
	Bias	+0.49	−0.46	+3.94	−0.08	−10.29

towards the open ocean throughout the year. This circulation pattern is most intense in late spring and weakest in early winter. The dynamics of the circulation pattern may explain a delayed response of the seasonal cycle of nitrate concentration with respect to nitrate fluxes (about three months). After reaching a minimum in early spring (September–October), nitrate concentrations begin to rise in October and reach a maximum during the spring/summer upwelling season (November–March). The high nitrate concentration during this period is sustained by a decrease in biological uptake. Variation in plankton biomass is due to horizontal advection from the south and the net biological growth rate (growth minus grazing), while the main sinks are northward and westward advection. When adding positive terms vs negative terms, the relative contribution of fluxes to biomass variation due to advection can be estimated. For instance, for mesozooplankton, except in July when the opposite is true, southerly advection and net biological rates accounted for 60 % and 40 % of the total annual gain mean (65 % and 35 % in spring) and contributed to 56 % and 40 % of the total loss (i.e. export towards the exterior of the box) throughout the year. Plankton fluxes and biomass approximately follow the same seasonal pattern as nitrate fluxes (Fig. 10B and Fig. 10C). The maximum plankton biomass is typically found in late spring-summer and then decreases until reaching a minimum in early winter.

Table 3 represents the most relevant time-lags between nitrate inputs and the response in plankton productivity (biomass and production). These delays were determined through a lagged correlation analysis, which identified the time lags corresponding to the most significant correlations ( $p < 0.05$ ) across the time series. Nitrate upwelling is followed by southerly nitrate advection with a 2-day lag, which could indicate the time required for an upwelling-favourable wind event to generate a coastal upwelling geostrophic current. Diatom production responds to nitrate upwelling with a 4-day lag and to southerly diatom biomass advection with a 3-day lag. Mesozooplankton production takes longer to respond, as attested by an 8-day lag with southerly diatom advection and a 7-day lag with local diatom production. The response of mesozooplankton biomass is still slower, as attested by an 18-day lag with local diatom production. This means that it takes around 11 days for mesozooplankton biomass to respond to mesozooplankton production.

### 3.3. Spatial variability

Two approaches were adopted to examine the extent to which the variations in zooplankton biomass simulated at Station 18 represent what is occurring in the upwelling region under study.

First, the seasonal cycle of zooplankton biomass simulated in the box centred at Station 18 (Box 1) was also simulated in a similar box (Box 2) located off Punta Lavapié, in the southern part of the study area. As expected, the annual cycles of mesozooplankton biomass appear very similar between boxes and are strongly correlated ( $p < 0.01$ ) (Fig. 11).

Secondly, the spatial autocorrelation of diatom biomass and zooplankton between grid points and Station 18 resulting from their mod-

elled estimates was assessed. In the upper layer (0–20 m), there was a highly significant correlation ( $p < 0.01$ ) of chl-a concentration within a coastal band of about 50 km (Fig. 12A). Zooplankton biomass in the upper layer also exhibited a highly significant correlation within the coastal band, extending up to 70 km offshore (Fig. 12B). The spatial autocorrelation patterns of chl-a and zooplankton biomass indicate that they are being transported northward by the coastal upwelling jet. Furthermore, there is evidence of a westward advection pattern in the form of a filament-like structure oriented towards the northwest, which extends up to 200 km offshore. The variability of mesozooplankton biomass below 20 m (20–80 m layer) at Station 18 is representative of a much-reduced area, with autocorrelations being only significant within a 20 km radius around Station 18 (Fig. 12C).

## 4. Discussion

Our findings indicate that alongshore and cross-shelf advection is a major driver causing variations in mesozooplankton biomass in the coastal upwelling zone of central-southern Chile, as it may occur in all eastern boundary upwelling systems known to exhibit a physical unstable environment (Xiu et al., 2018; Corredor-Acosta et al., 2020). Horizontal advection can control biomass gains and losses within the coastal band around Station 18 (ca. 50 km). As a result, a significant portion of the temporal variability observed in time series data, which is commonly conducted at stationary stations, can be attributed to the alongshore and cross-shelf flows that arise from small-scale and meso-scale processes. This advection originates over various spatial-temporal scales. Over a large-scale, the geostrophic current field for the entire period indicates a major northward flow (Fig. 1). In addition to this, the study area is strongly subject to mesoscale activity driven by instability of the eastern boundary current and the wind-driven upwelling circulation (Hormazábal et al., 2013). A recent study (Corredor-Acosta et al., 2020) also shows the formation of several cyclonic and anticyclonic eddies over the continental shelf in the area, giving rise to a net northward flow. The chl-a distribution shown in Fig. 12A also illustrates how phytoplankton becomes advected northward, so indicating that our biophysical model ROMS-PISCES could capture such meso-scale variability during active upwelling.

Local production certainly contributes to variations in mesozooplankton biomass across the upwelling region. However, our findings derived from the model analysis suggest that this factor may only account for 30–40 % of the biomass gain within the upwelling zone and 25–50 % of the biomass export from it (see Table 3). Indeed, many factors might interact to influence zooplankton biomass in the coastal zone. This is particularly true in highly dynamic coastal upwelling zones characterised by a highly advective environment, where physical forces can play a crucial role in causing variations in biomass (Marín et al., 2001; Reese et al., 2005). Coastal circulations can have a significant impact on the population dynamics of dominant species in coastal zooplankton, which make up most of the biomass, such as copepods (Peterson, 1998; Escribano, 1998). Other studies have also found that mesoscale activity can strongly affect plankton biomass in the upwelling zone by promoting offshore transport (Keister et al., 2009; Morales et al., 2010). All these physical processes and their effects on the variation of zooplankton biomass have rarely been considered in the analysis of *in situ* time series observations (Hugget et al., 2009; Mackas and Beaugrand, 2010; Escribano et al., 2012).

Our study findings can have important implications for ocean observations. Time series studies at coastal fixed stations seldom account for advection effects on plankton biomass; hence, using this variable as a proxy for ocean productivity (Miloslavich et al., 2018; Muller-Karger et al., 2018) may result in biased analyses if advective processes are not considered. Our analysis of model simulations suggests that there may be a 10-day lag between the peaks of mesozooplankton production and biomass in the highly advective coastal upwelling study region. The es-

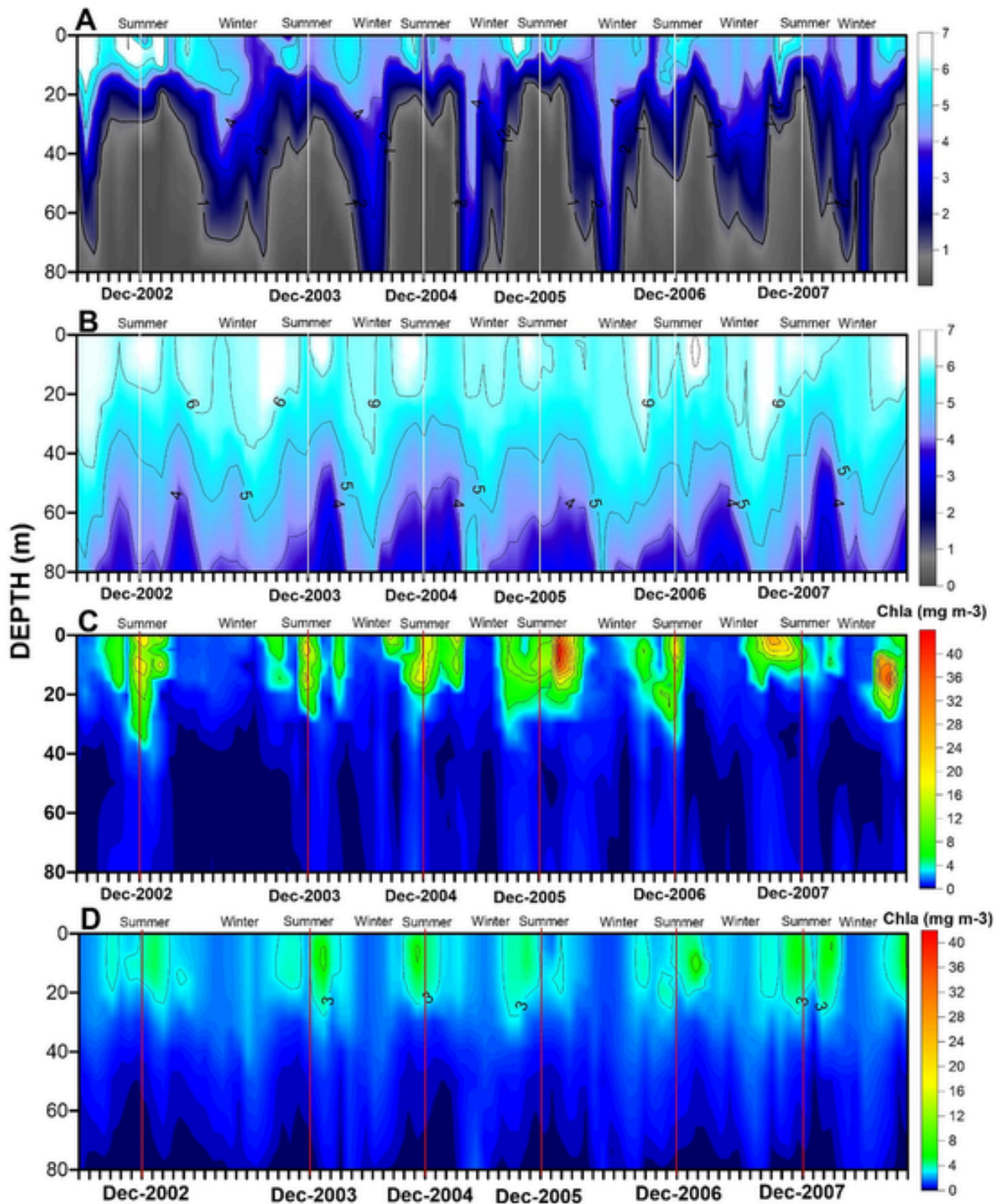


Fig. 8. Monthly time series at Station 18 (2002–2008) of dissolved oxygen from *in situ* measurements (A) and simulated by the model (B) and of chlorophyll-a from *in situ* measurements (C) and simulated by the model (D).

timination of mesozooplankton production based solely on biomass observations may be biased. Yet there are important implications for estimating zooplankton production in the ocean (Sigman and Hain, 2012; Yebra et al., 2018). The estimates of zooplankton secondary production rely heavily on accurate measurements of biomass, which can be challenging to replicate in field conditions (e.g. Kimmerer et al., 2007;

Kobari et al., 2019). Biased estimates of zooplankton biomass can lead to erroneous interpretations when examining the relative impact of bottom-up and top-down effects on zooplankton dynamics in highly productive upwelling systems (Escribano et al., 2016).

Our physical-biogeochemical model attempted to determine how plankton productivity responds to nutrient inputs and physical



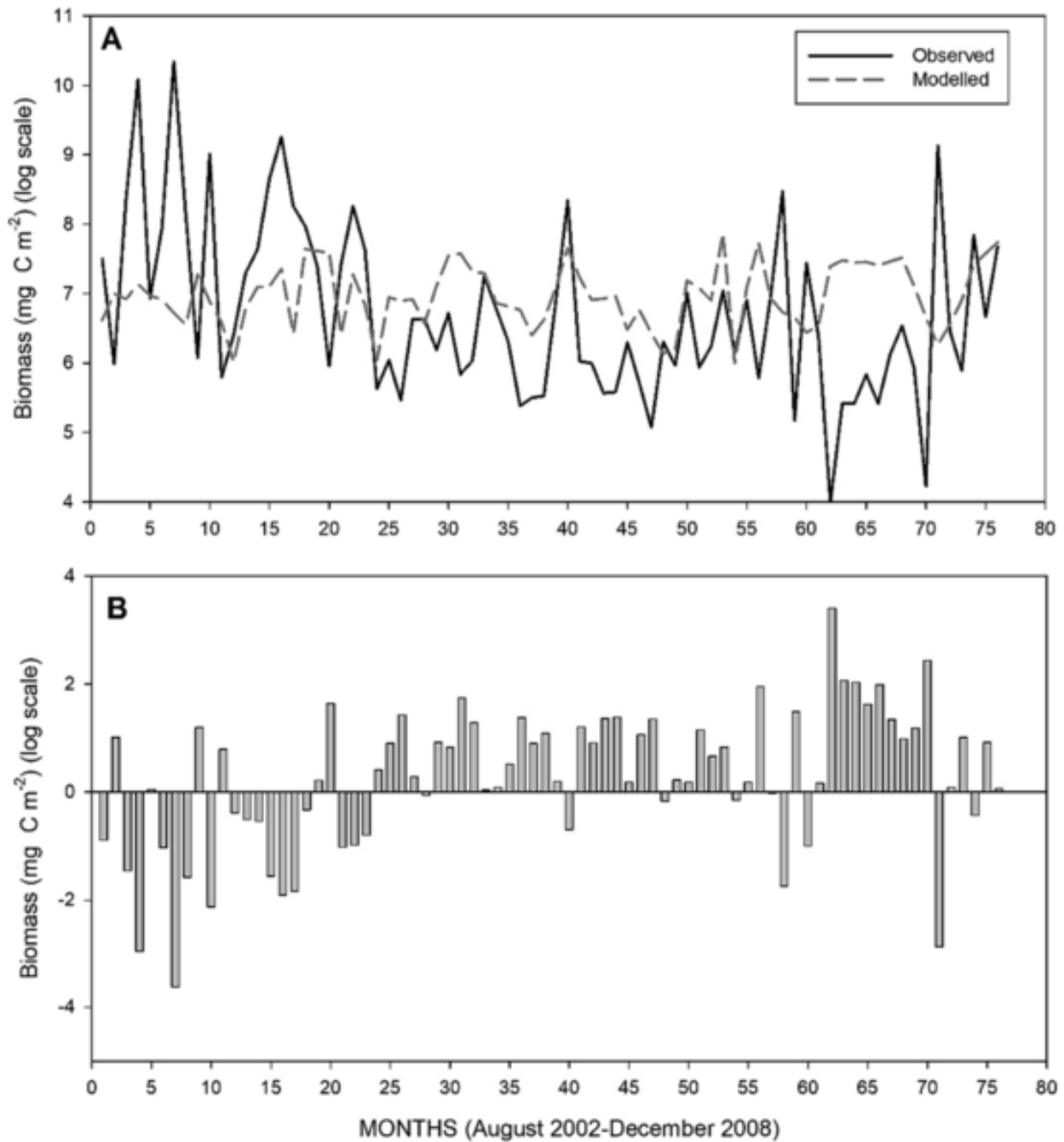


**Fig. 9.** Time series of depth-integrated (0–80 m) zooplankton biomass at Station 18 over the 2002–2008 period (A) from monthly measurements and model estimates. The y-axis represents the deviations between modelled and observed data (B).

processes throughout the year. To accomplish this, we estimated the time delay between the most important fluxes and biomass (i.e. the time lags for maximum correlation) using the complete time series. The 2-day lag between southerly nitrate advection and nitrate upwelling may represent the time required for the upwelling-favourable wind to generate coastal upwelling geostrophic current. There is then a lag between both the nitrate upwelling and southerly diatom biomass on the one hand and diatom production on the other hand (4 and 3 days, respectively). This is the response time of phytoplankton communities to coastal upwelling. Mesozooplankton production still takes longer to respond, as attested by a 7-day lag in response to local diatom production. In terms of the lag between primary and secondary producers, the simulated timing of responses between primary production on the one hand and zooplankton production and biomass on the other hand (7 and 18

days, respectively) falls within the expected range for these relationships (Almén and Tamelander, 2020).

A key concern is related to how well the observations at Station 18 could represent the variability over a wider area in the coastal upwelling region off Concepcion. According to the model outputs, the autocorrelation patterns of plankton biomass (Fig. 12) suggest that Station 18 could be representative of the entire coastal band that experiences wind-driven upwelling (both north and south of Station 18). Autocorrelations are stronger in the upper 20 m, which is the surface layer where the production of diatom biomass is intensified, along with prey-predator interactions between phytoplankton and zooplankton. The filament-like pattern oriented towards the northwest suggests that the drifting biomass, including diatoms and zooplankton, is primarily being carried away from the upwelling zone in this direction. Nevertheless,

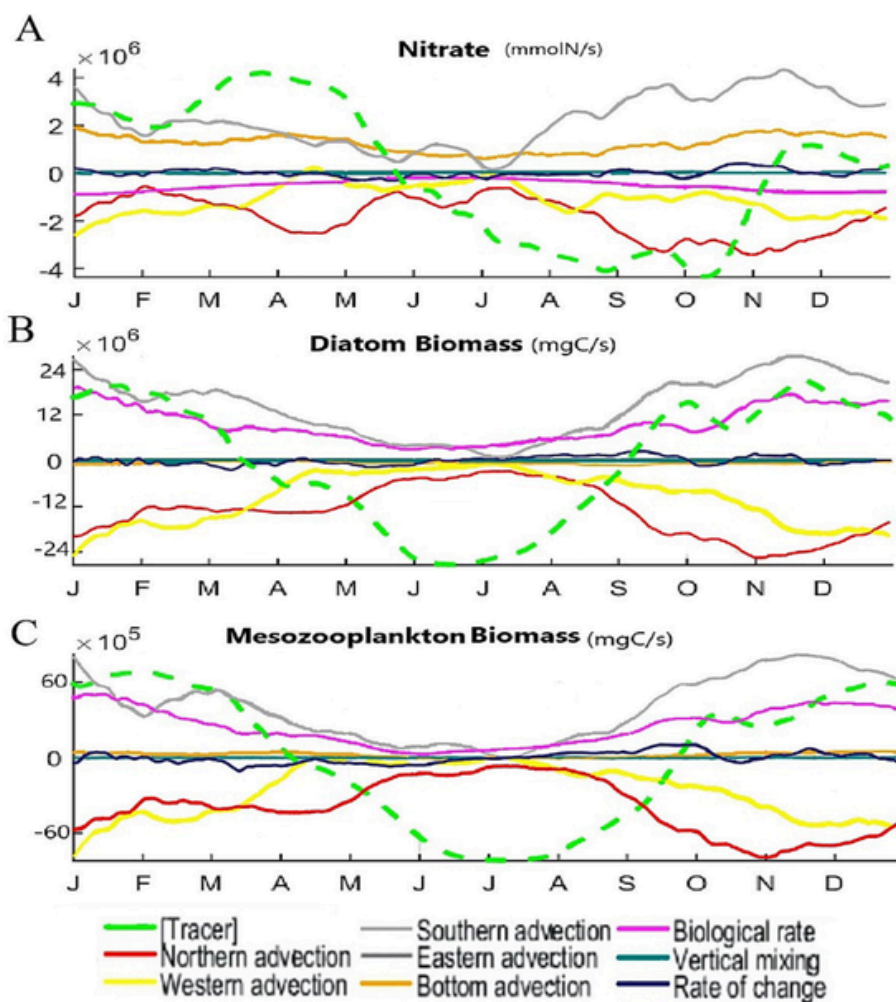


Fig. 10. Mean annual cycle of the source and sink terms for nitrate concentration (A), diatom biomass (B), and mesozooplankton biomass (C). Fluxes are estimated for a geographic box with its centre at Station 18 (see Fig. 1).

Table 3

Summary of forcings, corresponding responses, and time lag for responses between correlated physical and biological variables and processes derived from the PISCES biogeochemical model at Station 18 in the upwelling zone of central/southern Chile. Nitrate flow is in  $\text{mm m}^{-2} \text{s}^{-1}$ , and diatoms and zooplankton production and biomass are in  $\text{mg C/m}^{-2}(-|-\)  $\text{s}^{-1}$ .$

Forcing (Variable/Process)	Response (Variable/Process)	Time lag (d)
Upward Flow, $\text{NO}_3$	Northward Flow, $\text{NO}_3$	2
Upward Flow, $\text{NO}_3$	Diatoms Production	4
Northward, diatoms	Diatoms Production	3
Northward, diatoms	Zooplankton Production	8
Diatoms Production	Zooplankton Production	7
Northward, diatoms	Diatoms Biomass	20
Diatoms Production	Zooplankton Biomass	18

the results of the model should be considered with caution. Modelled data for the seasonal cycle, acquired from monthly climatology, show patterns that closely match *in situ* observations of physical variables, with significant correlations between the time series. However, there are also significant discrepancies between field observations and the distribution of data over the course of the year. For instance, the model overestimates temperatures during the spring-summer, but it agrees well with measurements collected *in situ* during the winter. Also, the model fails to accurately reproduce the extremely low salinities observed during winter at Station 18 in near-surface water, whereas higher salinities in near-surface water are simulated accurately

throughout spring and summer due to the intense upwelling of ESSW (Schneider et al., 2016). First, they strongly depend on spatial resolution (1/12 degrees) and coastal topography. The irregular morphology of the coastal area under study can cause small-scale circulation patterns that are not properly accounted for by the model, such as mesoscale and sub-mesoscale processes. All these factors can directly impact the dynamics of nutrients and biomass for both phytoplankton and zooplankton (Chaigneau et al., 2008; Chaigneau et al., 2009).

Moreover, the model underestimates nutrient and chlorophyll concentrations, which are proxies for phytoplankton biomass. This is most likely due to an overestimation of the diapycnal mixing of the nutrient-rich Peru-Chile undercurrent (PCUC), which is the source of upwelling waters in the study region (Silva et al., 2009), with the nutrient-poor surrounding waters. This is due to a weakness in the diffusion-advection scheme used for biogeochemical tracers in the model (V. Echevin, pers. comm.). Underestimating the strength of the oxygen minimum zone can lead to more hypoxic conditions in the water column than what is predicted by the model. In fact, the upper boundary of the oxygen minimum zone ( $1 \text{ mL O}_2 \text{ L}^{-1}$ ) is much shallower in depth. During the upwelling season, observations indicate the presence of a feature extending up to 30 m, while the model data failed to account for it, at least within the upper 80 m. Furthermore, the model configuration did not include the contribution of river runoff within the simulation domain. However, two major rivers in the region, Bio-Bio and Itata, can play important roles in the ecosystem functioning of central-southern Chile. They strongly influence the near-surface salinity and

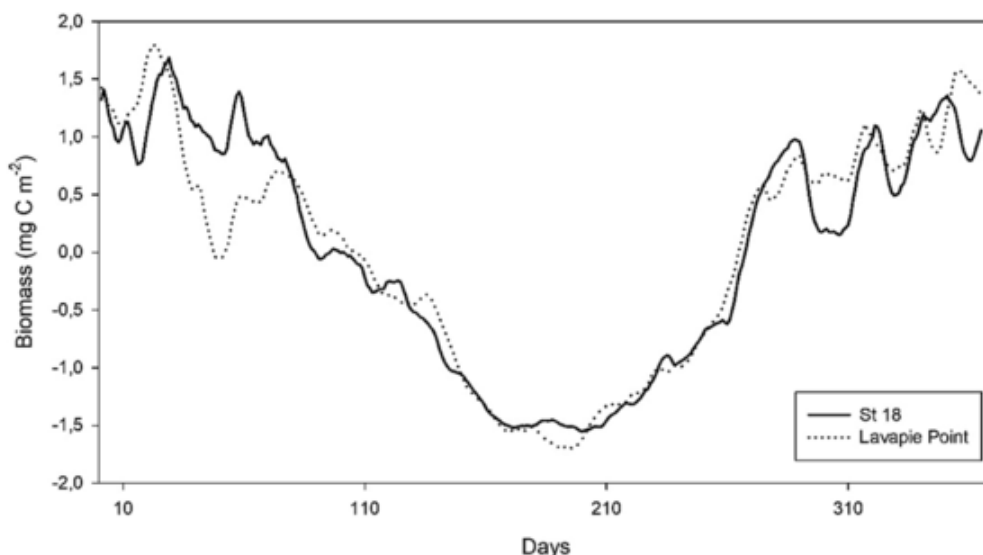


**Fig. 11.** Mean annual cycle of depth-integrated (0–80 m) mesozooplankton biomass ( $\text{mg C m}^{-2}$ ) estimated by the model in two boxes defined in different locations of the upwelling zone at central-southern Chile: at Station 18 (northern box) and off Punta Lavapié (southern box). The geographic location of the boxes is illustrated in Fig. 1.

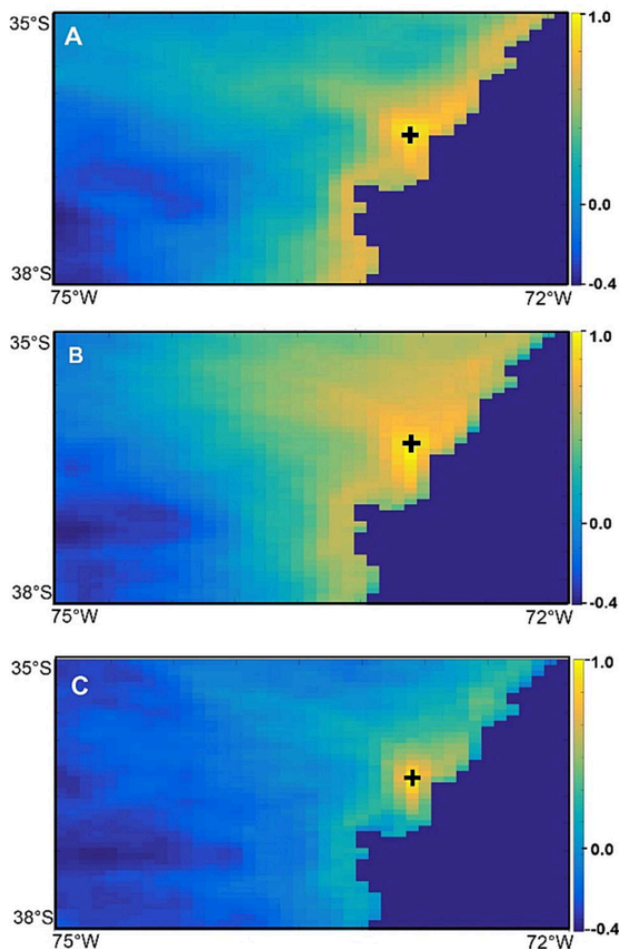


**Fig. 12.** Spatial autocorrelation (Pearson correlation coefficient) of model data over the study grid: A) Chlorophyll-a in the 0–20 m layer (A), mesozooplankton biomass in the 0–20 m layer (B), and mesozooplankton biomass in the 20–80 m layer (C).

stratification (Sobarzo et al., 2007) and contribute to the nutrient budget of the upwelling zone (Vargas et al., 2016).

Modelled data also overestimated observed values of mesozooplankton biomass over most occasions during the time series, and these overestimates became greater by the end period of the series (Fig. 9). These results may also relate to an underestimated upwelling intensity which is a key process controlling temperature, oxygenation, and food sources in the photic zone where zooplankton mostly reside. All these factors can affect the dynamics of zooplankton and its biomass. For instance, a greater hypoxia driven by a shallow OMZ (more intense upwelling) is known to increase mortality of zooplankton (e.g. Ekau et al., 2010), resulting in less biomass than that predicted by ROMS-PISCES Model. Other studies have shown that upwelling intensity has been incrementing in recent decades in eastern boundaries systems, apparently driven by ongoing global warming (e.g. Schneider et al., 2016, Xiu et al., 2018), impacting negatively on zooplankton biomass in the more recent decade (e.g. Escribano et al., 2016).

## 5. Conclusions

The modelling approach adopted in this study indicates that the primary sources of variance for phytoplankton and zooplankton productivity in the coastal upwelling zone of central-southern Chile are the advective processes that occur along the shore and across the shelf. The physical-biogeochemical hindcast simulation was shown to reasonably reproduce the seasonal cycle of physical, chemical, and biological variables observed at the fixed Station 18, although with significant deviations, mostly attributed to underestimated nutrient inputs. The temporal delays in the biological responses to physical processes were consistent with expected ranges, providing support for an appropriate modeling approach to represent the dynamics of a highly unstable and heterogeneous upwelling environment. The findings suggest that caution should be exercised when interpreting data from fixed time series stations that are susceptible to strong advective processes in eastern boundary upwelling systems.

## CRediT authorship contribution statement

**Ana Venegas:** Conceptualization, Formal analysis, Investigation, Methodology, Writing – original draft. **Pierre Amael-Auger:** Conceptualization, Formal analysis, Methodology, Software, Writing – review &

editing. **Ruben Escribano:** Conceptualization, Data curation, Formal analysis, Investigation, Supervision, Validation, Writing – original draft, Writing – review & editing. **Carolina Parada:** Conceptualization, Methodology, Supervision.

### Declaration of competing interest

The authors declare the following financial interests/personal relationships which may be considered as potential competing interests: Ruben Escribano reports financial support was provided by Millennium Institute of Oceanography. Carolina Parada reports financial support was provided by National Agency for Research and Development.

### Data availability

Data are public and available at DOI: 10.5281/zenodo.10378471

### Acknowledgements

The oceanographic time series at Station 18 was funded by FONDAP COPAS Center. Graduate studies of A. Venegas have been supported by ANID Graduate studies funded by CONICYT-PFCHA/doctorado nacional/2018-21180829 and IMO Scholarship. Data analysis and paper writing were supported by the Millennium Institute of Oceanography (IMO), Grant, IC\_120019. This work is a contribution to ECLIPSE project ANID ANILLO ACT210071 and the EBUS SCOR WG 155, Fondecyt 1191606 and Concurso de Fortalecimiento al Desarrollo Científico de Centros Regionales 2020-R20F0008-CEAZA. We thank to two anonymous reviewers for their very helpful comments to improve our work.

### Appendix A. Supplementary data

Supplementary data to this article can be found online at <https://doi.org/10.1016/j.pocean.2023.103193>.

### References

- Albert, A., Echevin, V., Lévy, M., Aumont, O., 2010. Impact of nearshore wind stress curl on coastal circulation and primary productivity in the Peru upwelling system. *J. Geophys. Res.* 115, C12033. <https://doi.org/10.1029/2010JC006569>.
- Almén, A., Tamelander, T., 2020. Temperature-related timing of the spring bloom and match between phytoplankton and zooplankton. *Mar. Biol. Res.* <https://doi.org/10.1080/17451000.2020.1846201>.
- Anabalón, V., Morales, C.E., González, H.E., Menschel, E., Schneider, W., Hormazabal, S., Valencia, L., Escribano, R., 2016. Micro-phytoplankton community structure in the coastal upwelling zone off Concepción (central Chile): annual and inter-annual fluctuations in a highly dynamic environment. *Progr. Oceanogr.* 149 (2016), 174–188.
- Arcos, D.A., Cubillos, L.A., Núñez, S.P., 2001. The jack mackerel fishery and El Niño 1997–98 effects off Chile. *Progr. Oceanogr.* 49, 597–617.
- Auger, P.-A., Gorgues, T., Machu, E., Aumont, O., Brehmer, P., 2016. What drives the spatial variability of primary productivity and matter fluxes in the north-west African upwelling system? A modelling approach. *Biogeosciences*, 13, 6419–6440, 2016 [www.biogeosciences.net/13/6419/2016/](http://www.biogeosciences.net/13/6419/2016/), doi:10.5194/bg-13-6419-2016.
- Auger, P.A., Machu, E., Gorgues, T., Grima, N., Waelles, M., 2015. Comparative study of potential transfer of natural and anthropogenic cadmium to plankton communities in the North-West African upwelling. *Sci. Total Environ.* 505, 870–888. <https://doi.org/10.1016/j.scitotenv.2014.10.045>.
- Aumont, O., Bopp, L., 2006. Globalizing results from ocean in-situ iron fertilization studies. *Glob. Biogeochem. Cy.* 20, GB2017. <https://doi.org/10.1029/2005GB002591>.
- Aumont, O., Ethé, C., Tagliabue, A., Bopp, L., Gehlen, M., 2015. PISCES-v2: An ocean biogeochemical model for carbon and ecosystem studies. *Geosci. Model Dev. Discuss.* 8, 1375–1509. <https://doi.org/10.5194/gmdd-8-1375-2015>.
- Beaugrand, G., Reid, P.C., 2003. Long-term changes in phytoplankton, zooplankton and salmon linked to climate. *Glob. Change Biol.* 9, 801–817.
- G. Beaugrand Long-term changes in copepod abundance and diversity in the north-east Atlantic in relation to fluctuations in the hydroclimatic environment. *Fish. Oceanogr.* 12 4/5 2003 270 283 doi.org/10.1046/j.1365-2419.2003.00248.x.
- Chaigneau, A., Gizolme, A., Grados, C., 2008. Mesoscale eddies off Peru in altimeter records: Identification algorithms and eddy spatio-temporal patterns. *Progr. Oceanogr.* 79, 106–119. <https://doi.org/10.1016/j.pocean.2008.10.013>.
- Chaigneau, A., Eldin, G., Dewitte, B., 2009. Eddy activity in the four major upwelling systems from satellite altimetry (1992–2007). *Progr. Oceanogr.* 83, 117–123. <https://doi.org/10.1016/j.pocean.2009.07.012>.
- A. Corredor-Acosta C.E. Morales A. Rodríguez-Santana V. Anabalón L.P. Valencia S. Hormazabal The influence of diapycnal nutrient fluxes on phytoplankton size distribution in an area of intense mesoscale and submesoscale activity off Concepción Chile. *J. Geophys. Res.: Oceans* 125 2020 e2019JC015539 10.1029/2019JC015539.
- Echevin, V., Aumont, O., Ledesma, J., Flores, G., 2008. The sea-seasonal cycle of surface chlorophyll in the Peruvian upwelling system: A modelling study. *Progr. Oceanogr.* 79, 167–176. <https://doi.org/10.1016/j.pocean.2008.10.026>.
- Echevin, V., Albert, A., Lévy, M., Graco, M., Aumont, O., Piétri, A., Garric, G., 2014. Intraseasonal variability of nearshore productivity in the Northern Humboldt Current System: The role of coastal trapped waves. *Cont. Shelf Res.* 73, 14–30. <https://doi.org/10.1016/j.csr.2013.11.015>.
- Ekau, W., Auel, H., Portner, H.O., Gilbert, D., 2010. Impacts of hypoxia on the structure and processes in pelagic communities (zooplankton, macro-invertebrates and fish). *Biogeosciences* 7, 1669–1699.
- Escribano, R., 1998. Population dynamics of *Calanus chilensis* from northern Chile. *Fish. Oceanogr.* 7, 245–251.
- Escribano, R., Schneider, W., 2007. The Structure and Functioning of the Coastal Upwelling System off Central/south of Chile. *Progr. Oceanogr.* 75, 343–346.
- Escribano, R., Hidalgo, P., González, H.E., Giesecke, R., Riquelme-Bugueño, R., Manríquez, K., 2007. Interannual and seasonal variability of metazooplankton in the Central/south upwelling region off Chile. *Progr. Oceanogr.* 75, 470–485.
- Escribano, R., Morales, C.E., 2012. Spatial and temporal scales of variability in the coastal upwelling and coastal transition zone off central-southern Chile (35–40°S). *Progr. Oceanogr.* 92–95, 1–7.
- Escribano, R., Hidalgo, P., Fuentes, M., Donoso, K., 2012. Zooplankton time series in the coastal zone off Chile: variation in upwelling and responses of the copepod community. *Progr. Oceanogr.* 97–100, 174–186.
- Escribano, R., Hidalgo, P., Valdés, V., Frederick, L., 2014. Temperature effects on development and reproduction of copepods in the Humboldt Current: the advantage of rapid growth. *J. Plank. Res.* 36, 104–116.
- Escribano, R., Bustos-Ríos, E., Hidalgo, P., Morales, C.E., 2016. Non-limiting food conditions for growth and production of the copepod community in a highly productive upwelling zone. *Cont. Shelf Res.* 126, 1–14. <https://doi.org/10.1016/j.csr.2016.07.018>.
- D. Espinoza-Morriberón V. Echevin F. Colas J. Tam J. Ledesma L. Vásquez M. Graco Impacts of El Niño events on the Peruvian upwelling system productivity. *J. Geophys. Res.* Oceans 122 2017 10.1002/2016JC012439.
- Garreaud, R.D., Falvey, M., 2009. The coastal winds off western subtropical South America in future climate scenarios. *Int. J. Clim.* 29, 543–554.
- Gorgues, T., Menkes, C., Slemmons, L., Aumont, O., Dandonneau, Y., Radenac, M.-H. Alvaín, S., Moulin, C., 2010. Revisiting the La Niña 1998 phytoplankton blooms in the equatorial Pacific, Deep Sea Res. Part I: Oceanographic Research Papers, Volume 57, Issue 4, Pages 567-576, ISSN 0967-0637, doi.org/10.1016/j.dsr.2009.12.008.
- Gorgues, T., Menkes, C., Aumont, O., Vialard, J., Dandonneau, Y., Bopp, L., 2005. Biogeochemical impact of tropical instability waves in the Equatorial Pacific. *Geophys. Res. Lett.* 32, L24615. <https://doi.org/10.1029/2005GL024110>.
- Hays, G., Richardson, A., Robinson, C., 2005. Climate change and marine plankton. *Trends in Ecol. Evol.* 20, 337–344. <https://doi.org/10.1016/j.tree.2005.03.004>.
- Hirst, A.G., Bunker, A.J., 2003. Growth of marine planktonic copepods: global rates and patterns in relation to chlorophyll-a, temperature, and body weight. *Limnol. Oceanogr.* 48, 1988–2010.
- Hormazabal, S., Combes, V., Morales, C.E., Correa-Ramírez, M.A., Di Lorenzo, E., Nuñez, S., 2013. Intrathermocline eddies in the coastal transition zone off central Chile (31–41°S). *J. Geophys. Res. Oceans* 118, 4811–4821.
- Huggett, J., Verhey, H., Escribano, R., Fairweather, T., 2009. Copepod biomass, size composition and production in the Southern Benguela: spatio-temporal patterns of variation, and comparison with other eastern boundary upwelling systems. *Progr. Oceanogr.* 83, 197–207.
- Huntley, M., Boyd, C., 1984. Food-Limited Growth of Marine Zooplankton, *The Am. Nat. Vol.* 124, No. 4.
- Keister, J.E., Cowles, T.J., Peterson, W.T., Morgan, C.A., 2009. Do upwelling filaments result in predictable biological distributions in coastal upwelling ecosystems? *Progr. Oceanogr.* 83 (1–4), 303–313. <https://doi.org/10.1016/j.pocean.2009.07.042>.
- Kimmerer, W.J., Hirst, A.G., Hopcroft, R.R., McKinnon, A.D., 2007. Estimating juvenile copepod growth rates: corrections, inter-comparisons and recommendations. *Mar. Ecol. Progr. Ser.* 336, 187–202.
- Kobari, T., Sastri, A.R., Yebra, L., Liu, H., Hopcroft, R.R., 2019. Evaluation of trade-offs in traditional methodologies for measuring metazooplankton growth rates: assumptions, advantages and disadvantages for field applications. *Progr. Oceanogr.* 178, 102137. <https://doi.org/10.1016/j.pocean.2019.102137>.
- C. Le Quéré Reply to Horizons Article 'Plankton functional type modelling: running before we can walk' Anderson (2005): I Abrupt changes in marine ecosystems?, *J. Plank. Res. Volume 28: 9* 2006 doi.org/10.1093/plankt/fbi014.
- D. Mackas G. Beaugrand Comparisons of zooplankton time series. *J. Mar. Sys.* 79 3–4 2010 286 304 doi.org/10.1016/j.jmarsys.2008.11.030.
- Mann, K.H., Lazier, J.R.N., 1991. Dynamics of Marine Ecosystems. Blackwell Scientific Publications, Oxford.
- Marín, V.H., Escribano, R., Delgado, L.E., Olivares, G., Hidalgo, P., 2001. Nearshore circulation in a coastal upwelling site off the northern Humboldt Current System. *Cont. Shelf Res.* 21, 1317–1329.
- McGowan, J.A., Bograd, S.J., Lynn, R.J., Miller, A.J., 2003. The biological response to the 1977 regime shift in the California Current. *Deep Sea Res. Part II.* 50, 2567–2582.
- Medellin-Mora, J., Atkinson, A., Escribano, R., 2019. Community structured production of zooplankton in the eastern boundary upwelling system off central/southern Chile (2003–2012). *ICES J. Mar. Sc.* 77 (1), 419–435. <https://doi.org/10.1093/icesjms/fsz193>.

- Miloslavich, P., Bax, N., Simmons, S.E., Klein, E., Appeltans, W., Aburto-Oropeza, O., et al., 2018. Essential Ocean Variables for sustained observations of marine biodiversity and ecosystems. *Gl. Change Biol.* 24, 2416–2433. <https://doi.org/10.1111/gcb.14108>.
- Montero, P., Daneri, G., Cuevas, L.A., González, H.E., Jacob, B., Lizárraga, L., Menschel, E., 2007. Productivity cycles in the coastal upwelling area off Concepción: The importance of diatoms and bacterioplankton in the organic carbon flux. *Progr. Oceanogr.* 75, 518–530.
- Montes, I., Dewitte, B., Gutknecht, E., Paulmier, A., Dadou, I., Oshlies, A., Garçon, V., 2010. High-resolution modeling of the Eastern Tropical Pacific Oxygen Minimum Zone: Sensitivity to the tropical oceanic circulation. *J. Geophys. Res. Oceans* 119. <https://doi.org/10.1002/2014JC009858>.
- Morales, C.E., Torreblanca, M.L., Hormazábal, S., Correa-Ramírez, M., Nuñez, S., Hidalgo, P., 2010. Mesoscale structure of copepod assemblages in the coastal transition zone and oceanic waters off central-southern Chile. *Progr. Oceanogr.* 84, 158–173.
- Muller-Karger, F.E., Miloslavich, P., Bax, N.J., Simmons, S., Costello, M.J., Sousa Pinto, I., Canonico, G., Turner, W., Gill, M., Montes, E., et al., 2018. Advancing Marine Biological Observations and Data Requirements of the Complementary Essential Ocean Variables (EOVs) and Essential Biodiversity Variables (EBVs) Frameworks. *Front. Mar. Sci.* 2018 (5), 211.
- Pauly, D., Christensen, V., Guénette, S., et al., 2002. Towards sustainability in world fisheries. *Nature* 418, 689–695. <https://doi.org/10.1038/nature01017>.
- Peterson, W., 1998. Life cycle strategies of copepods in coastal upwelling zones. *J. Mar. Sys.* 15, 313–326.
- Peterson, W.T., Emmet, R., Goericke, R., Venrick, E., Mantyla, A.W., Bograd, S.J., Schwing, F.B., Hewitt, R., Lo, N.C.H., Watson, W.H., Barlow, J., Lowry, M., Ralston, M., Forney, K.A., Lavaniegos-Espejo, B.E., Sydeman, W.J., Hyrenbach, K.D., Bradley, R.W., Chávez, F.P., Warzybok, P., Hunter, K., Benson, S., Weise, M., Harvey, J., GaxiolaCastro, G., Durazo-Arvizu, R., 2006. The state of the California current, 2005–2006: Warm in the north, cold in the south. *CalCOFI Report* 47, 30–74.
- Reese, D.C., Miller, T.W., Brodeur, R.D., 2005. Community structure of near-surface zooplankton in the northern California Current in relation to oceanographic conditions. *Deep Sea Res. Part II Topical Studies in Oceanography* 52, 29–50. <https://doi.org/10.1016/j.dsr2.2004.09.027>.
- Richardson AJ, Schoeman D.S., 2004. Climate impact on plankton ecosystems in the Northeast Atlantic. *Science* 305: 1609-1612. *Science (New York, N.Y.)*. 305. 1609-12. 10.1126/science.1100958.
- Riquelme-Bugueño, R., Escribano, R., Gómez-Gutiérrez, J., 2013. Somatic and molt production of *Euphausia mucronata* off central-southern Chile: the influence of coastal upwelling variability. *Mar. Ecol. Progr. Ser.* 476: 39–57, 2013.
- Ryakaczewski, R.R., Dunne, J.P., Sydeman, W.J., García-Reyes, M., Black, B.A., Bograd, S.J., 2015. Poleward displacement of coastal upwelling-favorable winds in the ocean's eastern boundary currents through the 21st century. *Geophys. Res. Lett.* 42, 6424–6431.
- Schmoker, C., Hernández-León, S., 2013. Stratification effects on the plankton of the subtropical Canary Current. *Progr. Oceanogr.* 119, 24–31. <https://doi.org/10.1016/j.pocean.2013.08.006>.
- Schneider, W., Donoso, D., Garcés-Vargas, J., Escribano, R., 2016. Water-column cooling and sea surface salinity increase in the upwelling region off central-south Chile driven by a poleward displacement of the South Pacific. *Progr. Oceanogr.* 141, 38–58.
- Seibel, B.A., 2011. Critical oxygen levels and metabolic suppression in oceanic oxygen minimum zones. *J. Exp. Biol.* 214, 326–336.
- Schepetkin, A., McWilliams, J., 2005. The Regional Oceanic Modeling System (ROMS): a split-explicit, free-surface, topography-following-coordinate ocean model. *Ocean Model.* 9, 347–404. <https://doi.org/10.1016/j.ocemod.2004.08.002>.
- Sigman, D.M., Hain, M.P., 2012. The Biological Productivity of the Ocean. *Nature Education Knowledge* 3 (10), 21.
- Sobarzo, M., Bravo, L., Donoso, D., Garcés-Vargas, J., Schneider, W., 2007. Coastal upwelling and seasonal cycles that influence the water column over the continental shelf off central Chile, *Progr. Oceanogr.*, Volume 75, Issue 3, 2007, Pages 363-382, ISSN 0079-6611, [doi.org/10.1016/j.pocean.2007.08.022](https://doi.org/10.1016/j.pocean.2007.08.022).
- Sunda, W.G., Huntsman, S.A., 1997. 1997 Interrelated influence of iron, light and cell size on marine phytoplankton growth. *Nature* 390, 389–392.
- Vargas, C., Escribano, R., Poulet, S., 2006. Phytoplankton diversity determines time-windows for successful zooplankton reproductive pulses. *Ecology* 87, 2992–2999.
- Vargas, C., Martínez, R., Escribano, R., Lagos, N., 2010. The relative influence of food quantity, quality, and feeding behavior on zooplankton growth regulation in coastal food webs. *J. Mar. Biol. Ass. UK*. <https://doi.org/10.1017/S0025315409990804>.
- Vargas, C., Contreras, P., Pérez, C., Sobarzo, M., Saldías, G., Salisbury, J., 2016. Influences of riverine and upwelling waters on the coastal carbonate system off Central Chile and their ocean acidification implications. *J. Geophys. Res. Biogeo.* 121. <https://doi.org/10.1002/2015JG003213>.
- Vergara, O., Echevin, V., Sepúlveda, H.H., Quiñones, R.A., 2017. Controlling factors of the seasonal variability of productivity in the southern Humboldt Current System (30–40°S): A biophysical modelling approach. *Cont. Shelf Res.* <https://doi.org/10.1016/j.csr.2017.08.013>.
- Wang, D., Gouhier, T.C., Menge, B.A., Ganguly, A.R., 2015. Intensification and spatial homogenization of coastal upwelling under climate change. *Nature* 518, 390–406.
- Xiu, P., Chai, F., Curchitser, E.N., Castruccio, F.S., 2018. Future changes in coastal upwelling ecosystems with global warming: The case of the California Current System. *Sci. Rep.* 8, 2866.
- Yebra, L., Herrera, I., Mercado, J.M., Cortés, D., Gómez-Jakobsen, F., Alonso, A., et al., 2018. Zooplankton production and carbon export flux in the western Alboran sea gyre (SW Mediterranean). *Progr. Oceanogr.* 167, 64–77. <https://doi.org/10.1016/j.pocean.2018.07.009>.

## Capitulo II:

“Assessing the functional response Holling type IV for the diatoms-zooplankton interaction”.

“Evaluando la respuesta funcional Holling tipo IV para la interacción diatomeas-zooplancton”.

Ecological Modelling (en revisión)

## Resumen

En el ecosistema marino, la interacción predador-presa entre diatomeas y zooplancton constituye un proceso clave en los procesos de transferencia de carbono desde los productores primarios a los niveles tróficos superiores. Esta relación es también un componente fundamental de los modelos biogeoquímicos NPZ (Nitrógeno-Fitoplancton-Zooplancton). El modelamiento matemático de estas relaciones se conoce como respuesta funcional de la tasa de consumo del depredador frente a la concentración de presas. Sin embargo, los procesos biológicos involucrados en esta relación y sus consecuencias son inciertas. Por ejemplo, las observaciones en la naturaleza sugieren la existencia de algunas respuestas por parte de las diatomeas ante el zooplancton a través de la liberación de compuestos tóxicos que pueden retardar o inhibir el crecimiento de sus predadores, como un mecanismo de defensa. Este fenómeno puede ocurrir durante la floración primaveral de diatomeas en los sistemas altamente productivos de surgencia costera. En este estudio desarrollamos una prueba analítica para el efecto potencial de este factor inhibidor en la dinámica NPZ. Usamos un sistema de tres ecuaciones diferenciales basado en la respuesta funcional tipo Holling IV para describir la dinámica de los componentes del NPZ examinando el comportamiento de las soluciones en el infinito sobre un espacio 3-D. Esta aproximación analítica del modelamiento NPZ indica que ante la presencia de un parámetro inhibidor el sistema no alcanza el equilibrio, o sea, las diatomeas y el zooplancton mantienen una dinámica impredecible. Estos hallazgos son consistentes con los datos obtenidos de la estación costera del centro sur de Chile y con las simulaciones de datos originadas por el modelo geoquímico ROMS-PISCES, para la misma localidad durante una ventana de tiempo de 60 días. Nuestro estudio, por lo tanto, sugiere que de hecho pueden existir mecanismos de respuesta en la relación diatomeas – zooplancton, en sistemas altamente productivos de afloramiento costero, y que deberían ser incorporados en los modelos biogeoquímicos del tipo NPZ.

# ASSESSING THE FUNCTIONAL RESPONSE HOLLING TYPE IV FOR THE DIATOMS-ZOOPLANKTON INTERACTION

ANA BELÉN VENEGAS<sup>1,2,4</sup>, Y. PAULINA MANCILLA-MARTÍNEZ<sup>2</sup>, RUBEN ESCRIBANO<sup>3,4</sup>

ABSTRACT. In the marine ecosystem, the prey-predator interaction comprised by diatoms and zooplankton constitutes a key process for C transfer from primary producers to the higher trophic levels. This relationship is also a fundamental component of the biogeochemical NPZ (Nitrogen-Phytoplankton-Zooplankton) models. The mathematical modelling of this relationship is known as a functional response of predator feeding rate as a function of the prey concentration, although the biological processes involved in such relationship and their consequences are uncertain. For instance, observations in nature suggest the existence of some feedback responses of diatoms with their grazers (zooplankton) through the release of toxic compounds which can retard or inhibit the growth of their predators, as a defence mechanism. This phenomenon may occur during the spring bloom of diatoms in highly productive coastal upwelling systems. In this study, we performed an analytical test of the potential effect of this inhibitory factor on the NPZ dynamics. We used a 3-differential equation system based on the Holling IV type functional response to describe the dynamics of the NPZ components by examining the behaviour of solutions in the infinite over a 3-D space. The analytical approach of NPZ modelling indicated that under presence of an inhibitory parameter the system does not reach an equilibrium, i.e., diatoms and zooplankton maintain unpredictable dynamics. These findings were consistent with field data observed at a coastal station in central-southern Chile, and with data simulations derived from application of a biogeochemical (ROMS-PISCES) applied to same location during a time window of 60 days. Our study thus suggests that feedback mechanisms can indeed exist in the diatoms-zooplankton relationship in highly productive coastal upwelling systems, and they should be incorporated in the biogeochemical NPZ models.

## 1. INTRODUCTION AND STATEMENT OF THE MAIN RESULT

Zooplankton play a pivotal role in the marine food web, being the main link for transferring organic C from primary production to higher trophic levels. In the coastal zones of the world ocean this C transfer is mostly mediated by the prey-predator relationship between diatoms and zooplankton [1][2]. In highly productive coastal upwelling areas of subtropical and temperate regions, the spring bloom of diatoms sustains the growth and secondary production of zooplankton [3] [4]. In these regions, the diatoms-zooplankton link has long called the attention of ecologists and biological oceanographers [5]; [6], motivating the search for establishing mathematical equations which could properly describe the functional response between the food concentration (diatoms density) and the feeding rate of zooplankton grazers. Several models have been proposed for such relationship, and they have traditionally been known as functional responses, in which the specific consumption rate of food (per predator biomass and time unit) is a function of the prey density [7][8] [9]. The diatoms-zooplankton relationship has also been one of the key components for the development of biogeochemical models, which are fundamentally based on the variation of diatoms and zooplankton biomasses (in terms of C

---

*Key words and phrases.* Polynomial vector fields, Diatoms, Zooplankton, Functional-response, Biogeochemical Model, Upwelling Zone .



or N). These approaches are known as NPZ (Nitrogen, Phytoplankton, Zooplankton) models, because they include the relationships among these 3 basal components of the biological production in the ocean, i.e., nutrients, phytoplankton, and zooplankton. These NPZ models have been widely used to study the dynamics of plankton communities [10]. They basically consist in a system of equations accounting for the evolution of nutrients, phytoplankton, and zooplankton in which the effects of mortality, nutrient consumption by phytoplankton, and the consumption of phytoplankton by zooplankton are included. In these models, one of the essential assumptions is that the NPZ relationships occur within the photic zone [11].

NPZ models use simple linear or non-linear relationships between the three components, and because of that they may not account for some more complex relationships taking place in field conditions. For example, some field observations indicate that a large proportion of phytoplankton biomass may sink in highly productive coastal zones without being grazed by zooplankton [12], meaning that zooplankton may not fully exploit their prey (diatoms). A possible explanation for this suggests that diatoms reaching a high concentration (during the spring bloom) may release some toxic compounds which can inhibit zooplankton growth, and such phenomenon is viewed as a mechanism of defence of diatoms against their predators [13] [14] [15] [16]. These toxic effects induced by highly concentrated diatoms on herbivores zooplankton has also been suggested as a process preventing an exacerbated predation, so that allowing diatoms to recover their populations more rapidly [17] [18], [19]. For instance, in field studies [20] and laboratory [21] [22], it has been shown that diatoms toxicity can act as a strong factor impacting the feeding rate and the growth of planktonic copepods (main grazers) with negative consequences on their population dynamics. These copepods-diatoms interactions have been however matter of debate regarding their actual impact on zooplankton dynamics in the ocean [23][24]. The existence and effect of such feedback mechanisms of diatoms against zooplankton predation has not yet been assessed when developing and applying NPZ models. In this work, we test the hypothesis that the inhibition of zooplankton growth by highly concentrated diatoms will affect the dynamics of a hypothetical planktonic system in a coastal upwelling zone, and such an effect will have implications in the applicability of NPZ models. For this, we studied the behaviour of the solutions for the three components N, P, Z, using a 3- differential equation system based on the Holling IV type functional response [25]. Ultimately, we aimed at describing the dynamics of this simplified ecosystem by examining the behaviour of solutions in the infinite over a 3-D space.

**Theorem 1.** *The global dynamics on the Poincaré ball of system NPZ in the positive region is as is shown in Figure 1*

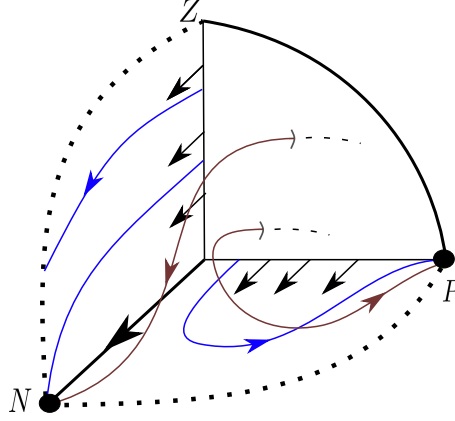


FIGURE 1. Global dynamics of system NPZ in the positive region.

## 2. PROOF OF THEOREM 1

The analytical model  $NPZ$  (0D) that will be developed in this article is based on the NPZ model structure presented by Franks (2002) [10]. The model NPZ represents the nutrient-phytoplankton-zooplankton interaction locally in an upwelling system, with a constant input of nutrients and dominated by diatoms (it is adjusted as the only food for the zooplankton), where diatoms in high concentrations have an inhibitory effect on zooplankton, thus progressing their growth.

The model has the form

$$(1) \quad \begin{aligned} \dot{N} &= a + \delta_p P + \delta_z Z + \frac{\mu\gamma PZ}{K_z + P + \beta P^2} - \frac{rNP}{K_p + N}, \\ \dot{P} &= \frac{rNP}{K_p + N} - \delta_p P - \frac{\mu PZ}{K_z + P + \beta P^2}, \\ \dot{Z} &= \frac{\epsilon\mu PZ}{K_z + P + \beta P^2} - \delta_z Z. \end{aligned}$$

where  $N$  represent the nutrient,  $P$  the phytoplankton and  $Z$  the zooplankton, the dot  $(\dot{\phantom{x}})$  represent the derivative with respect the time. The parameters are all positives.

- $r$ : Maximum specific growth rate of phytoplankton.
- $K_z, K_p$ : Average saturation constant for zooplankton and phytoplankton respectively.
- $\delta_z, \delta_p$ : Mortality rate of zooplankton and phytoplankton respectively.
- $\epsilon$ : Zooplankton assimilation efficiency.
- $\gamma$ : Fraction not assimilated by zooplankton.
- $\beta$ : Inhibitory parameter of phytoplankton.
- $\mu$ : Maximum specific growth rate of zooplankton.

Our system (1) is rational, and in order to study its dynamics of a mathematical point of view we can introduce a reparametrization of the time to get a polynomial vector field. In fact, we consider the re-scaling in the time

$$(2) \quad \frac{dt}{d\tau} = (K_z + P + \beta P^2)(K_p + N) > 0,$$

and the rational vector field (1) becomes

$$(3) \quad \begin{aligned} N' &= (K_z + P + \beta P^2)(-rNP + a(K_p + N) + \delta_p P(K_p + N) + \delta_z Z(K_p + N)) + \\ &\quad \mu\gamma PZ(K_p + N), \\ P' &= P(K_z + P + \beta P^2)(rN - \delta_p(K_p + N)) - \mu PZ(K_p + N), \\ Z' &= -Z(K_p + N)(K_z\delta_z + P(\delta_z + \beta\delta_z P + \mu(\gamma - 1))), \end{aligned}$$

where ( )' denotes the derivative with respect to  $\tau$ . Since our system represent a biological model, we are interested in the positive octant, i.e. in  $\Omega = \{(N, P, Z) : N \geq 0, P \geq 0, Z \geq 0\}$  where the model has a biological meaning. Note that  $(K_z + P + \beta P^2)(K_p + N)$  is positive on  $\Omega$ .

We consider different approach to analyze the dynamics of system (3).

Considering the conditions on the parameters (all positives), the finite equilibria of system (3) are not in the region of interest  $\Omega$ , so we do not have finite equilibria to analyze in our region of study.

We can note that the planes  $P = 0$  and  $Z = 0$  are invariant for the vector field. So we do a study of the vector field on these planes.

- If  $P = 0$  we have a two dimensional vector field:

$$(4) \quad \begin{aligned} N' &= K_z(a(K_p + N) + \delta_z(K_p + N)Z), \\ Z' &= -K_z\delta_z(K_p + N)Z, \end{aligned}$$

We can see that on the  $N$ -axis, the flow is increasing in the  $N$ -direction and invariant on the  $Z$ -direction. On the other hand, on the  $Z$ -axis the flow is increasing in the  $N$ -direction and decreasing on the  $Z$ -direction. Also we can note that  $N' > 0$  and  $Z' < 0$  in the positive region. We do a rescaling on the time of system (4) by the common factor  $K_z(K_p + N)$  to get

$$(5) \quad N' = (a + \delta_z Z), \quad Z' = -\delta_z Z.$$

On the infinite region, system (5) on the local chart  $U_1$  has the form

$$(6) \quad \begin{aligned} z_1' &= -z_1(az_2 + \delta_z(1 + z_1)), \\ z_2' &= -z_2(az_2 + \delta_z z_1) \end{aligned}$$

On the infinite, i.e. for  $z_2 = 0$  system (6) has two equilibria  $p_1 = (0, 0)$  and  $p_2 = (-1, 0)$ , the last equilibrium has eigenvalues  $\delta_z > 0$  of multiplicity two, and then it is a unstable node, however it is not located at the positive region. The origin of  $U_1$  is a semi-hyperbolic

equilibrium with eigenvalues  $-\delta_z < 0$  and  $0$ . Doing the study of the dynamics for the semi-hyperbolic equilibrium (see Theorem 2.19 in [26]) we arrive that the equilibrium is a saddle-node with a stable separatrix on  $z_2 = 0$  and the invariant  $z_2$ -axis is decreasing in the  $z_2$ -direction, see Figure 2 (b).

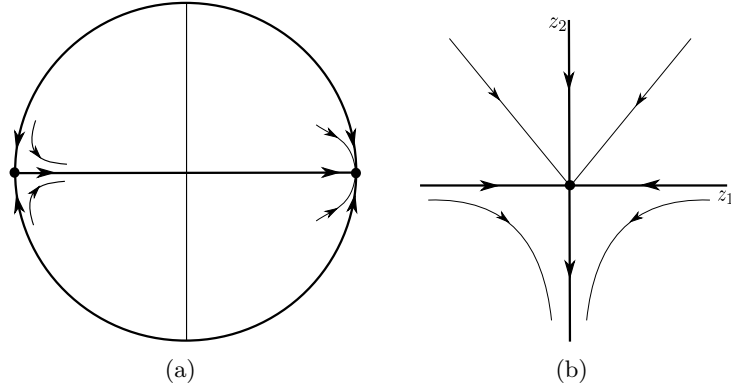


FIGURE 2. Study of the infinity of system (5). (a): representation of the origin of  $U_1$  in the Poincaré disk (our interest is in the positive region). (b): Origin of  $U_1$ .

The study on the local chart  $U_2$  does not give the origin as an equilibrium point. Considering the analysis of the finite and infinite region we have that on the plane  $P = 0$  the dynamics of system (5) is as is shown in Figure 3. We recall that here we eliminate a common factor of the original system.

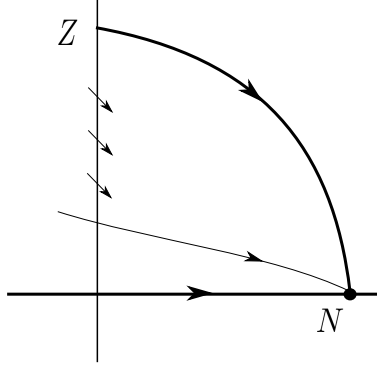


FIGURE 3. Global dynamics in the positive quadrant of system (5).

- If  $Z = 0$ , we have that  $Z' = 0$ , so we can consider the planar vector field:

$$(7) \quad \begin{aligned} N' &= (K_z + \beta P^2 + P)(a(K_p + N) + \delta_p P(K_p + N) - NPr), \\ P' &= P(K_z + \beta P^2 + P)(Nr - \delta_p(K_p + N)). \end{aligned}$$

On the  $P$ -axes we have that  $N'|_{N=0} > 0$  and  $P'|_{N=0} < 0$ , and on the  $N$ -axis we have  $N'|_{P=0} > 0$  and  $P'|_{P=0} = 0$ . Note that  $(K_z + \beta P^2 + P)$  is a common factor of system (7), we eliminate the common factor in order to study the infinite region.

The study at the infinity give that on the local chart  $U_1$ , the system becomes:

$$(8) \quad \begin{aligned} z_1' &= -z_1(-r - rz_1 + az_2 + aK_p z_2^2 + \delta_p + z_1 \delta_p + K_p z_2 \delta_p + K_p z_1 z_2 \delta_p), \\ z_2' &= -z_2(-rz_1 + az_2 + aK_p z_2^2 + z_1 \delta_p + K_p z_1 z_2 \delta_p). \end{aligned}$$

System (8) has the origin as the unique equilibrium point in the non negative region, and this is degenerate. We apply a blow-up  $z_2 = wz_1$  to study the behaviour next to the origin and get the system

$$(9) \quad \begin{aligned} z_1' &= -z_1^3(-r - rz_1 + awz_1 + aK_p w^2 z_1^2 + \delta_p + z_1 \delta_p + K_p w z_1 \delta_p + K_p w z_1^2 \delta_p) \\ w' &= -w z_1^2 (r - \delta_p - K_p w z_1 \delta_p) \end{aligned}$$

After eliminate the common factor  $z_1^2$  we get

$$(10) \quad \begin{aligned} z_1' &= -z_1(-r - rz_1 + awz_1 + aK_p w^2 z_1^2 + \delta_p + z_1 \delta_p + K_p w z_1 \delta_p + K_p w z_1^2 \delta_p) \\ w' &= -w(r - \delta_p - K_p w z_1 \delta_p) \end{aligned}$$

On  $z_1 = 0$  we get the equilibria  $(0, 0)$  that is a saddle with eigenvalues  $\pm\beta(r - \delta_p)$  with stable separatrix on the  $z_1$ -axis and unstable separatrix on the  $w$ -axis.

Thus we can going back through the blow up to obtain the local dynamics of the origin of system (8), this is shown in Figure 4.

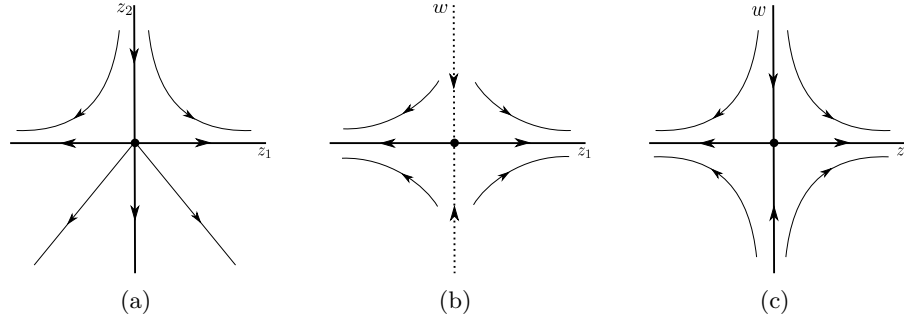


FIGURE 4. Reconstruction of the local dynamics of the origin of system (8). (a): Origin of system (8), (b): Origin of system (9), (c): Origin of system (10).

On the local chart  $U_2$  the associated system has the form:

$$(11) \quad \begin{aligned} z_1' &= (-rz_1(1+z_1) + (z_1 + K_p z_2)(az_2 + \delta_p + z_1 \delta_p)) \\ z_2' &= z_2(-rz_1 + z_1 \delta_p + K_p z_2 \delta_p), \end{aligned}$$

where the origin is a semi-hyperbolic equilibrium with eigenvalues 0 and  $\beta(r - \delta_p)$ . Applying the analysis to semi-hyperbolic equilibria via Theorem 2.19 of [26], we had to do a change of variables  $z_1 \rightarrow -z_1$  (due to the eigenvalues not null is negative), and applying the Jordan decomposition, we arrive that the equilibrium point is a saddle, with stable separatrix on the  $z_1$  axes, and unstable separatrix on the  $z_2$  axis. Reconstructing the local dynamics of the equilibria on the original variables, system (11) has an stable node at the origin (see Figure 5, the reconstruction is shown from left to right).

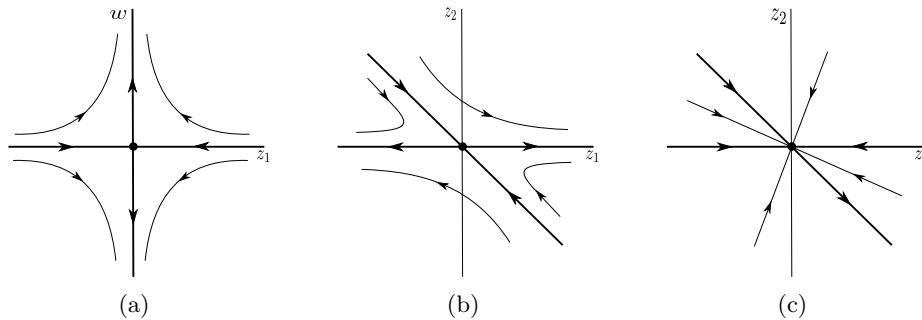


FIGURE 5. Reconstruction of the local dynamics of the origin of system (11).

From the analysis of the finite and infinite region, we have that the dynamics of system (7) is as in Figure 6.

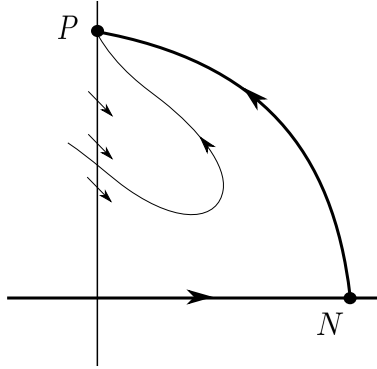


FIGURE 6. Dynamics of the positive region of system (7).

- Consider  $N = 0$ . We can note that  $N = 0$  is not an invariant plane for system (3). The vector field (3) on  $N = 0$  is

$$(12) \quad \begin{aligned} N' &= K_p(K_z + P + P^2\beta)(a + P\delta_p + Z\delta_z) + K_pPZ\gamma\mu \\ P' &= -K_pP(K_z\delta_p + \delta_pP + \beta\delta_pP^2 + Z\mu), \\ Z' &= -K_pZ(K_z\delta_z + \delta_zP + \mu(-1 + \gamma)P + \beta\delta_zP^2). \end{aligned}$$

Where  $K_p > 0$  is a common factor. On the axes  $y = 0$  we have that  $N'|_{y=0} > 0$ ,  $P'|_{y=0} = 0$  and  $Z'|_{y=0} < 0$ . On the other axes  $z = 0$  we have  $N'|_{z=0} > 0$ ,  $P'|_{z=0} < 0$  and  $Z'|_{z=0} = 0$ . Then for initial conditions on the axes  $N$  and  $Z$ , the solutions remains on the planes  $NY$  and  $NZ$  respectively. We recall that system does not have finite equilibria in the non-negative region  $\Omega$ , so we do not have equilibria on plane  $PZ$  positive.

We also can observe that  $N' > 0$ ,  $P' < 0$  under our hypothesis on the parameters. The sense of the flow on the  $Z$ -direction can be positive, zero or negative under some conditions.

This implies that the solution in the bounded positive region goes to  $N \rightarrow \infty$  and  $P \rightarrow 0$ , where for the previous analysis, the unique attractor is located at the infinite of  $N$ -axes positive.

**2.1. Poincaré Compactification on  $\mathbb{R}^3$ .** Due to our original polinomial system (3) is tridimensional we present an analysis of the infinite region in the three dimensional space, that give us more information about the dynamics at the infinity (however we prefer exhibit the before the previous analysis on the planes since its understanding is easier).

Systems (3) on the local charts of  $\mathbb{D}^3$  (see Appendix) are presented in the next.

- On  $U_1 = \{(x, y, z) \in \mathbb{D}^3 : x > 0\}$  doing  $x \rightarrow 1/z_3, y \rightarrow z_1/z_3$  and  $z \rightarrow z_2/z_3$  the related system is

$$\begin{aligned}\dot{z}_1 &= z_1(-z_3(z_1 + K_z z_3) + z_1^2 \beta)(-r(1 + z_1) + (1 + K_p z_3)(az_3 + \delta_p + z_1 \delta_p + z_2 \delta_z)) - \\ &\quad z_2 z_3 (1 + K_p z_3)(1 + z_1 \gamma) \mu \\ \dot{z}_2 &= -z_2(z_3(z_1 + K_z z_3) + z_1^2 \beta)(-r z_1 + (1 + K_p z_3)(az_3 + z_1 \delta_p + \delta_z + z_2 \delta_z)) - \\ &\quad z_1 z_2 z_3 (1 + K_p z_3)(-1 + \gamma + z_2 \gamma) \mu \\ \dot{z}_3 &= z_3(-z_3(z_1 + K_z z_3) + z_1^2 \beta)(-r z_1 + (1 + K_p z_3)(az_3 + z_1 \delta_p + z_2 \delta_z)) - \\ &\quad z_1 z_2 z_3 (1 + K_p z_3) \gamma \mu\end{aligned}$$

that on the equator (the infinity)  $z_3 = 0$  becomes

$$\begin{aligned}\dot{z}_1 &= \beta z_1^3 (-r(1 + z_1) + (\delta_p + z_1 \delta_p + z_2 \delta_z)) \\ \dot{z}_2 &= -\beta z_1^2 z_2 (-r z_1 + (z_1 \delta_p + \delta_z + z_2 \delta_z)) \\ \dot{z}_3 &= 0\end{aligned}$$

We have  $(-1, 0)$  as an equilibrium point with eigenvalues  $\beta(-r + \delta_p)$ ,  $\beta(-r + \delta_p)$  and  $-\beta(r - \delta_p + \delta_z)$ , however is not in the region of biological meaning of our systems, so it is not relevant. On the other hand  $z_1 = 0$  is a curve of equilibria  $(0, z_2, 0)$  located at the infinite of the plane  $P = 0$  on the Poincaré disk.

- On  $U_2 = \{(x, y, z) \in \mathbb{D}^3 : y > 0\}$  doing  $x \rightarrow z_1/z_3, y \rightarrow 1/z_3$  and  $z \rightarrow z_2/z_3$  the related system is

$$\begin{aligned}\dot{z}_1 &= -r z_1 (1 + z_1)(z_3 + K_z z_3^2 + \beta) + (z_1 + K_p z_3)((z_3 + K_z z_3^2 + \beta)(az_3 + \delta_p + \\ &\quad z_1 \delta_p + z_2 \delta_z) + z_2 z_3 (z_1 + \gamma) \mu) \\ \dot{z}_2 &= z_2(z_3 + K_z z_3^2 + \beta)(-r z_1 + (z_1 + K_p z_3)(\delta_p - \delta_z)) + z_2 z_3 (z_1 + K_p z_3)(1 + z_2 - \gamma) \mu \\ \dot{z}_3 &= z_3((z_3 + K_z z_3^2 + \beta)(-r z_1 + (z_1 + K_p z_3)\delta_p) + z_2 z_3 (z_1 + K_p z_3) \mu).\end{aligned}$$

Taking  $z_1 = z_3 = 0$  we get  $\dot{z}_1 = 0, \dot{z}_2 = 0, \dot{z}_3 = 0$ . Thus  $(0, z_2, 0)$  is a curve of equilibria on the infinite on the local chart  $U_2$ .

- On  $U_3 = \{(x, y, z) \in \mathbb{D}^3 : z > 0\}$  doing  $x \rightarrow z_1/z_3, y \rightarrow z_2/z_3$  and  $z \rightarrow 1/z_3$  the related system is

$$\begin{aligned}\dot{z}_1 &= (z_3(z_2 + K_z z_3) + z_2^2 \beta)(-r z_1 z_2 + (z_1 + K_p z_3)(az_3 + z_2 \delta_p + \delta_z + z_1 \delta_z)) + \\ &\quad z_2 z_3 (z_1 + K_p z_3)(z_1(-1 + \gamma) + \gamma) \mu \\ \dot{z}_2 &= z_2(z_3(z_2 + K_z z_3) + z_2^2 \beta)(r z_1 - (z_1 + K_p z_3)(\delta_p - \delta_z)) + z_2 z_3 (z_1 + K_p z_3)(-1 + \\ &\quad z_2(-1 + \gamma)) \mu \\ \dot{z}_3 &= z_3(z_1 + K_p z_3)(K_z z_3^2 \delta_z + z_2^2 \beta \delta_z + z_2 z_3(\delta_z + (-1 + \gamma) \mu)).\end{aligned}$$

Where clearly the origin is an equilibrium point, but it is degenerate. Note that is located on the curves of equilibria at the infinite region.

From the analysis on the local charts we get the equilibria on the infinite region, that are on our region of study are shown in Figure 2.1.



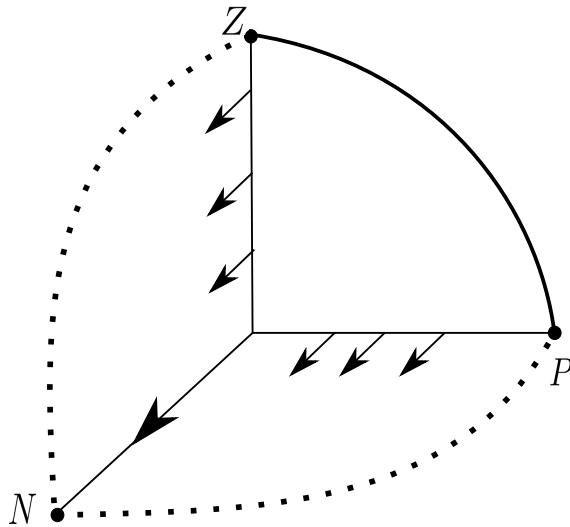


FIGURE 7. Equilibria at the infinite region of system (3).

The previous analysis give us the global dynamics on the positive region which is shown in Figure 1.

This complete the proof of Theorem 1.

### 3. DATA COMPARISON

For testing the performance of our model, we used field data obtained from a time series study carried out in the coastal zone of central-southern Chile at Station 18 ( $36^{\circ}30' S$ ) (described in [27]). From this time series, we used data for the period January through February 2003. Data for Nitrate concentration and Phytoplankton biomass (chlorophyll-a) were for the upper 20  $m$  layer. The time series also included monthly estimates of zooplankton biomass, obtained as described in Escrivano et al.2007 [28]. Biomass was measured as dry weight ( $mgm^{-2}$ ), which was then converted to  $mgCm^{-2}$ , assuming a  $C$  content of 40% of the bulk of biomass [28], although to standardize with the other variables in the NPZ model, both chlorophyll-a and zooplankton biomass were thereafter converted to using the  $C : N$  Redfield ratios [29]. For further test against a NPZ model, we used data from a ROMS-PISCES model, obtained from a 3 -  $D$  physical-biogeochemical simulation with a spatial resolution of  $1/12^{\circ}$ . This biogeochemical model PISCES (Pelagic Interactions Scheme for Carbon and Ecosystem Studies) [30][31]; was forced by the regional circulation model ROMS (Regional Ocean Modelling System) [32]. PISCES is a biogeochemical model based on functional groups of plankton [33], simulating the biogeochemical cycles of  $C$  and nutrients (nitrate, ammonium, phosphate, silicate, and iron). The model simulates two size classes of functional groups of phytoplankton (nanophytoplankton and diatoms) and zooplankton (micro- and mesozooplankton), also detritus (dead cells and faecal particles). The metabolism of  $C$  performed by phytoplankton depends on light, temperature, and nutrients availability. The model was set for outputs intervals of 3 days since August 2002 through December 2008 for 32 depths, which were interpolated according to available depths at Station 18 of the field time series (0, 5, 10, 15, 20, 30, 40, 50, 80 m), also adjusting the dates and geographic position to the nearest field observations. Data on diatoms and zooplankton biomass and nitrate were

standardized in at the depth of 20m which was assumed as representing a mid-depth of the photic zone at Station 18.

To evaluate the performance of the model, a simulation was carried out for a period of 60 days, considered as an active upwelling period, for which the parameters described in Table 3, the time series data and the output of the Roms-PISCES model were used.

Parametro	
$a$	1
$r$	$\frac{6}{10} d^{-1}$
$K_z$	$20 \mu mol CL^{-1}$
$K_p$	$\frac{39}{100} \mu mol NL^{-1}$
$\delta_z$	$\frac{3}{100} d^{-1}$
$\delta_p$	$\frac{1}{100} d^{-1}$
$\epsilon$	$\frac{4}{10}$
$\gamma$	$\frac{6}{10}$
$\beta$	$\frac{5}{4}$
$\mu$	$\frac{3}{10}$

TABLE 1. Values of the parameters for numerical simulations.

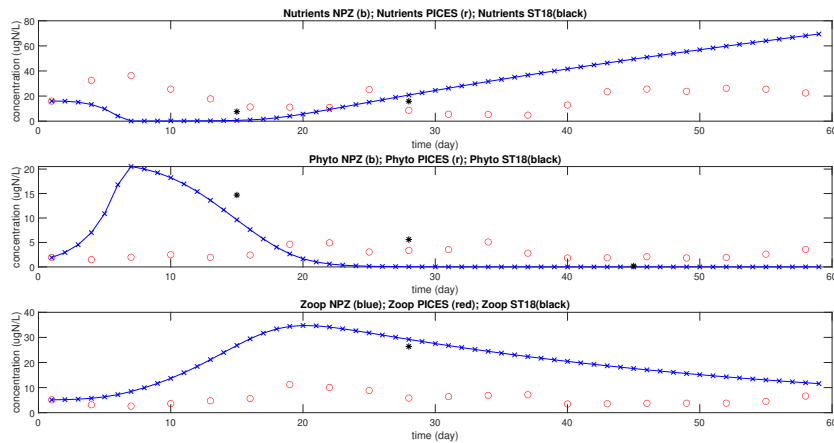


FIGURE 8. Comparison of time series data, Roms-PISCES model, NPZ model.

Fig. 7 illustrates a graphical simulation of the NPZ model from the data obtained with the ROMS-PISCES. It can be seen that our model outputs are similar to those observed at the time series, while when compared to those of the ROMS-PISCES model our results exhibit steeper slopes, although zooplankton biomasses are highly correlated ( $p < 0.05$ ,  $r = 0.76$ ).

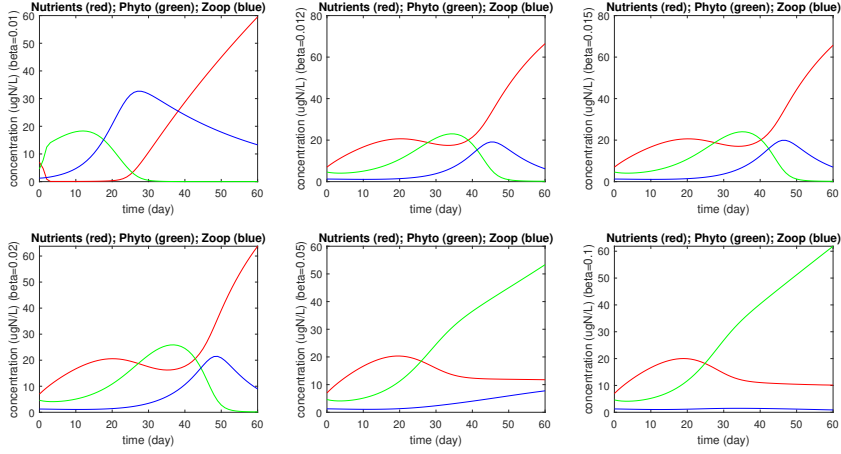


FIGURE 9. Simulations for different values of the inhibitory parameter.

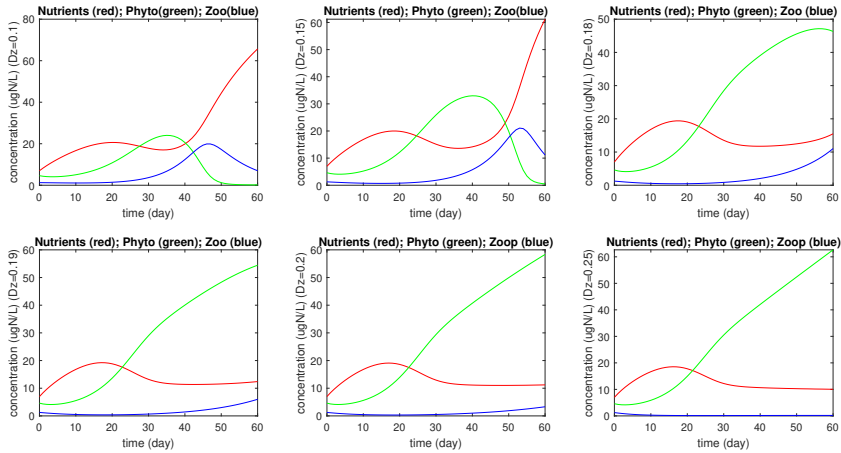


FIGURE 10. Simulations for different values of the zooplankton mortality parameter.

The NPZ model is highly sensitive to the inhibition parameter ( $\beta$ ), and small changes in this parameter can cause drastic fluctuations in the phytoplankton and zooplankton dynamics. Greater values of  $\beta$  result in zooplankton collapses, preventing its growth in biomass during the upwelling season. Like  $\beta$ , the mortality parameter is also highly sensitive to small changes causing drastic fluctuations in the model dynamics.

Our analytical approach of NPZ modelling equations indicates that under presence of toxicity conditions of diatoms (prey) affecting zooplankton (predators) the system does not reach an equilibrium,

i.e., diatoms and zooplankton maintain unpredictable dynamics. Moreover, under a condition of phytoplankton extinction, nutrients increased while zooplankton diminished, both in finite and infinite time scales. These dynamics appeared consistent with observations in natural situations. For instance, severe toxicity induced by high diatoms aggregation in the upwelling zone of central-southern Chile, zooplankton becomes greatly depleted up to an apparently local extinction [34]. The phenomenon has also been observed upon greatly increased phytoplankton patches where zooplankton tend to disappear or seem to be uncoupled to phytoplankton biomass [16],[35] [36]. Our findings from our analytical approach are also consistent with the time series obtained by the ROMS-PISCES model, as well as those from field data at Station 18 for a time window of 60 days (January-February), with same initial conditions of nutrients, phytoplankton and zooplankton. However, the number of observations at Station 18 are too few (two observational points in 2003) for statistical comparisons with analytical results. Further observations indicate that our analytical model is highly sensitive to the inhibition parameter ( $\beta$ ). Such that small variations in this parameter can result in drastic changes in the dynamics of phytoplankton and zooplankton. For instance, values greater than result in a collapse of zooplankton, which cannot increase in biomass and finally become non-sustainable. It can also be seen that  $\beta$  is strongly related to the carrying capacity of the system ( $K$ ), and so becoming an essential parameter for the zooplankton dynamics in the proposed system. It is important to mention that our analytical model can hardly reproduce field data, or those obtained with the ROMS-PISCES model. This because, there are multiple factors not considered in our model which can influence phytoplankton and zooplankton in a natural situation, or which can be included in the ROMS-PISCES model. For example, variation in light intensity, advection, diffusion, allochthonous inputs and interactions with other organisms [37],[38] [31]. The study of prey-predator interactions has long captured the interest of the ecology mostly because it is assumed as a fundamental process for understanding and modelling ecosystems [39]. In this respect, diatoms can produce several toxins, such as the domoic acid (DA), which is a neurotoxic compound. It has been estimated that copepods can accumulate between 5% to 50% of consumed DA [40] [41] Other studies showed that adults and copepodite stages of *Calanus* sp. while grazing may cause an increase in DA of the diatom *Pseudonitzschia seriata*, and so inducing the production of DA in *P. obtusa* which is non-toxic [42], [43]. Also, this compound has been found affecting the grazing patterns of some copepods and Krill. Other compounds related to diatoms toxicity are the poli-unsaturated aldehydes (PUA), which are synthesized from the fatty acids when the cells become damaged [44] [45]. These aldehydes act by inhibiting the reproductive success of copepods [34]. This effect has been observed in the field associated with a high diatoms concentration, for example in the Adriatic Sea [24] Bahía Dabob: Pacífico norte [36], in shallow Waters off Roscoff in the English Channel [46], and in the upwelling system in southeast Pacific [47], Norway fjors [48], also in laboratory when copepods are fed with monocultures of certain species [49][24] [13]. The inhibition of copepods reproduction by diatoms has been interpreted as a defence mechanism of diatoms against grazing [13].

Our analytical approach of the NZ dynamics allowed us to conclude that feedback mechanisms may indeed exist in the diatoms-zooplankton relationship in nature, and their consideration in the biogeochemical NPZ models will strengthen their predictions and help to provide more realistic outcomes when simulating variation in the C budget in highly productive coastal upwelling systems.

#### 4. APPENDIX: IRREDUCIBLE INVARIANT ALGEBRAIC CURVES AND PUISEUX SERIES

Below we provide definitions and results used in the article.

#### 4.1. Study of equilibria. Let

$$(13) \quad \mathcal{X} = f(x)$$

be the vector field associated to a polynomial system  $X' = f(X)$ . Let  $q$  be an equilibrium point of  $\mathcal{X}$ .

If some of the two eigenvalues  $\lambda_1, \lambda_2$  of the linear part of the vector field  $\mathcal{X}$  at the equilibrium point  $q$  is not zero, then this equilibrium is called *elementary*.

The local phase portrait of an elementary equilibrium  $q$  that has both eigenvalues non-zero, i.e. is an hyperbolic equilibrium point, can be studied using, for instance, Theorem 2.15 of [26], and can be a saddle, a node, a focus or a center.

If an elementary equilibrium point  $q$  has one eigenvalue zero is called a *semi-hyperbolic* equilibrium point. The local phase portrait of a finite semi-hyperbolic equilibrium point of a polynomial system can be a saddle, a node or a saddle-node, see again for example [26]. The local phase portrait of a semi-hyperbolic equilibrium  $q$  can be described using, for instance, Theorem 2.19 of [26].

When both eigenvalues are equals to zero, but the linear part of  $\mathcal{X}$  at the equilibrium point  $q$  is not identically the zero matrix, we say that  $q$  is a *nilpotent* equilibrium point. The local phase portrait of a nilpotent equilibrium point can be studied using Theorem 3.5 of [26]. If  $q$  is a finite nilpotent equilibrium point, it only can be a saddle, a center, or a cusp.

Finally, we have a degenerate equilibrium point  $q$  if the Jacobian matrix of  $\mathcal{X}$  at  $q$  is identically zero, if also  $q$  is isolated inside the set of all equilibrium points we say that  $q$  is a *linearly zero* equilibrium point. The study of the local phase portraits of such equilibria needs special changes of variables called blow-ups, see for more details Chapter 3 of [26].

#### 4.2. Poincaré compactification of $\mathbb{R}^3$ . In order to give a detailed proof of Theorem 1 we need to introduce the Poincaré compactification.

We consider a polynomial vector field  $\mathcal{X} = (P, Q, R)$  associated to the polynomial differential system

$$\dot{x} = P(x, y, z), \quad \dot{y} = Q(x, y, z), \quad \dot{z} = R(x, y, z).$$

The polynomial differential system has degree  $n$ , where  $n$  is defined as  $n = \max\{\deg(P), \deg(Q), \deg(R)\}$ .

Now we shall describe the equations of the Poincaré compactification of a polynomial differential system in  $\mathbb{R}^3$ .

We consider the local charts  $(U_k, \phi_k)$  and  $(V_k, \psi_k)$  for  $k = 1, 2, 3$  on the disc  $\mathbb{D}^3$  defined by

$$\begin{aligned} U_k &= \{x = (x_1, x_2, x_3) \in \mathbb{D}^3 : x_k > 0\}, \\ V_k &= \{x = (x_1, x_2, x_3) \in \mathbb{D}^3 : x_k < 0\}, \end{aligned}$$

where the diffeomorphisms  $\phi_k : U_k \rightarrow \mathbb{R}^3$  for  $k = 1, 2, 3$  are

$$\begin{aligned} \phi_1(x) &= \left( \frac{x_2}{x_1}, \frac{x_3}{x_1}, \frac{1}{x_1} \right) = (z_1, z_2, z_3), \\ \phi_2(x) &= \left( \frac{x_1}{x_2}, \frac{x_3}{x_2}, \frac{1}{x_2} \right) = (z_1, z_2, z_3), \\ \phi_3(x) &= \left( \frac{x_1}{x_3}, \frac{x_2}{x_3}, \frac{1}{x_3} \right) = (z_1, z_2, z_3), \end{aligned}$$

and  $\psi_k(x) = -\phi_k(x)$ .

Note that the coordinates  $(z_1, z_2, z_3)$  have different meaning depending on local chart. The points of the infinity, i.e. the points of the boundary  $\mathbb{S}^2$  of  $\mathbb{D}^3$  all have the coordinate  $z_3 = 0$ .

Now we give the expression of the compactified vector field  $p(\mathcal{X})$  of the polynomial vector field  $X = (P, Q, R)$  in each local chart. The expression of the compactified analytical vector field  $p(\mathcal{X})$  of  $\mathcal{X}$  of degree  $n$  on the local chart  $U_1$  of  $\mathbb{D}^3$  is

$$(14) \quad z_3^n (-z_1 P(z) + Q(z), -z_2 P(z) + R(z), -z_3 P(z)),$$

where  $z = (1/z_3, z_1/z_3, z_2/z_3)$ .

In a similar way the expression of  $p(\mathcal{X})$  in  $U_2$  is

$$(15) \quad z_3^n (-z_1 Q(z) + P(z), -z_2 Q(z) + R(z), -z_2 Q(z)),$$

where  $z = (z_1/z_3, 1/z_3, z_2/z_3)$ .

Finally the vector field  $p(\mathcal{X})$  in  $U_3$  is

$$(16) \quad z_3^n (-z_1 R(z) + P(z), -z_2 R(z) + Q(z), -z_2 R(z)),$$

where  $z = (z_1/z_3, z_2/z_3, 1/z_3)$ .

The singular points of  $p(\mathcal{X})$  which are on the boundary  $\mathbb{S}^2$  of  $\mathbb{D}^3$  (at  $z_3 = 0$ ) are called *infinite singular points*, and we call *finite singular points* to the ones which are in the interior of  $\mathbb{D}^3$ .

From equations (14), (15) and (16) it follows that the infinity  $\mathbb{S}^2$  of the Poincaré disc is invariant under the flow of the compactified vector field  $p(\mathcal{X})$ . For studying its infinite singular points,  $z_3 = 0$ , we need to study the ones that are on the local chart  $U_1$ , the ones in  $U_2$  with  $z_1 = 0$ , and the origin of the local chart  $U_3$  (if it is a singular point).

In the local chart  $V_k$ , the expression for  $p(\mathcal{X})$  is the same as in  $U_k$  multiplied by the factor  $(-1)^{n-1}$ . For more details on the Poincaré compactification in  $\mathbb{R}^3$  see [50] and chapter 5 of [26].

Two compactified polynomial differential systems on the Poincaré ball  $\mathbb{D}^3$  are *topologically equivalent* if there is a homeomorphism of  $\mathbb{D}^3$  sending orbits of one to the other system, either preserving or reversing the orientation of all the orbits.

**4.3. Poincaré compactification of  $\mathbb{R}^2$ .** Now we shall see how to characterize the phase portrait of a compactified vector field  $p(X)$  in the Poincaré disc  $\mathbb{D}^2$ .

Let  $Y$  a two-dimensional polynomial system. A *separatrix* of  $p(Y)$  is an orbit which is either an equilibrium point, or a trajectory which lies in the boundary of a hyperbolic sector of a finite or an infinite equilibrium point, or any orbit contained in  $\mathbb{S}^1$  (the boundary of  $D^2$ , i.e. the infinity of the plane), or a limit cycle. Neumann [52] proved that the set formed by all separatrices of  $p(Y)$ , denoted by  $S(p(Y))$  is closed.

The open connected components of  $\mathbb{D}^2 \setminus S(p(Y))$  are called canonical regions of  $Y$  or of  $p(Y)$ . A *separatrix configuration* is the union of  $S(p(Y))$  plus one orbit chosen in each canonical region. Two separatrix configurations  $S(p(Y))$  and  $S(p(\mathcal{Y}))$  are *topologically equivalent* if there is an orientation preserving or reversing homeomorphism which maps the trajectories of  $S(p(Y))$  into the trajectories of  $S(p(\mathcal{Y}))$ . The following result is due to Markus [51], Neumann [52] and Peixoto [53], who found it independently.

**Theorem 2.** *The phase portraits in the Poincaré disc  $\mathbb{D}^2$  of two compactified polynomial vector fields  $p(Y)$  and  $p(\mathcal{Y})$  are topologically equivalent, if and only if, their separatrix configurations  $S(p(Y))$  and  $S(p(\mathcal{Y}))$  are topologically equivalent.*

#### ACKNOWLEDGEMENTS

Graduate studies of A. Venegas have been supported by ANID Graduate studies funded by CONICYT-PFCHA/doctorado nacional/2018-21180829 and the Instituto Milenio de Oceanografía (IMO), Grant, IC-120019. This work is a contribution to ECLIPSE project ANID ANILLO ACT210071. The second author is supported by Anid Fondecyt Iniciación en Investigación 11230544.

#### REFERENCES

- [1] Lebour, M.V. 1922. The food of plankton organisms. *J. Mar. Biol. Assoc. UK.* 12:644-677.
- [2] Marshall, S.M. and Orr, A.P., 1955. *The Biology of a Marine Copepod, Calanus finmarchicus (Gunnerus)*, Oliver and Boyd.
- [3] Turner, J.T., 1984. The feeding ecology of some zooplankters that are important prey items of larval fish. NOAA Technical Reports. Washington, DC. NMFS7, p1-28.
- [4] Mann, K.H., 1993. Physical oceanography, foodchains & fishstocks: a review. *ICES. J. Mar. Sci.* 50:105-119.
- [5] Frost B.W., 1972 Effects of size and concentration of food particles on the feeding behavior of the marine planktonic copepod *calanus pacificus*, *Limnology and Oceanography*, Volume 17, Pages 805-815
- [6] Mullin M.M., Fuglister E., Fuglister F. J., 1975 Ingestion by planktonic grazers as a function of concentration of food, *Limnology and oceanography*.
- [7] Solomon, M.E., 1949. The natural control of animal populations. *Journal of Animal Ecology*. 18, 1-35.
- [8] Holling, C.S., 1959. Some characteristics of simple types of predation & parasitism. *Canadian Entomologist*. 91, 824-839.
- [9] Begon, M., Townsend, C.R. & Harper, J.L., 2005. *Ecology: from Individuals to Ecosystems*, fourth ed. London. Blackwell Publishing.
- [10] Franks, P.J.S., 2002. NPZ models of plankton dynamics: their construction, coupling to physics, & application. *Journal of Oceanography*. 58, 379-387.
- [11] Steele, J.H., 1958. The quantitative ecology of marine phytoplankton. *Biol. Rev.* 34:129-158.
- [12] Vargas, C.A., Cuevas, L.A., González, H.E. y G. Daneri, 2007, "Bacterial Growth Response to Copepod Grazing in Aquatic Ecosystems", *Journal of the Marine Biological Association* 87, 667-674.
- [13] Ban, S., Burns, C., Castel, J., Chaudron, Y., Christou, E., Escribano, R., Fonda Umani, S., Gasparini, S., Guerrero Ruiz, F., Hoffmeyer, M., Ianora, A., Kang, H.K., Laabir, M., Lacoste, A., Miralto, A., Ning, X., Poulet, S., Rodriguez, V., Runge, J., Shi, J., Starr, M., Uye, S., Wang, Y., 1997. The paradox of diatom-copepod interactions. *Mar. Ecol. Prog. Ser.* 157, 287-293.
- [14] Colebrook, J.M., 1982. Continuous plankton records: seasonal variation in the distribution & abundance of plankton in the North Atlantic Ocean & the North Sea. *J. Plankton Res.* 4, 435-462.
- [15] Verity, P.G. and Smetacek, V., 1996. Organism life cycles, predation and structure of pelagic ecosystems. *Mar. Ecol. Prog. Ser.* 130, 277-293.

- [16] Miralto, A., Guglielmo, L., Zagami, G., Buttino, I., Granata, A. and Ianora, A., 2003. Inhibition of population growth in the copepods *Acartia clausi* and *Calanus shelgolandicus* during diatom bloom. *Mar.Ecol.Prog.Ser.*254,253–268.
- [17] Teegarden, G.J., 1999. Copepod grazing selection and particle discrimination on the basis of PSP toxin content. *Marine Ecology Progress Series.*181,163–176.
- [18] Wolfe, G., 2000. The chemical defense ecology of marine unicellular plankton: constraints, mechanisms & impacts. *Biological Bulletin.*198,225-244.
- [19] Sukhanov, V. and Omelko, A., 2002. Dynamics of feeding preferences by a predator. *Ecological Modelling.*154,203-206.
- [20] Nielsen, T.G., Lokkegaard, B., Richardson, K., Pedersen, F.B. and Hansen, L., 1993. *Marine Ecology Progress Series.*95:115-131.
- [21] Ives, J.D., 1987. Possible mechanisms underlying copepod grazing responses to levels of toxicity in red tide dinoflagellates. *J.Exp.Mar. BioI.Ecol.* 112,131-145.
- [22] Nejstgaard, J.C. and Solberg, P.T., 1996. Repression of copepod feeding and fecundity by the toxic haptophyte *Prymnesium patelliferum*. *Sarsia* 81,339–344.
- [23] Irigoien, X., Huisman, J. & Harris, R., 2004 Global biodiversity patterns of marine phytoplankton and zooplankton. *Nature* 429, 863–867. <https://doi.org/10.1038/nature02593>
- [24] Ianora, A., Miralto, A., Poulet, S.A., Carotenuto, Y., Buttino, I., Romano, G., Casotti, R., Pohnert, G., Wichard, T., Colucci-D'Amato, L., Terrazzano, T. and Smetacek, V. 2004. Aldehyde suppression of copepod recruitment in blooms of a ubiquitous planktonic diatom. *Nature.* 429,403-407.
- [25] Andrews, J. F., 1968. A mathematical model for the continuous culture of microorganisms utilizing inhibitory substrates. *Biotechnol. Bioeng.* Vol. 10, No. 6, 707–723.
- [26] Dumortier, F., Llibre, J. and Artés, J.C., 2006. *Qualitative theory of planar differential systems.* Universitext. Springer-Verlag, Berlin.
- [27] Rubén Escribano, Carmen E. Morales, 2012 Spatial and temporal scales of variability in the coastal upwelling and coastal transition zones off central-southern Chile (35-40°S), *Progress in Oceanography*, Volumes 92-95, Pages 1-7, ISSN 0079-6611,
- [28] Escribano, R., Hidalgo, P., González, H., Giesecke, R., Riquelme-Bugueño, R. & Manríquez, K. 2007. Seasonal & interannual variation of mesozooplankton in the coastal upwelling zone off central-southern Chile. *Progress in Oceanography.*75,470-485.
- [29] Redfield, A.C., B.H. Ketchum, and F.A. Richards. 1963. The influence of organisms on the composition of sea-water. Pp. 26–77 in *The Sea. Volume 2: The Composition of Sea-Water: Comparative and Descriptive Oceanography.* M.N. Hill, ed., Interscience Publishers, New York.
- [30] Aumont, O. and Bopp, L. 2006, Globalizing results from ocean in-situ iron fertilization studies, *Global Biogeochem. Cy.*, 20, GB2017, doi:10.1029/2005GB002591.
- [31] Aumont, O. Ethé, C. Tagliabue, A., Bopp, L., Gehlen, M., 2015 PISCES-v2: An ocean biogeochemical model for carbon and ecosystem studies. *Geoscientific Model Development Discussions* Vol. 8, 1375-1509, doi:10.5194/gmdd-8-1375-2015
- [32] Shchepetkin, Alexander & McWilliams, James. 2005. The Regional Oceanic Modeling System (ROMS): a split-explicit, free-surface, topography-following- coordinate ocean model. *Ocean Modelling.* 9. 347-404. 10.1016/j.ocemod.2004.08.002.
- [33] Le Quere, C., Harrison, S. P., Prentice, I. C., Buitenhuis, E. T., Aumont, O., Bopp, L., Cluastre, H., Cotrim da Cunha, L., Geider, R., Giraud, X., Klaas, C., Kohfeld, K. E., Legendre, L., Manizza, M., Platt, T., Rivkin, R. B., Sathyendranath, S., Uitz, J., Watson, A. J. and Wolf-Gladrow, D. 2005. Ecosystem dynamics based on plankton functional types for global ocean biogeochemistry models. *Global Change Biology*, 11 (11). pp. 2016-2040. ISSN 1354-1013



- [34] Poulet, S.A., Escribano, R., Hidalgo, P., Cueff, A., Wichard, T., Aguilera, V., Vargas, C.A. & Pohnert, G. 2007. Collapse of *Calanus chilensis* reproduction in a marine environment with high diatom concentration. *Journal of Experimental Marine Biology and Ecology*. 352 187–199.
- [35] Leising, A.W., Pierson, J.J., Halsband-Lenk, C., Horner, R., Postel, J., 2005. Copepod grazing during spring blooms: does *Calanus pacificus* avoid harmful diatoms? *Prog. Oceanogr.* 67, 384–405.
- [36] Halsband-Lenk, C., J. J. Pierson, and A. W. Leising. 2005. Reproduction of *Pseudocalanus newmani* (Copepoda: Calanoida) is deleteriously affected by diatom blooms: a field study. *Progress in Oceanography* 67:332–348.
- [37] Mitra, A., Castellani, C., Gentleman, W.C., Jónasdóttir, S.H., Flynn, K.J., Bode, A., Halsband, C., Kuhn, P., Licandro, P.B., Agersted, M.D., Calbet, A., Lindeque, P.K., Koppelman, R., Møller, E.F., Gislason, A., Nielsen, T.G. & John, M. 2004. Bridging the gap between marine biogeochemical and fisheries sciences; configuring the zooplankton link. *Progress in Oceanography*. 129, 176–199.
- [38] Merico, A., Bruggeman, J., and Wirtz, K. 2009: A trait-based approach for downscaling complexity in plankton ecosystem models, *Ecol. Model.*, 220, 3001–3010, doi:10.1016/j.ecolmodel.2009.05.005,
- [39] Flynn, K.J. & Mitra, A. 2016. Why Plankton Modelers Should Reconsider Using Rectangular Hyperbolic (Michaelis-Menten, Monod) Descriptions of Predator-Prey Interactions. *Frontiers in Marine Science*. 3, 165.
- [40] Maneiro, I., Iglesias, P., Guisande, C., Riveiro, I., Barreiro, A., Zervoudaki, S. & Granéli, E. 2005. Fate of domoic acid ingested by the copepod *Acartia clausi*. *Mar. Biol.* 1(48), 123–130
- [41] Tammilehto, A., Nielsen, T.G., Krock, B., Møller, E.F., Lundholm, N., 2012. *Calanus* spp.- vectors for the biotoxin, domoic acid, in the arctic marine ecosystem? *Harmful Algae* 20, 165–174.
- [42] Harðardóttir, S., Pancic, P., Tammilehto, A., Nielsen, T.G., Krock, B., Møller, E.F., & Lundholm, N. 2015. Dangerous relations in the arctic Marine food web: interactions between toxin producing *Pseudo-nitzschia* diatoms & *calanus* copepodites. *Marine Drugs*. 1(3), 3809–3835
- [43] Tammilehto, A., Nielsen, T.G., Krock, B., Møller, E.F. & Lundholm, N. 2015. Induction of domoic acid production in the toxic diatom *Pseudo-nitzschia seriata* by calanoid copepods. *Aquat. Toxicol.* 159, 52–61.
- [44] Miralto, A., Barone, G., Romano, G., Poulet, S.A., Ianora, A., Russo, G.L., Buttino, I., Mazzarella, G., Laabir, M., Cabrini, M. & Giacobbe, M.G. 1999. The insidious effect of diatoms on copepod reproduction. *Nature*. 402, 173–176.
- [45] Pohnert, G., Lumineau, O., Cueff, A., Adolph, S., Cordevant, C., Lange, M., Poulet, S.A. 2002. Are volatile unsaturated aldehydes from diatoms the main line of chemical defense against copepods? *Mar. Ecol. Prog. Ser.* 245, 33–45.
- [46] Poulet, S.A., Wichard, T., Ledoux, J.B., Lebreton, B., Marchetti, J., Dancie, C., Bonnet, D., Cueff, A., Morin, P. & Pohnert, G. 2006. Influence of diatoms on copepod reproduction. I. Field and laboratory observations related to *Calanus helgolandicus* egg production. *Mar. Ecol. Prog. Ser.* 308, 129–142.
- [47] Vargas, Cristian & Manríquez, Patricio & Navarrete, Sergio. (2006). Feeding by larvae of intertidal invertebrates: Assessing their position in pelagic food webs. *Ecology*. 87. 444–57. 10.1890/05-0265.
- [48] Koski, M. 2007. High reproduction of *Calanus finmarchicus* during a diatom-dominated spring bloom. *Mar. Biol.* 151, 1785–1798.
- [49] Ianora, A., Poulet, S.A., Miralto, A. & Grotoli, R. 1996. The diatom *Thalassiosira rotula* affects reproductive success in the copepod *Acartia clausi*. *Mar. Biol.* 125:279–286.

- [50] Cima, A. and Llibre, J., 1990. Algebraic and topological classification of the homogeneous cubic vector fields in the plane, *J. Math. Anal. Appl.*, 147(2),420-488.
- [51] Markus L., 1954. Global structure of ordinary differential equations in the plane: *Trans. Amer. Math Soc.*76, 127–148.
- [52] Neumann D.A., 1975. Classification of continuous flows on 2–manifolds, *Proc. Amer. Math. Soc.* 48, 73–81.
- [53] Peixoto M.M., 1973. *Dynamical Systems. Proceedings of a Symposium held at the University of Bahia*, 389–420, Acad. Press, New York.
- [54] Perko, L., 1996. *Differential Equations and Dynamical Systems. Texts in Applied Mathematics*, Springer New York.

<sup>1</sup> DOCTORAL PROGRAM IN OCEANOGRAPHY, DEPARTAMENT OF OCEANOGRAPHY, FACULTAD DE CIENCIAS NATURALES Y OCEANOGRÁFICAS, UNIVERSIDAD DE CONCEPCIÓN, CONCEPCIÓN, CHILE

<sup>2</sup> DEPARTAMENTO DE MATEMÁTICA, FACULTAD DE CIENCIAS, UNIVERSIDAD DEL BÍO-BÍO, CASILLA 5–C, VIII–REGIÓN, CONCEPCIÓN, CHILE

<sup>3</sup> DEPARTAMENTO DE OCEANOGRAFÍA, UNIVERSIDAD DE CONCEPCIÓN, CHILE

<sup>4</sup> INSTITUTO MILENIO DE OCEANOGRAFÍA, UNIVERSIDAD DE CONCEPCIÓN, CHILE

## DISCUSIÓN GENERAL

El objetivo de esta tesis fue evaluar qué factores contribuyen en mayor porcentaje a la variabilidad de la biomasa del zooplancton presente en la zona de surgencia del centro-sur de Chile. Se evidenció que los procesos advectivos a lo largo de la costa son un factor clave que modulan gran parte de los cambios en la biomasa del zooplancton, especialmente en los periodos de surgencia activa (primavera-verano). La advección horizontal en una banda costera circundante a la estación 18, contribuye a la pérdida de biomasa producto de la advección hacia el norte y mar afuera, y a la ganancia de biomasa, producto de la advección desde el sur. Por lo tanto, una parte importante de la variabilidad percibida en los datos de la estación de monitoreo pueden deberse a los procesos advectivos que ocurren en la zona circundante a la estación, puesto que la zona de surgencia de Chile centro-sur está fuertemente influenciada por la surgencia inducida por el viento.

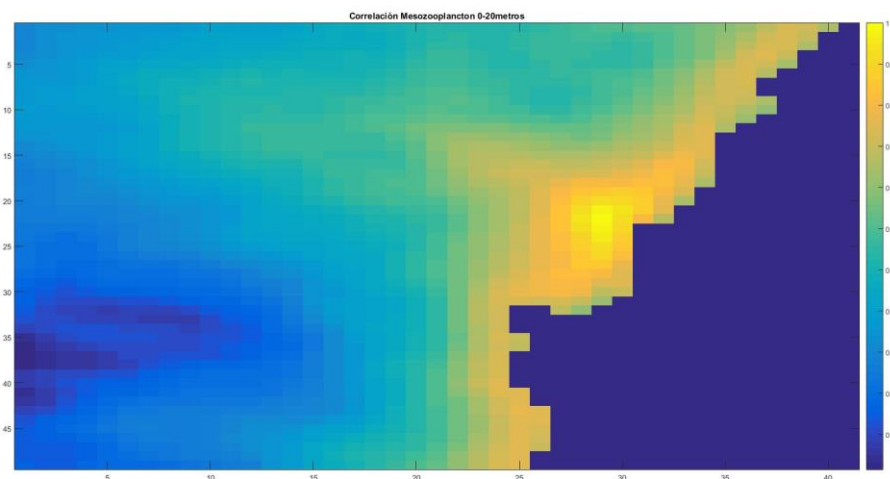


**Figura 2.** Correlación espacial del punto de grilla de la estación 18 con cada punto del dominio de estudio, para la biomasa del mesozooplancton.

En la Fig. 2 de autocorrelación espacial entre los puntos de grilla representativos de la estación 18 y los demás puntos del dominio, se puede observar un flujo hacia al norte y mar afuera, altamente correlacionado con dicho punto que puede ser explicado por la actividad de mesoescala impulsada por la surgencia (Hormazábal et al., 2013), lo cual indicaría que el modelo está capturando los procesos de mesoescala característicos de la zona de estudio.

Al evaluar los factores que influyen en la variabilidad de la biomasa, si bien la productividad local contribuye a la variabilidad observada, el modelo indica que son los procesos advectivos en los periodos de surgencia los que modulan gran porcentaje de la variabilidad observada en la zona de estudio. Esto es concordante con otros estudios realizados los cuales indican que los procesos de circulación en la costa pueden tener un impacto significativo en la dinámica poblacional de las especies dominantes del zooplancton costero, que constituyen la mayor parte de la biomasa, como los copépodos (Peterson, 1998; Escribano, 1998). Estudios realizados en la zona de transición costera central de Chile, determinaron que los remolinos de mesoescala influyen en la distribución y la biomasa de las comunidades de fitoplancton y zooplancton, además, debido a la advección de nutrientes y fitoplancton, contribuyen a extender el área de alta productividad primaria (Morales et al., 2010; Hormazábal et al., 2013), a pesar de esto los procesos advectivos no son considerados en el análisis de observaciones de series temporales *in situ* (Hugget et al., 2009; Mackas y Beaugrand, 2010; Escribano et al., 2012).

El no considerar los procesos advectivos en el estudio de datos obtenidos de estaciones de monitoreo fijas puede dar lugar a análisis sesgados sobre los procesos que modulan la variabilidad en la biomasa del plancton y, por consiguiente, en determinar la producción secundaria de los océanos. Estas estimaciones erróneas en la determinación de la biomasa pueden conducir a interpretaciones incorrectas sobre los procesos que subyacen estas variaciones, es decir control top-down o bottom-up, en particular en los sistemas de surgencia (Escribano et al., 2016).

Considerando el objetivo fundamental que fue determinar los factores que influyen en la variabilidad de la biomasa del zooplancton, una de las variables importante a estudiar fue el tiempo de respuesta de las variables biológicas/oceanográficas frente a los factores físicos. Para esto se utilizó la serie temporal obtenida del modelo, es decir, desde 2008 a 2012, y se calculó un promedio anual, obteniendo así una serie promedio diaria de esos años. Para lograr esto, estimamos el retraso temporal entre los flujos más importantes y la biomasa (es decir, los retrasos para la máxima correlación) utilizando la serie temporal completa. El desfase de 2 días entre la advección de nitrato del sur y el afloramiento de nitrato puede estar representando el tiempo necesario para que el viento favorable al afloramiento genere una corriente de afloramiento costero. Entonces hay un desfase entre el afloramiento de nitratos y la biomasa de diatomeas del sur, por un lado, y la producción

de diatomeas, por el otro (4 y 3 días, respectivamente). Este tiempo representaría el tiempo necesario de respuesta de las comunidades del fitoplancton al afloramiento costero. La producción de mesozooplancton tarda más tiempo en responder a los cambios producto de la dinámica física, lo cual queda demostrado en un retraso de 7 días a la producción local de las diatomeas. El tiempo simulado de respuestas entre la producción primaria y la producción y biomasa del zooplancton (7 y 18 días, respectivamente) resulta acorde al rango esperado para estas relaciones (Almén & Tamelander, 2020).

A pesar de que el modelo reproduce en cierta medida los ciclos estacionales de la biomasa, tanto de zooplancton como fitoplancton y los nutrientes, debemos tener en cuenta las restricciones y desviaciones obtenidas en las simulaciones. Tal es el caso de la sobreestimación de la temperatura especialmente en la capa profunda y una subestimación de los nutrientes durante este mismo periodo, lo cual se puede deber posiblemente a una subestimación de la intensidad del afloramiento de la corriente Perú-Chile (PCUC), rica en nutrientes (Silva et al., 2009). Esto se debe a una debilidad en el esquema de difusión-advección utilizado para los trazadores biogeoquímicos en el modelo (V. Echevin, com. pers.).

Por otra parte, el modelo no reproduce las salinidades bajas que presentan las aguas circundantes a la estación 18 en el periodo de invierno, mientras que salinidades más altas en aguas cercanas a la superficie se simulan con precisión durante la primavera y el verano debido al intenso afloramiento de agua ecuatorial subsuperficial (ESSW) (Schneider et al., 2016). Eso puede ser producto de la influencia de la descarga de agua dulce proveniente de los ríos Bío-Bío e Itata, los cuales tienen una gran influencia en la zona de la estación 18 (Sobarzo et al., 2007) y los cuales no fueron considerados en la configuración de la simulación utilizada, por lo cual las salinidades muestran claras discrepancias, además debemos considerar que la descarga de ríos no solo influye en la salinidad si no que afecta directamente en la dinámica de los nutrientes (Vargas et al., 2016).

Además se debe tener en cuenta que se utilizó una resolución espacial de  $1/12^\circ$  la cual no es lo suficientemente fina para capturar los procesos de meso- y submesoescala propios de una zona costera con topografía irregular, lo cual puede influir en la dinámica de los nutrientes y biomasa del fitoplancton y zooplancton, dado que estas estructuras pueden concentrar los nutrientes y biomasa al igual que extender por ejemplo la biomasa tanto del fitoplancton como el zooplancton desde la zona costera a la zona de transición costera

(Chaigneau et al., 2008; Chaigneau et al., 2009). El modelo también muestra una sobreestimación de la concentración de oxígeno disuelto presente, dado que en los datos *in situ* indican la presencia de la zona mínima de oxígeno (1 ml de  $O_2$  por litro) hasta alrededor de los 30 metros lo cual no se observa en los datos modelados, de hecho el modelo no muestra la zona de mínimo oxígeno dentro de los 80 metros del estudio, lo cual también se puede deber a la subestimación de la intensidad del afloramiento.

Todas estas desviaciones pueden ser provocadas por la falta de ríos en la configuración del modelo y a la subestimación del fenómeno de surgencia. Ambos procesos influyen en factores tales como temperatura, oxigenación y disponibilidad de nutrientes; los cuales afectan directamente en la dinámica del zooplancton y su biomasa. Por lo cual a pesar de reproducir de buena forma el ciclo estacional y poder medir la influencia de los procesos advectivos los cuales generalmente no son considerados en estudios de la biomasa del zooplancton, estos resultados deben ser considerados con cautela y teniendo en cuenta las limitaciones propias del modelado.

Para el segundo objetivo, se describió un modelo analítico NPZ (Nitrato- Fitoplancton - Zooplancton) en el cual se utilizó una respuesta funcional Holling IV para el pastoreo del zooplancton al fitoplancton. Este modelo se propuso considerando un sistema altamente productivo en el cual dominan las diatomeas las cuales a altas concentraciones se ha estudiado que se vuelven tóxicas para el zooplancton, afectando principalmente la eficiencia de eclosión y por lo tanto a la biomasa total (Poulet et al., 2007). Se debe tener en cuenta que los modelos NPZ son altamente simplificados de la dinámica del plancton, los cuales son resueltos en la capa fótica sin la influencia de la física del sistema (Franks, 2002). Nuestro objetivo fue hacer un análisis cualitativo del comportamiento de las soluciones del sistema y comparar los resultados con los obtenidos de la estación 18 y con los resultados obtenidos del modelo ROMS-PISCES en la zona de surgencia del centro sur de Chile, de tal forma de evaluar cuan significativo es el uso de este tipo de respuestas funcionales en los modelos aplicados a estas regiones altamente productivas. Sin embargo, se debe considerar que al ser sistemas simplificados es de esperar que no reproduzcan fehacientemente los datos obtenidos, al no considerar variables tales como, intensidad de la luz, advección, difusión, aporte de ríos, lluvias, otros organismos que interactúan, etc. (Mitra et al., 2004, Merico et al., 2009, Aumont et al., 2015). A pesar de lo anterior, el modelo NPZ reproduce en magnitud los datos obtenidos tanto por el modelo biogeoquímico como la serie de datos *in situ*, sin embargo, no es posible realizar un

estudio cuantitativo (ejemplo, correlaciones) con los datos obtenidos en la serie de tiempo debido a que se cuenta con 2 a 3 datos por variable en el periodo de estudio, pero podemos observar que los datos del modelo NPZ se ajustan significativamente a los datos obtenidos *in situ* y en cuanto a los datos obtenidos por el modelo RMOS-PISCES se observan ciclos muchos menos suaves pero concordantes en su evolución.

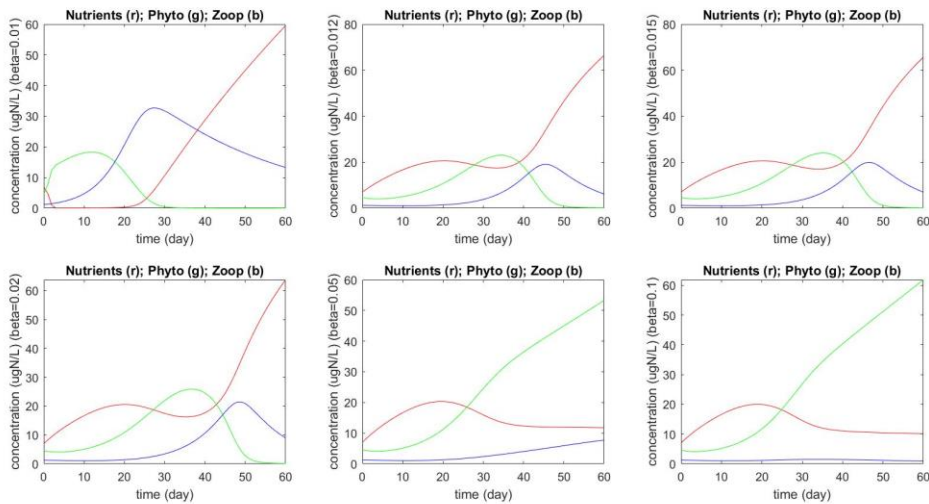


**Figura 3.** Graficas simulación del modelo NPZ para diferentes valores del parámetro inhibitorio (Beta) (rojo= nutrientes, verde= fitoplancton, azul= zooplancton).

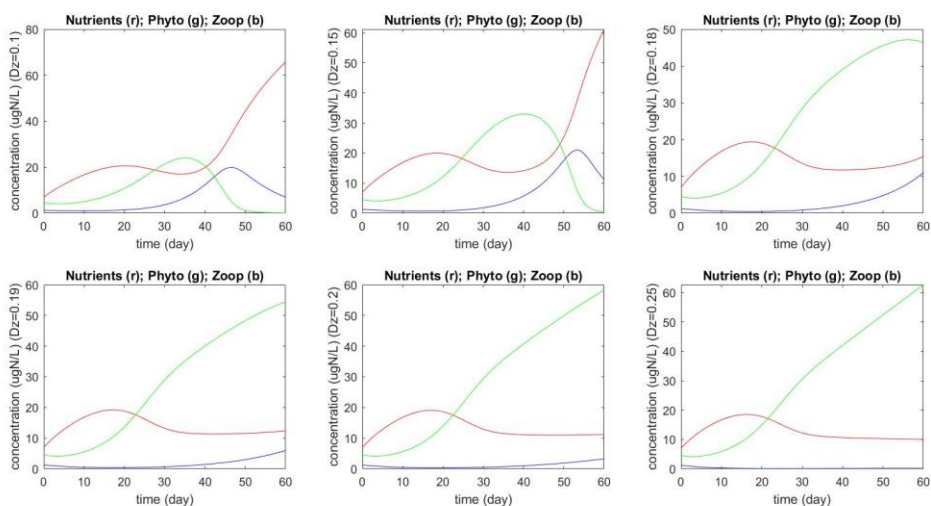


**Figura 4.** Graficas simulación del modelo NPZ para diferentes valores del parámetro de mortalidad (rojo= nutrientes, verde= fitoplancton, azul= zooplancton).

Se puede observar que el modelo plantado es altamente sensible a los parámetros de mortalidad e inhibición (parámetro inhibitorio), dado que variaciones pequeñas en estos parámetros se traducen en cambios bruscos en la dinámica del sistema. En este sentido, nuestro objetivo fue evidenciar que es necesaria la utilización de una respuesta funcional Holling IV en los estudios de modelado. Este tipo de estudios han sido de interés desde hace años debido a la importancia de comprender las interacciones entre los niveles tróficos de los ecosistemas y de esta forma mejorar el proceso de modelado (Flynn & Mitra, 2016).

El efecto de la toxicidad de las diatomeas se ha estimado que puede producirse por diversas toxinas, entre ellas el ácido domoico (AD) el cual es un compuesto neurotóxico, el cual es acumulado por los copépodos (bioacumulación) al consumir estas diatomeas, (Windeest, 1992; Maneiro et al., 2005; Tammilehto et al., 2012). Este compuesto se ha estudiado que afecta los patrones de pastoreo de algunas especies de zooplancton tales como el krill. Otro de los compuestos estudiados en la interacción zooplancton-fitoplancton son los aldehídos poliinsaturados (PUA) los cuales actúan inhibiendo el éxito de reproductivo del zooplancton (Miralto et al., 1999; Pohnert, 2002).

En conclusión, los enfoques de modelado son herramientas útiles para el estudio y comprensión de la dinámica e interacciones que ocurren en los ecosistemas y en particular los ecosistemas marinos, los cuales son altamente dinámicos e influenciados por la física. Sin embargo estos resultados deben considerados con cautela y tomando en cuenta todas las limitantes y restricciones propias de estos enfoques y por lo tanto es necesario contrarrestar con datos y estudios de campo los cuales permitan validar los resultados obtenidos.



## CONCLUSIONES

De acuerdo con los resultados vistos anteriormente, podemos afirmar que los procesos advectivos son claves en la modulación de la biomasa del zooplancton en la zona de surgencia, contribuyendo a una pérdida significativa de la biomasa en la zona costera de Chile centro-sur hacia la zona de transición y hacia el sur. Por lo cual, para la interpretación de los datos obtenidos en series de tiempo fijas, es necesario considerar estos procesos para una mejor comprensión e interpretación de los datos obtenidos. Por otra parte se pudo observar que al considerar una respuesta funcional Holling tipo IV para un modelo simple, este es capaz de reproducir los ciclos y magnitudes observadas en los datos de las observaciones.

El estudio propone la necesidad de analizar e incluir este tipo de respuestas funcionales que han sido observadas en laboratorios en modelos más detallados tales como PISCES, con configuraciones específicas para las zonas de surgencia y, de este modo, obtener representaciones más precisas de los procesos que influyen en la variabilidad de la biomasa del zooplancton. No obstante, en la interpretación de los resultados se deben considerar aquellos factores y procesos que los modelos no son capaces de reproducir y por lo cual son limitantes en el momento de la interpretación de los resultados obtenidos mediante este tipo de metodología.

La tesis provee evidencia para apoyar las hipótesis planteadas y sugiere que ambos procesos de base física (dinámica advectiva) y biológica (interacciones diatomeas-zooplancton) deberían ser considerados en las observaciones de campo y en el desarrollo de modelos biogeoquímicos que involucran la dinámica del zooplancton y su producción en biomasa en sistemas de surgencia altamente productivos.

## BIBLIOGRAFÍA.

- Albert, A., Echevin, V., Lévy, M., and Aumont, O. 2010. Impact of nearshore wind stress curl on coastal circulation and primary productivity in the Peru upwelling system. *Journal of Geophysical Research*. 115, C12033. doi:10.1029/2010JC006569
- Almén, A., Tamelander, T. 2020. Temperature-related timing of the spring bloom and match between phytoplankton and zooplankton, *Marine Biology Research*, DOI: 10.1080/17451000.2020.1846201
- Anabalón, V., Morales, C.E., González, H.E., Menschel, E., Schneider, W., Hormazabal, S., Valencia, L., Escribano, R. 2016. Micro-phytoplankton community structure in the coastal upwelling zone off Concepción (central Chile): annual and inter-annual fluctuations in a highly dynamic environment. *Progress in Oceanography*. 149 (2016) 174–188.
- Andrews, J. F., 1968. A mathematical model for the continuous culture of microorganisms utilizing inhibitory substrates. *Biotechnol. Bioeng.* Vol. 10, No. 6, 707–723.
- Arcos, D.A., Cubillos, L.A., Núñez, S.P., 2001. The jack mackerel fishery and El Niño 1997-98 effects off Chile. *Progress in Oceanography*. 49, 597–617.
- Auger, P.-A. Gorgues, T., Machu, E., Aumont, O., Brehmer, P. 2016 What drives the spatial variability of primary productivity and matter fluxes in the north-west African upwelling system? A modelling approach, *Biogeosciences*, 13, 6419–6440, 2016 [www.biogeosciences.net/13/6419/2016/](http://www.biogeosciences.net/13/6419/2016/), doi:10.5194/bg-13-6419-2016.
- Auger, P. A., Machu, E., Gorgues, T., Grima, N., and Waeles, M.: Comparative study of potential transfer of natural and anthropogenic cadmium to plankton communities in the North -West African upwelling. *Science of the Total Environment*. 505, 870–888, doi:10.1016/j.scitotenv.2014.10.045, 2015.
- Aumont, O. and Bopp, L. 2006, Globalizing results from ocean in-situ iron fertilization studies, *Global Biogeochem. Cy.*, 20, GB2017, doi:10.1029/2005GB002591.
- Aumont, O. Ethé, C. Tagliabue, A., Bopp, L., Gehlen, M., 2015 PISCES-v2: An ocean biogeochemical model for carbon and ecosystem studies. *Geoscientific Model Development Discussions* Vol. 8, 1375-1509, doi:10.5194/gmdd-8-1375-2015.
- Ban, S., Burns, C., Castel, J., Chaudron, Y., Christou, E., Escribano, R., Fonda Umani, S., Gasparini, S., Guerrero Ruiz, F., Hoffmeyer, M., Ianora, A., Kang, H.K., Laabir, M., Lacoste, A., Miralto, A., Ning, X., Poulet, S., Rodriguez, V.,

- Runge, J., Shi, J., Starr, M., Uye, S., Wang, Y., 1997. The paradox of diatom-copepod interactions. *Mar.Ecol.Prog.Ser.*157, 287-293.
- Begon, M., Townsend, C.R. & Harper, J.L., 2005. *Ecology: from Individuals to Ecosystems*, fourth ed. London. Blackwell Publishing.
  - Beaugrand, G., 2003: Long-term changes in copepod abundance and diversity in the north-east Atlantic in relation to fluctuations in the hydroclimatic environment. *Fishery Oceanography* 12:4/5, 270–283, doi.org/10.1046/j.1365-2419.2003.00248.x
  - Beaugrand, G. and Reid, P.C. (2003) Long-term changes in phytoplankton, zooplankton and salmon linked to climate. *Global Change Biology* 9: 801–817.
  - Brun, P. et al. Climate change has altered zooplankton-fuelled carbon export in the North Atlantic. *Nat. Ecol. Evol.* 3, 416–423 (2019).
  - Chaigneau, A., A. Gizolme, Grados, C., 2008: Mesoscale eddies off Peru in altimeter records: Identification algorithms and eddy spatio-temporal patterns. *Progress in Oceanography*, 79, 106 - 119, doi:10.1016/j.pocean.2008.10.013.
  - Chaigneau, A., G. Eldin, B. Dewitte, 2009: Eddy activity in the four major upwelling systems from satellite altimetry (1992 - 2007). *Progress in Oceanography*, 83, 117 - 123, doi:10.1016/j.pocean.2009.07.012.
  - Cima, A. and Llibre, J., 1990. Algebraic and topological classification of the homogeneous cubic vector fields in the plane, *J. Math. Anal. Appl.*, 147(2), 420-488.
  - Colebrook, J.M., 1982. Continuous plankton records: seasonal variation in the distribution & abundance of plankton in the North Atlantic Ocean & the North Sea. *J. Plankton Res.*4, 435–462.
  - Corredor-Acosta, A., Morales, C. E., Rodríguez-Santana, A., Anabalón, V., Valencia, L. P., Hormazabal, S., 2020. The influence of diapycnal nutrient fluxes on phytoplankton size distribution in an area of intense mesoscale and submesoscale activity off Concepción, Chile. *Journal of Geophysical Research: Oceans*, 125, e2019JC015539. <https://doi.org/10.1029/2019JC015539>.
  - Echevin, V., Aumont, O., Ledesma, J., and Flores, G.: The sea-sonal cycle of surface chlorophyll in the Peruvian upwelling system: A modelling study, *Progress in Oceanography*, 79, 167–176, doi:10.1016/j.pocean.2008.10.026, 2008.
  - Echevin, V., Albert, A., Lévy, M., Graco, M., Aumont, O., Piétri, A., Garric, G., 2014. Intraseasonal variability of nearshore productivity in the Northern Humboldt Current System: The role of coastal trapped waves. *Continental Shelf Research* 73, 14–30. <http://dx.doi.org/10.1016/j.csr.2013.11.015>.

- Escribano, R. 1998. Population dynamics of *Calanus chilensis* from northern Chile. *Fisheries Oceanography* 7: 245-251.
- Escribano, R., Hidalgo, P., González, H., Giesecke, R., Riquelme-Bugueño, R. & Manríquez, K. 2007. Seasonal & interannual variation of mesozooplankton in the coastal upwelling zone off central-southern Chile. *Progress in Oceanography* 75, 470-485.
- Escribano, R., Morales, C. E. 2012 Spatial and temporal scales of variability in the coastal upwelling and coastal transition zones off central-southern Chile (35-40°S), *Progress in Oceanography*, Volumes 92-95, Pages 1-7, ISSN 0079-6611.
- Escribano, R., Morales, C.E., 2012. Spatial and temporal scales of variability in the coastal upwelling and coastal transition zone off central-southern Chile (35-40°S). *Progress in Oceanography* 92-95, 1-7.
- Escribano, R., Hidalgo, P., Fuentes, M., Donoso, K. 2012. Zooplankton time series in the coastal zone off Chile: variation in upwelling and responses of the copepod community. *Progress in Oceanography*, 97-100, 174-186.
- Escribano, R., Hidalgo, P., Valdés, V., Frederick, L. 2014. Temperature effects on development and reproduction of copepods in the Humboldt Current: the advantage of rapid growth. *Journal of Plankton Research* 36: 104–116.
- Escribano, R., Bustos-Ríos, E., Hidalgo, P., Morales, C.E. 2016. Non-limiting food conditions for growth and production of the copepod community in a highly productive upwelling zone. *Continental Shelf Research*. 126:1-14. Doi:10.1016/j.csr.2016.07.018.
- Espinoza-Morriberón, D., V. Echevin, F. Colas, J. Tam, J. Ledesma, L. Vásquez, and M. Graco (2017), Impacts of El Niño events on the Peruvian upwelling system productivity, *Journal of Geophysical Research Oceans*, 122, doi:10.1002/2016JC012439.
- Franks, P.J.S., 2002. NPZ models of plankton dynamics: their construction, coupling to Physics & application. *Journal of Oceanography*. 58, 379–387.
- Flynn, K.J. & Mitra, A. 2016. Why Plankton Modelers Should Reconsider Using Rectangular Hyperbolic (Michaelis-Menten, Monod) Descriptions of Predator-Prey Interactions. *Frontiers in Marine Science*. 3, 165.
- Frost B.W., 1972 Effects of size and concentration of food particles on the feeding behavior of the marine planktonic copepod *calanus pacificus*, *Limnology and Oceanography*, Volume 17, Pages 805-815.
- Garreaud, R. D. & Falvey, M. The coastal winds off western subtropical South America in future climate scenarios. *International Journal of Climatology* 29, 543–554 (2009).

- Gorgues, T., Menkes, C., Aumont, O., Vialard, J., Dandonneau, Y., and Bopp, L. 2005: Biogeochemical impact of tropical instability waves in the Equatorial Pacific, *Geophysical Research Letters* 32, L24615, doi:10.1029/2005GL024110.
- Gorgues, T., Menkes, C., Slemons, L., Aumont, O., Dandonneau, Y., Radenac, M.-H., Alvain, S., Moulin, C., 2010., Revisiting the La Niña 1998 phytoplankton blooms in the equatorial Pacific, *Deep Sea Research Part I: Oceanographic Research Papers*, Volume 57, Issue 4, Pages 567-576, ISSN 0967-0637, doi.org/10.1016/j.dsr.2009.12.008.
- Harördóttir, S., Pancic, P., Tammilehto, A., Nielsen, T.G., Krock, B., Møller, E.F., & Lundholm, N. 2015. Dangerous relations in the arctic Marine food web: interactions between toxin producing *Pseudo-nitzschia* diatoms & calanus copepodites. *Marine Drugs*.1(3),3809–3835.
- Halsband-Lenk, C., J. J. Pierson, and A. W. Leising. 2005. Reproduction of *Pseudocalanus newmani* (Copepoda: Calanoida) is deleteriously affected by diatom blooms: a field study. *Progress in Oceanography* 67:332–348.
- Hays, Graeme & Richardson, Anthony & Robinson, Carol. (2005). Climate change and marine plankton. *Trends in ecology & evolution*. 20. 337-44. 10.1016/j.tree.2005.03.004.
- Hirst, A.G., Bunker, A.J., 2003. Growth of marine planktonic copepods: global rates and patterns in relation to chlorophyll-a, temperature, and body weight. *Limnology and Oceanography* 48,1988–2010.
- Holling, C.S., 1959. Some characteristics of simple types of predation & parasitism. *Canadian Entomologist*.91,824–839.
- Hormazábal, S., Combes, V., Morales, C.E., Correa-Ramírez, M.A., Di Lorenzo, E., Nuñez, S., 2013. Intrathermocline eddies in the coastal transition zone off central Chile (31-41°S). *Journal of Geophysical Research Oceans* 118, 4811–4821.
- Huntley M. & Boyd C., 1984 Food-Limited Growth of Marine Zooplankton, *The American Naturalist*, Vol. 124, No. 4.
- Huggett, J., Verheye, H., Escribano, R., Fairweather, T., 2009. Copepod biomass, size composition and production in the Southern Benguela: spatio-temporal patterns of variation, and comparison with other eastern boundary upwelling systems. *Progress in Oceanography* 83,197–207.
- Ianora, A., Poulet, S.A., Miralto, A. & Grottole, R. 1996. The diatom *Thalassiosira rotula* affects reproductive success in the copepod *Acartia clausi*. *Mar. Biol.*125:279-286.
- Ianora, A., Miralto, A., Poulet, S.A., Carotenuto, Y., Buttino, I., Romano, G., Casotti, R., Pohnert, G., Wichard, T., Colucci-D'Amato, L., Terrazzano, T.

and Smetacek, V. 2004. Aldehyde suppression of copepod recruitment in blooms of a ubiquitous planktonic diatom. *Nature*. 429,403-407.

- Irigoien, X., Huisman, J. & Harris, R., 2004 Global biodiversity patterns of marine phytoplankton and zooplankton. *Nature* 429, 863–867. <https://doi.org/10.1038/nature02593>
- Ives, J.D., 1987. Possible mechanisms underlying copepod grazing responses to levels of toxicity in red tide dinoflagellates. *J. Exp. Mar. Biol. Ecol.* 112,131-145.
- Keister, J.E., T.J. Cowles, W.T. Peterson, C.A. Morgan. 2009. Do upwelling filaments result in predictable biological distributions in coastal upwelling ecosystems?, *Progress in Oceanography*, Volume 83, Issues 1–4: 303-313, <https://doi.org/10.1016/j.pocean.2009.07.042>.
- Kimmerer, W.J., Hirst, A.G., Hopcroft, R.R., McKinnon, A.D., 2007. Estimating juvenile copepod growth rates: corrections, inter-comparisons and recommendations. *Marine Ecology Progress Series* 336,187–202.
- Kobari, T., Sastri, A. R., Yebra, L., Liu, H., and Hopcroft, R. R. (2019). Evaluation of trade-offs in traditional methodologies for measuring metazooplankton growth rates: assumptions, advantages and disadvantages for field applications. *Progress in Oceanography* 178:102137. doi: 10.1016/j.pocean.2019.102137.
- Koski, M. 2007. High reproduction of *Calanus finmarchicus* during a diatom-dominated spring bloom. *Mar. Biol.* 151,1785–1798.
- Lauria, V., Attrill, M. J., Brown, A., Edwards, M. & Votier, S. C. Regional variation in the impact of climate change: evidence that bottom-up regulation from plankton to seabirds is weak in parts of the Northeast Atlantic. *Mar. Ecol. Prog. Ser.* 488, 11–22 (2013).
- Lebour, M.V. 1922. The food of plankton organisms. *J. Mar. Biol. Assoc. UK.* 12:644-677.
- Le Quere, C., Harrison, S. P., Prentice, I. C., Buitenhuis, E. T., Aumont, O., Bopp, L., Cluastre, H., Cotrim da Cunha, L., Geider, R., Giraud, X., Klaas, C., Kohfeld, K. E., Legendre, L., Manizza, M., Platt, T., Rivkin, R. B., Sathyendranath, S., Uitz, J., Watson, A. J. and Wolf-Gladrow, D. 2005. Ecosystem dynamics based on plankton functional types for global ocean biogeochemistry models. *Global Change Biology*, 11 (11). pp. 2016-2040. ISSN 1354-1013.
- Le Quéré C., Reply to Horizons Article ‘Plankton functional type modelling: running before we can walk’ Anderson (2005): I. Abrupt changes in marine ecosystems?, *Journal of Plankton Research*, Volume 28, Issue 9, September 2006, Pages 871–872, doi.org/10.1093/plankt/fbl014.

- Leising, A.W., Pierson, J.J., Halsband-Lenk, C., Horner, R., Postel, J., 2005. Copepod grazing during spring blooms: does *Calanus pacificus* avoid harmful diatoms? *Prog. Oceanogr.* 67, 384–405.
- Mackas, D., Beaugrand, G. 2010. Comparisons of zooplankton time series, *Journal of Marine Systems*, 79, Issues 3–4: 286-304, doi.org/10.1016/j.jmarsys.2008.11.030.
- Mann, K.H., Lazier, J.R. N., 1991. *Dynamics of Marine Ecosystems*. Blackwell Scientific Publications, Oxford.
- Marín, V.H., Escribano, R., Delgado, L.E., Olivares, G. & P. Hidalgo. (2001). Nearshore circulation in a coastal upwelling site off the northern Humboldt Current System. *Continental Shelf Research*. 21: 1317-1329.
- Marshall, S.M. and Orr, A.P., 1955. *The Biology of a Marine Copepod, Calanus finmarchicus* (Gunnerus), Oliver and Boyd.
- Markus L., 1954. Global structure of ordinary differential equations in the plane: *Trans. Amer. Math Soc.* 76, 127–148.
- Maneiro, I., Iglesias, P., Guisande, C., Riveiro, I., Barreiro, A., Zervoudaki, S. & Granéli, E. 2005. Fate of domoic acid ingested by the copepod *Acartia clausi*. *Mar. Biol.* 1(48), 123–130.
- Mann, K.H., 1993. Physical oceanography, foodchains & fishstocks: a review. *ICES. J. Mar. Sci.* 50:105-119.
- McGowan J. A., Bograd S. J., Lynn R. J., Miller A. J. (2003) The biological response to the 1977 regime shift in the California Current. *Deep Sea Res. Part II.*, 50, 2567–2582.
- Merico, A., Bruggeman, J., and Wirtz, K. 2009: A trait-based approach for downscaling complexity in plankton ecosystem models, *Ecol. Model.*, 220, 3001–3010, doi: 10.1016/j.ecolmodel.2009.05.005.
- Medellín-Mora, J., Atkinson, A., Escribano, R. 2019. Community structured production of zooplankton in the eastern boundary upwelling system off central/southern Chile (2003-2012). *ICES Journal of Marine Sciences*, 77(1) 419-435. doi:10.1093/icesjms/fsz193.
- Miralto, A., Guglielmo, L., Zagami, G., Buttino, I., Granata, A. and Ianora, A., 2003. Inhibition of population growth in the copepods *Acartia clausi* and *Calanus shelgolandicus* during diatom bloom. *Mar. Ecol. Prog. Ser.* 254, 253–268.
- Miralto, A., Barone, G., Romano, G., Poulet, S.A., Ianora, A., Russo, G.L., Buttino, I., Mazzarella, G., Laabir, M., Cabrini, M. & Giacobbe, M.G. 1999. The insidious effect of diatoms on copepod reproduction. *Nature*. 402, 173–176.

- Mitra, A., Castellani, C., Gentleman, W.C., Jónasdóttir, S.H., Flynn, K.J., Bode, A., Hals-band, C., Kuhn, P., Licandro, P.B., Agersted, M.D., Calbet, A., Lindeque, P.K., Koppelman, R., Møller, E.F., Gislason, A., Nielsen, T.G. & John, M. 2004. Bridging the gap between marine biogeochemical and fisheries sciences; configuring the zooplankton link. *Progress in Oceanography* 129, 176–199.
- Miloslavich, P., Bax, N., Simmons, S. E., Klein, E., Appeltans, W., Aburto-Oropeza, O., et al. (2018). essential Ocean Variables for sustained observations of marine biodiversity and ecosystems. *Global Change Biology* 24, 2416–2433. doi: 10.1111/gcb.14108
- Montero, P., Daneri, G., Cuevas, L.A., González, H.E., Jacob, B., Lizárraga, L., Menschel, E., 2007. Productivity cycles in the coastal upwelling area off Concepción: The importance of diatoms and bacterioplankton in the organic carbon flux. *Progress in Oceanography* 75, 518–530.
- Montes, Ivonne & Dewitte, Boris & Elodie, Gutknecht & Paulmier, A. & Dadou, Isabelle & Oschlies, Andreas & Garçon, V. 2014. High-resolution modeling of the Eastern Tropical Pacific Oxygen Minimum Zone: Sensitivity to the tropical oceanic circulation. *Journal of Geophysical Research: Oceans*. 119. 10.1002/2014JC009858.
- Morales, C.E., Torreblanca, M.L., Hormazábal, S., Correa-Ramírez, M., Nuñez, S., Hidalgo, P., 2010. Mesoscale structure of copepod assemblages in the coastal transition zone and oceanic waters off central-southern Chile. *Progress in Oceanography* 84, 158–173. Pauly et al. 2002.
- Muller-Karger, F.E.; Miloslavich, P.; Bax, N.J.; Simmons, S.; Costello, M.J.; Sousa Pinto, I.; Canonico, G.; Turner, W.; Gill, M.; Montes, E.; et al. 2018. Advancing Marine Biological Observations and Data Requirements of the Complementary Essential Ocean Variables (EOVs) and Essential Biodiversity Variables (EBVs) Frameworks. *Front. Mar. Sci.* 2018, 5, 211.
- Mullin M.M., Fuglister E., Fuglister F. J., 1975 Ingestion by planktonic grazers as a function of concentration of food, *Limnology and oceanography*.
- Nejstgaard, J.C. and Solberg, P.T., 1996. Repression of copepod feeding and fecundity by the toxic haptophyte *Prymnesium patelliferum*. *Sarsia* 81, 339–344.
- Nielsen, T.G., Lokkegaard, B., Richardson, K., Pedersen, F.B. and Hansen, L., 1993. *Marine Ecology Progress Series* 95:115-131.
- Neumann D.A., 1975. Classification of continuous flows on 2-manifolds, *Proc. Amer. Math. Soc.* 48, 73–81.
- Pauly, D., Christensen, V., Guénette, S. et al. Towards sustainability in world fisheries. *Nature* 418, 689–695 (2002). <https://doi.org/10.1038/nature01017>.
- Peixoto M.M., 1973. *Dynamical Systems. Proceedings of a Symposium held at the University of Bahia*, 389–420, Acad. Press, New York.



- Perko, L., 1996. *Differential Equations and Dynamical Systems*. Texts in Applied Mathematics, Springer New York.
- Peterson, W. T., Emmet, R., Goericke, R., Venrick, E., Mantyla, A. W., Bograd, S. J., Schwing, F. B., Hewitt, R., Lo, N. C. H., Watson, W. H., Barlow, J., Lowry, M., Ralston, M., Forney, K. A., Lavaniegos-Espejo, B. E., Sydeman, W. J., Hyrenbach, K. D., Bradley, R. W., Chávez, F. P., Warzybok, P., Hunter, K., Benson, S., Weise, M., Harvey, J., GaxiolaCastro, G. & Durazo-Arvizu, R. 2006. The state of the California current, 2005– 2006: Warm in the north, cold in the south. *California Cooperative Oceanic Fisheries Investigation Report* 47:30–74.
- Peterson, W., 1998. Life cycle strategies of copepods in coastal upwelling zones. *Journal of Marine Systems* 15, 313–326.
- Pohnert, G., Lumineau, O., Cueff, A., Adolph, S., Cordevant, C., Lange, M., Poulet, S.A. 2002. Are volatile unsaturated aldehydes from diatoms the main line of chemical defense against copepods? *Mar.Ecol.Prog.Ser.*245,33–45.
- Poulet, S.A., Wichard, T., Ledoux, J.B., Lebreton, B., Marchetti, J., Dancie, C., Bonnet, D., Cueff, A., Morin, P. & Pohnert, G. 2006. Influence of diatoms on copepod reproduction. I. Field and laboratory observations related to *Calanus helgolandicus* egg production. *Mar. Ecol. Prog.Ser.*308,129–142.
- Poulet, S.A., Escribano, R., Hidalgo, P., Cueff, A., Wichard, T., Aguilera, V., Vargas, C.A. & Pohnert, G. 2007. Collapse of *Calanus chilensis* reproduction in a marine environment with high diatom concentration. *Journal of Experimental Marine Biology and Ecology.*352 187–199.
- Redfield, A.C., B.H. Ketchum, and F.A. Richards. 1963. The influence of organisms on the composition of sea-water. Pp. 26–77 in *The Sea*. Volume 2: *The Composition of Sea-Water: Comparative and Descriptive Oceanography*. M.N. Hill, ed., Interscience Publishers, New York.
- Reese, D. C., Miller, T. W., and Brodeur, R. D. (2005). Community structure of near-surface zooplankton in the northern California Current in relation to oceanographic conditions. *Deep Sea Res. Part II Topical Studies in Oceanography* 52, 29–50. doi: 10.1016/j.dsr2.2004.09.027.
- Richardson AJ, Schoeman D.S. 2004. Climate impact on plankton ecosystems in the Northeast Atlantic. *Science* 305: 1609-1612. *Science* (New York, N.Y.). 305. 1609-12. 10.1126/science.1100958.
- Riquelme-Bugueño, R., Escribano, R., Gómez-Gutiérrez, J. 2013. Somatic and molt production of *Euphausia mucronata* off central-southern Chile: the influence of coastal upwelling variability. *Marine Ecology Progress Series* 476: 39–57, 2013.

- Rykaczewski, R. R. et al. Poleward displacement of coastal upwelling-favorable winds in the ocean's eastern boundary currents through the 21st century. *Geophysical Research Letters* 42, 6424–6431 (2015).
- Schmoker, C., Hernández-León, S. 2013. Stratification effects on the plankton of the subtropical Canary Current. *Progress in Oceanography* 119,24–31. <http://dx.doi.org/10.1016/j.pocean.2013.08.006>.
- Seibel, B.A. 2011. Critical oxygen levels and metabolic suppression in oceanic oxygen minimum zones. *Journal of Experimental Biology* 214, 326–336.
- Sigman, D. M. & Hain, M. P. 2012. The Biological Productivity of the Ocean. *Nature Education Knowledge* 3(10):21.
- Shchepetkin, Alexander & McWilliams, James. (2005). The Regional Oceanic Modeling System (ROMS): a split-explicit, free-surface, topography-following-coordinate ocean model. *Ocean Modelling*. 9. 347-404. 10.1016/j.ocemod.2004.08.002.
- Schneider, W., Donoso, D., Garcés-Vargas, J., Escibano, R. 2016. Water-column cooling and sea surface salinity increase in the upwelling region off central-south Chile driven by a poleward displacement of the South Pacific. *Progress in Oceanography*. 141:38-58.
- Shchepetkin, Alexander & McWilliams, James. 2005. The Regional Oceanic Modeling System (ROMS): a split-explicit, free-surface, topography-following-coordinate ocean model. *Ocean Modelling*. 9. 347-404. 10.1016/j.ocemod.2004.08.002.
- Sobarzo, M., Bravo, L., Donoso, D., Garcés-Vargas, J., Schneider, W., Coastal upwelling and seasonal cycles that influence the water column over the continental shelf off central Chile, *Progress in Oceanography*, Volume 75, Issue 3, 2007, Pages 363-382, ISSN 0079-6611, doi.org/10.1016/j.pocean.2007.08.022.
- Solomon, M.E., 1949. The natural control of animal populations. *Journal of Animal Ecology*. 18, 1–35.
- Steele, J.H., 1958. The quantitative ecology of marine phytoplankton. *Biol.Rev.*34:129-158.
- Sukhanov, V. and Omelko, A., 2002. Dynamics of feeding preferences by a predator. *Ecological Modelling*. 154, 203-206.
- Sunda, W. G. and Huntsman, S. A.: Interrelated influence of iron, light and cell size on marine phytoplankton growth, *Nature*, 390, 389–392, 1997.

- Tammilehto,A., Nielsen,T.G., Krock,B., Møller,E.F., Lundholm,N., 2012. Calanus spp.- vectors for the biotoxin, domoic acid, in the arctic marine ecosystem? Harmful Algae 20, 165-174.
- Tammilehto,A., Nielsen,T.G., Krock,B., Møller,E.F. \& Lundholm, N. 2015. Induction of domoic acid production in the toxic diatom Pseudo-nitzschia seriata by calanoid copepods. Aquat.Toxicol.159,52–61.
- Teegarden,G.J., 1999. Copepod grazing selection and particle discrimination on the basis of PSP toxincontent. Marine Ecology Progress Series.181,163–176.
- Turner,J.T., 1984. The feeding ecology of some zooplankters that are important prey items of larval fish. NOAA Technical Reports. Washington, DC.NMFS7,p1-28.
- Vargas, Cristian \& Manríquez, Patricio \& Navarrete, Sergio. 2006. Feeding by larvae of intertidal invertebrates: Assessing their position in pelagic food webs. Ecology. 87. 444-57. 10.1890/05-0265.
- Vargas, C.A., Cuevas, L.A., González, H.E. y G. Daneri, 2007, "Bacterial Growth Response to Copepod Grazing in Aquatic Ecosystems", Journal of the Marine Biological Association 87, 667-674.
- Vargas, C., Martínez, R., Escribano, R., Lagos, N. 2010. The relative influence of food quantity, quality, and feeding behavior on zooplankton growth regulation in coastal food webs. Journal of the Marine Biology Association, UK. doi:10.1017/S0025315409990804.
- Vargas, Cristian & Contreras, Paulina & Pérez, Claudia & Sobarzo, Marcus & Saldías, Gonzalo & Salisbury, J. (2016). Influences of riverine and upwelling waters on the coastal carbonate system off Central Chile and their ocean acidification implications. Journal of Geophysical Research: Biogeosciences. 121. 10.1002/2015JG003213.
- Vergara, O., Echevin, V., Sepúlveda, H.H., Quiñones, R.A. 2017. Controlling factors of the seasonal variability of productivity in the southern Humboldt Current System (30-40°S): A biophysical modelling approach. Continental Shelf Research. DOI: 10.1016/j.csr.2017.08.013.
- Verity,P.G. and Smetacek,V., 1996. Organism life cycles, predation and structure of pelagic ecosystems. Mar.Ecol.Prog.Ser.130, 277-293.
- Wang, D., Gouhier, T. C., Menge, B. A. & Ganguly, A. R. 2015. Intensification and spatial homogenization of coastal upwelling under climate change. Nature. 518, 390-406.
- Wolfe,G., 2000. The chemical defense ecology of marine unicellular plankton: constraints, mechanisms \& impacts. Biological Bulletin.198,225-244.

- Xiu, P., Chai, F., Curchitser, E. N. & Castruccio, F. S. 2018. Future changes in coastal upwelling ecosystems with global warming: The case of the California Current System. *Scientific Reports*. 8:2866.
- Yebra, L., Herrera, I., Mercado, J. M., Cortés, D., Gómez-Jakobsen, F., Alonso, A., et al. (2018). Zooplankton production and carbon export flux in the western Alboran sea gyre (SW Mediterranean). *Progress in Oceanography* 167, 64–77. doi: 10.1016/j.pocean.2018.07.009.

## ANEXOS

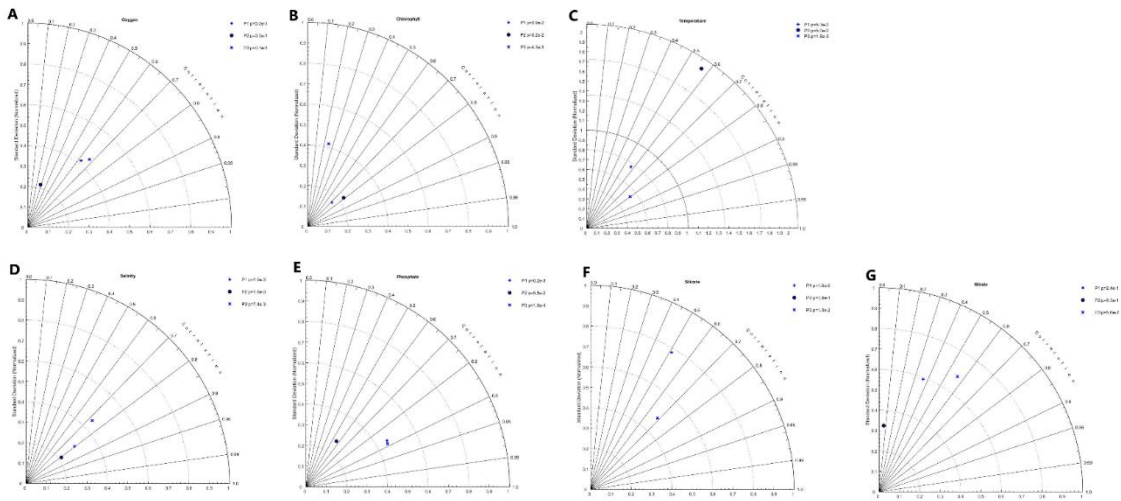


**Figura 1A.** Diagrama de Taylor correlaciones de datos de 0 a 80 metros, A. oxígeno, B. clorofila, C. temperatura, D. salinidad, E. fosfato, F. Silicato, G. nitrato.

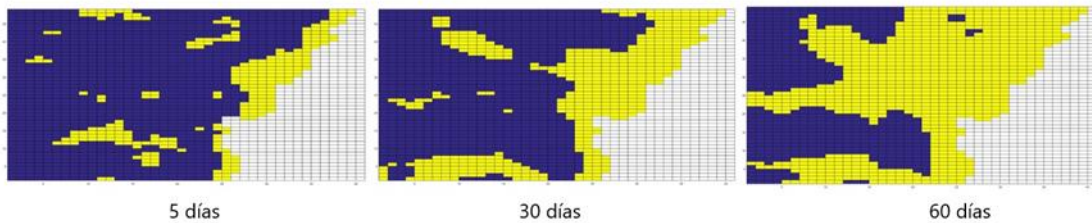


**Figura 2A.** Mapas de correlación del punto de grilla representativo de la estación 18 con los demás puntos de grilla del dominio, los recuadros amarillos representan correlaciones significativas  $p < 0.05$ .

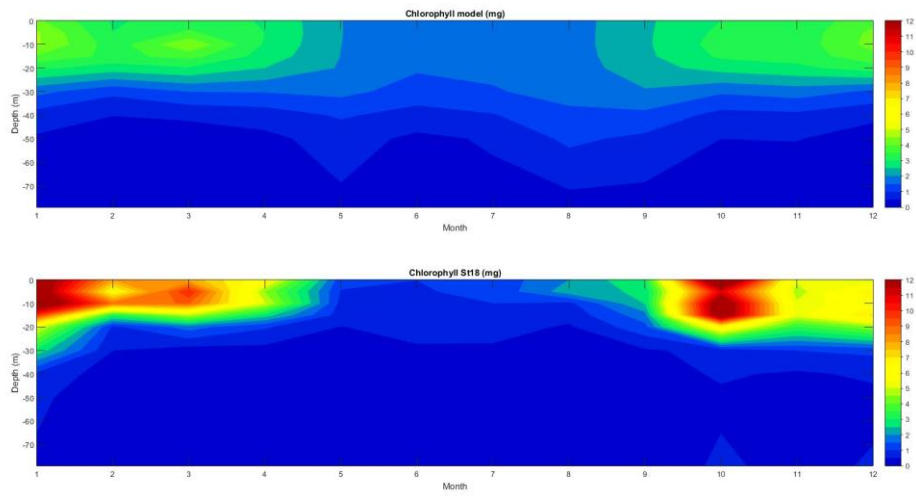


**Figura 3A.** Grafica Hovmoller climatológica de la clorofila, modelo panel superior, estación 18 panel inferior.

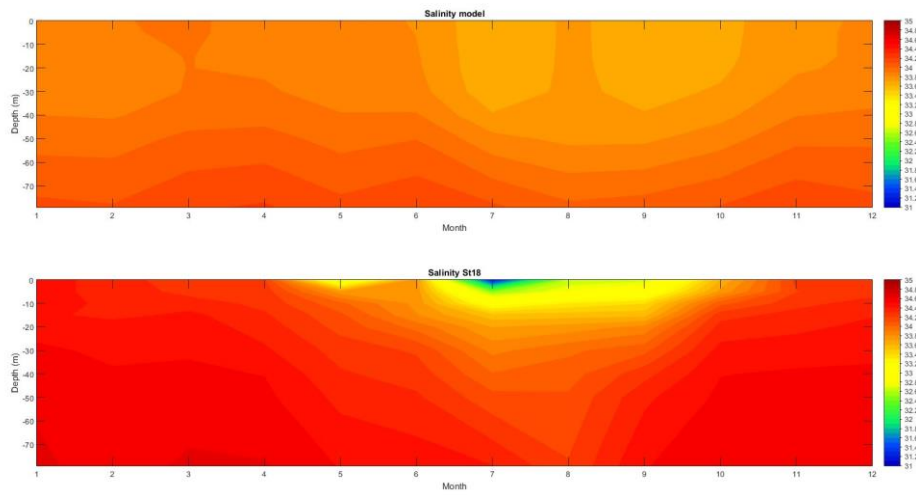


**Figura 4A.** Grafica Hovmoller climatológica de la salinidad, modelo panel superior, estación 18 panel inferior.

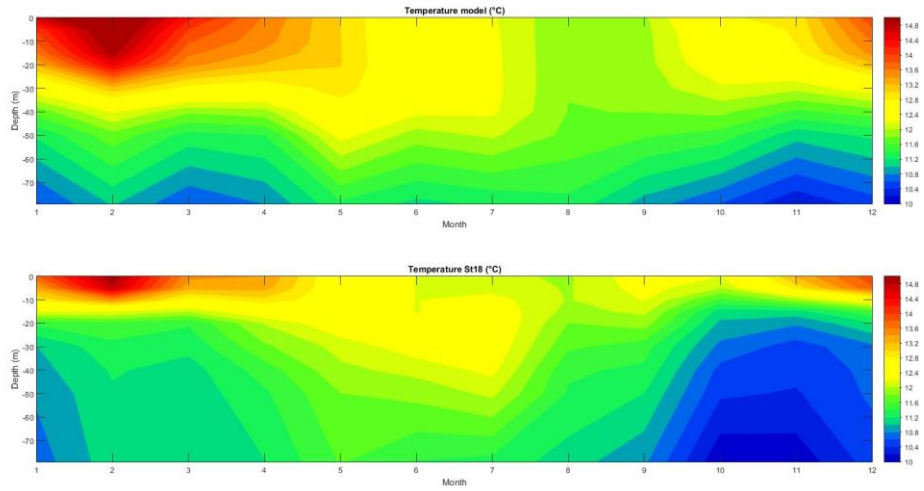


**Figura 5A.** Grafica Hovmoller climatológica de la Temperatura, modelo panel superior, estación 18 panel inferior

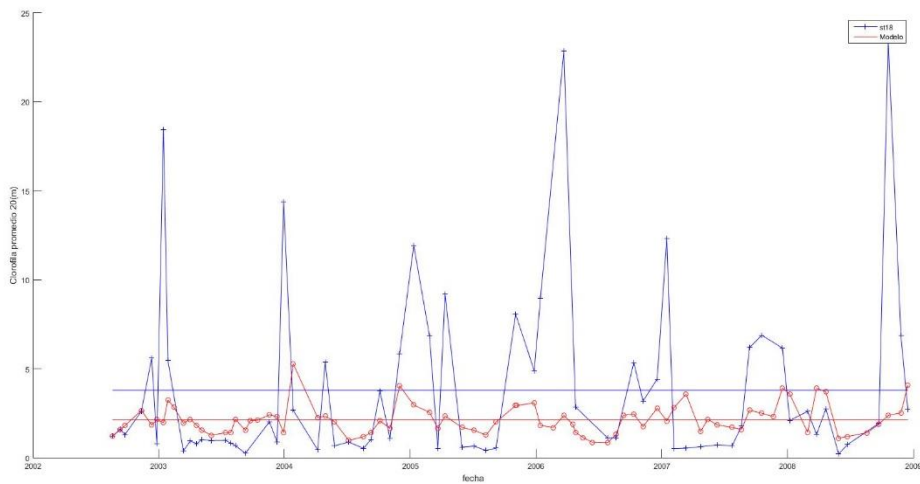


**Figura 6A.** Serie de tiempo para la clorofila junto a sus promedios en Promedios 0-20 metros datos modelo (rojo) y estación 18 (azul).

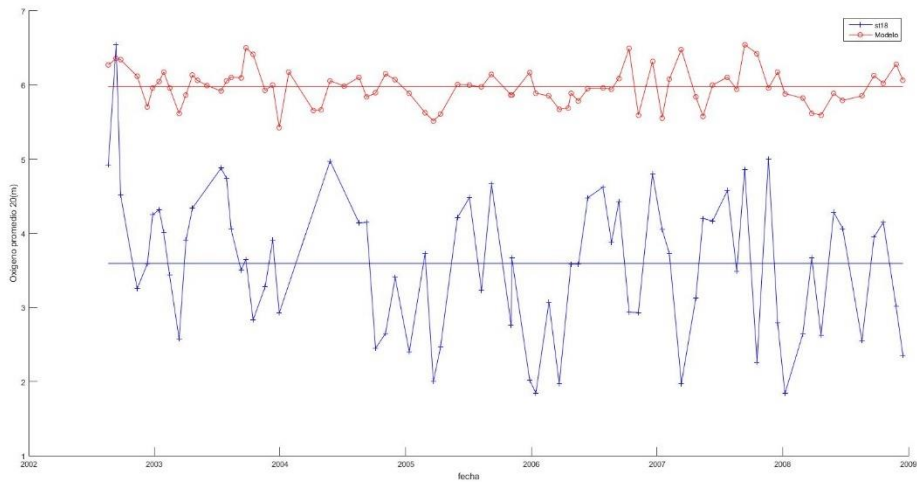


**Figura 7A.** Serie de tiempo para el oxígeno junto a sus promedios en 0-20 metros de Oxígeno, datos modelo (rojo) y estación 18 (azul).

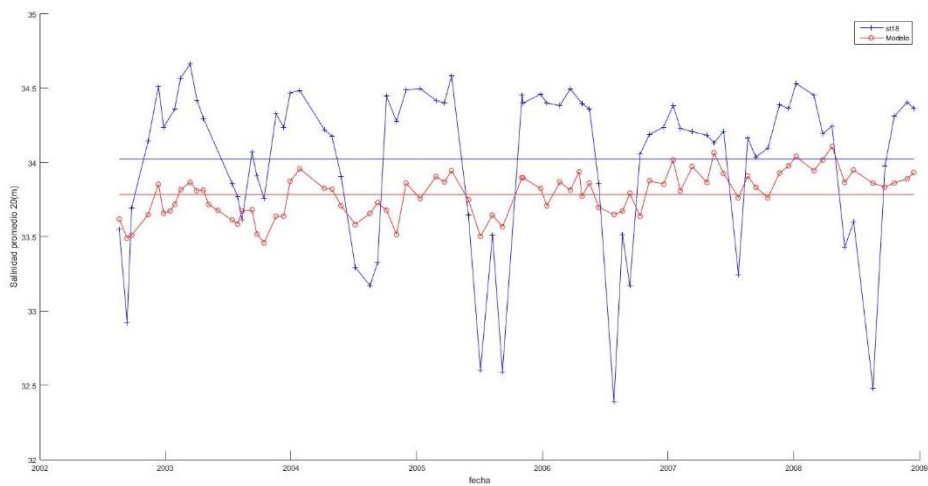


**Figura 8A.** Serie de tiempo para la salinidad junto a sus promedios en 0-20 metros, datos modelo (rojo) y estación 18 (azul).



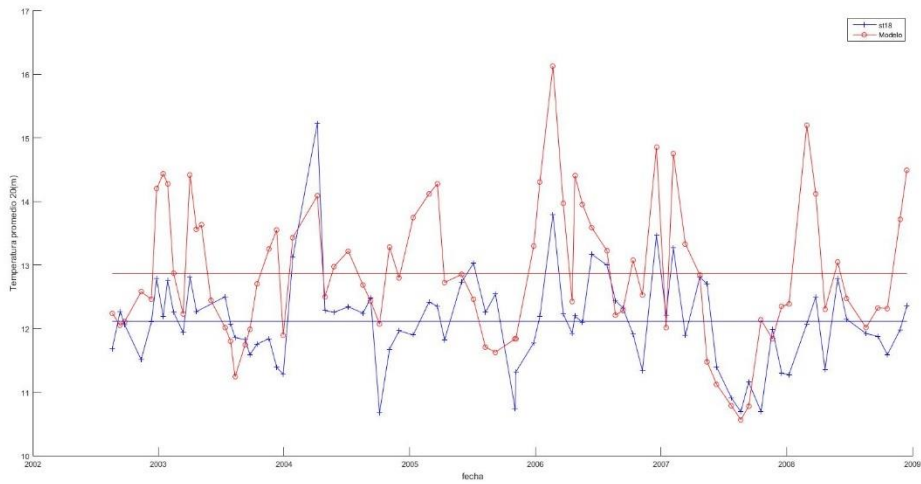


**Figura 9A.** Serie de tiempo para la temperatura junto a sus promedios en 0-20 metros, datos modelo (rojo) y estación 18 (azul).

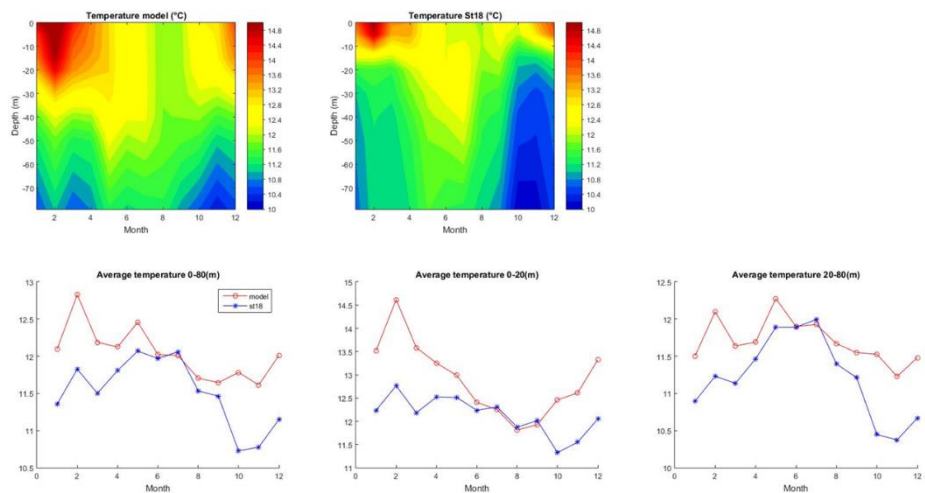


**Figura 10A.** Paneles superiores grafica Hovmoller climatología de la temperatura en la columna de agua, paneles inferiores promedios climatológicos (0-80 metros, 0-20 metros, 20-80 metros).

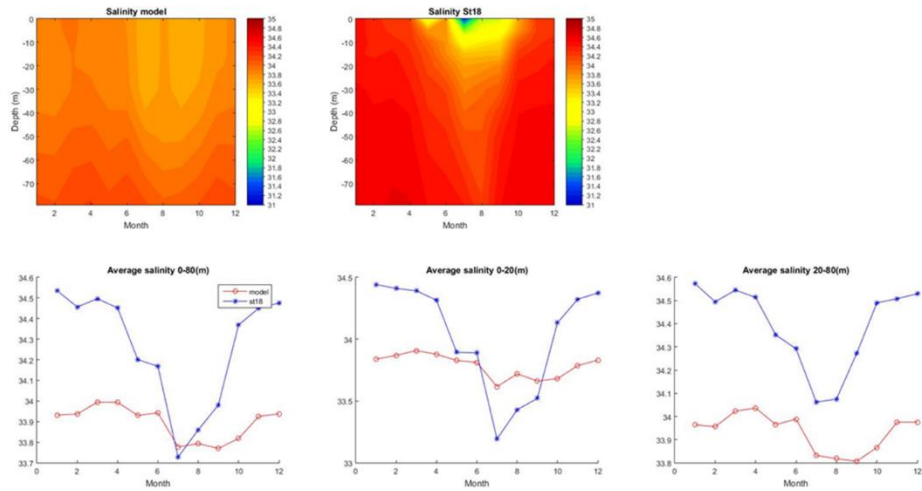


**Figura 11A.** Paneles superiores grafica Hovmoller climatología de la salinidad en la columna de agua, paneles inferiores promedios climatológicos (0-80 metros, 0-20 metros, 20-80 metros).

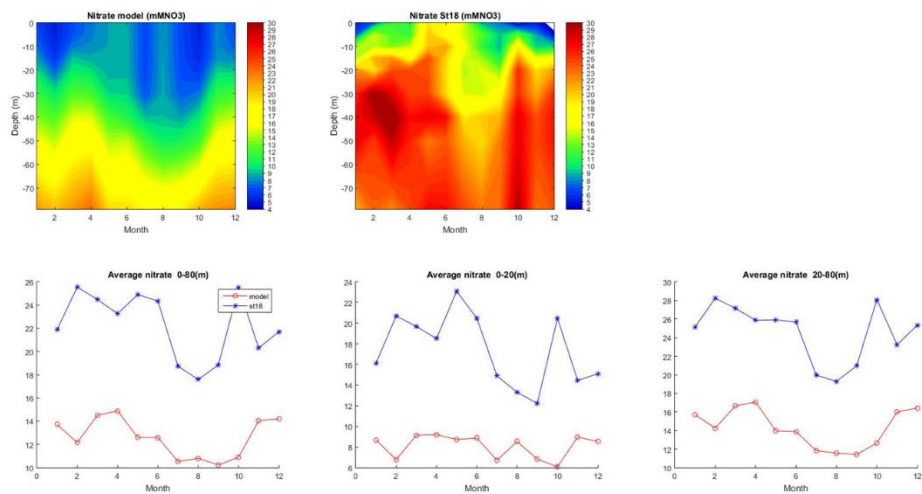


**Figura 12A.** Paneles superiores grafica Hovmoller climatología del nitrato en la columna de agua, paneles inferiores promedios climatológicos (0-80 metros, 0-20 metros, 20-80 metros).

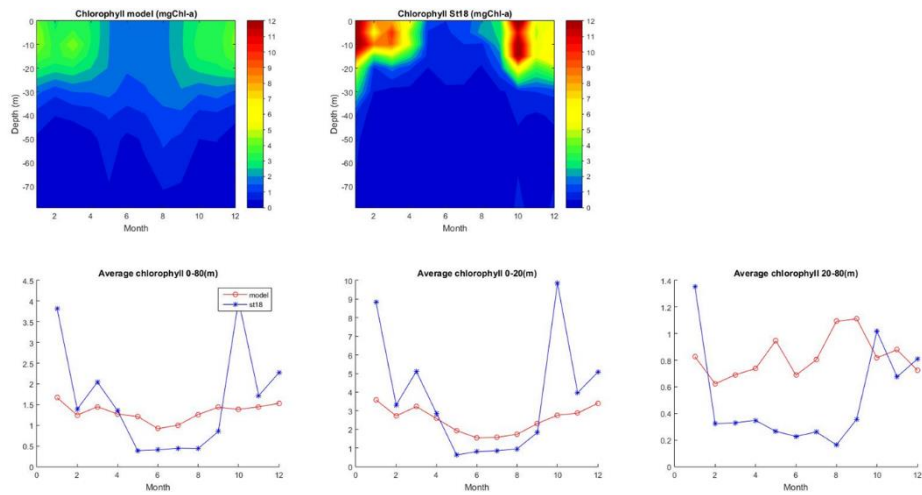


**Figura 13A.** Paneles superiores grafica Hovmoller climatología de la clorofila en la columna de agua, paneles inferiores promedios climatológicos (0-80 metros, 0-20 metros, 20-80 metros).

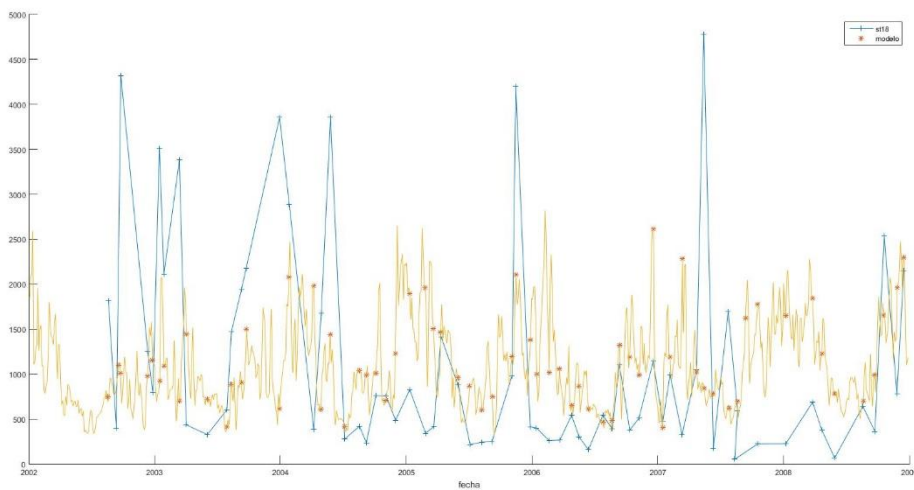


**Figura 14A.** Biomasa integrada de 0 a 80 metros desde agosto de 2002 a diciembre de 2008, datos estación 18 (azul), datos modelo (naranja).

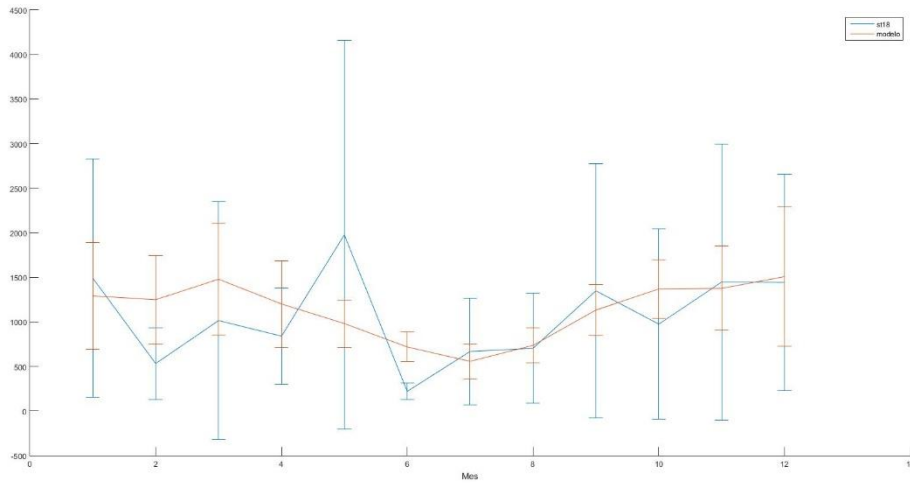


**Figura 15A.** Climatología biomasa integrada de 0 a 80 metros, datos estación 18 (azul), datos modelo (naranja).

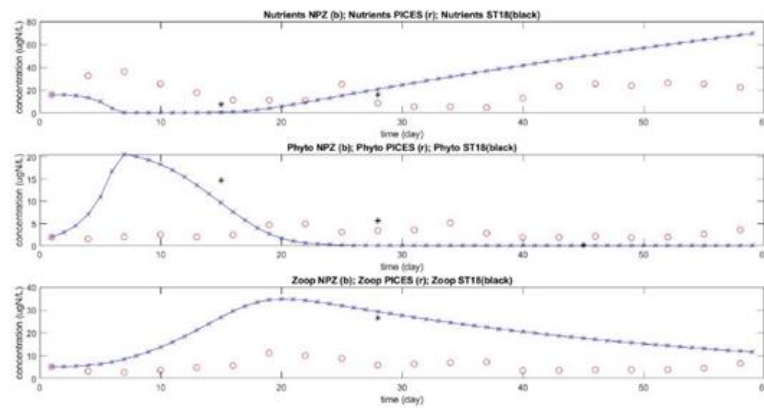


**Figura 16A.** Datos modelo NPZ (azul), modelo Roms-Pisces (naranja) y estación 18 (negro) para 60 días, panel superior concentración de nitrato, panel central biomasa del fitoplancton, panel inferior biomasa del zooplancton.